

**THERMOMECHANICAL MODELING OF STAMPING OF  
ADVANCED HIGH STRENGTH STEELS**

**A THESIS SUBMITTED TO  
GRADUATE SCHOOL OF NATURAL AND APPLIED SCIENCE  
OF  
KOCAELİ UNIVERSITY  
BY  
KADİR AKCAN**

**IN PARTIAL FULFILLMENT OF THE REQUIREMENTS  
FOR  
THE DEGREE OF DOCTOR OF PHILOSOPHY  
IN  
MECHANICAL ENGINEERING**

**KOCAELİ 2021**

**THERMOMECHANICAL MODELING OF STAMPING OF  
ADVANCED HIGH STRENGTH STEELS**

**A THESIS SUBMITTED TO  
GRADUATE SCHOOL OF NATURAL AND APPLIED SCIENCES  
OF  
KOCAELİ UNIVERSITY**

**BY**

**KADİR AKCAN**

**IN PARTIAL FULFILLMENT OF THE REQUIREMENTS  
FOR  
THE DEGREE OF DOCTOR OF PHILOSOPHY  
IN  
MECHANICAL ENGINEERING**

**Prof.Dr.H.İbrahim Saraç**  
**Supervisor, Kocaeli University** .....

**Prof.Dr.Mesut Gür**  
**Jury member, İstanbul Technical University** .....

**Prof.Dr.Cenk Çelik**  
**Jury member, Kocaeli University** .....

**Prof.Dr.Muharrem Yılmaz**  
**Jury member, Kocaeli University** .....

**Prof.Dr.Nedim Sözbir**  
**Jury member, Sakarya University** .....

**Thesis Defense Date: 10.02.2021**

## **ACKNOWLEDGEMENTS**

I cannot express enough thanks to my committee for their continued support and encouragement: consultant Prof. Dr. H.İbrahim Saraç, jury member Prof.Dr.Mesut Gür and Prof.Dr.Cenk Çelik. I offer my sincere appreciation for the learning opportunities provided by my committee. Prof.Dr.Taylan Altan helps with experienced ideas. Additionally thanks to Doç.Dr.Eren Billur who supported me during paper phase.

Completion of this project could not have been accomplished without the support of Dr. Alper Güner from AutoForm Engineering Deutschland GmbH and Mr. Nihat Kurtuluş from Grup Otomasyon. They shared Autoform software as free and supported this study technically.

My managers, Mr. Müjdat Tiryaki, Mr. Burak Gürler and Mr. Gürkan Erol, have supported to me for all doctorate duration in Ford Otosan.

Finally, to my caring, loving, and supportive wife, Şükran Akcan: my deepest gratitude. Your encouragement when the times got rough are much appreciated and duly noted. It was a great comfort and relief to know that you were willing to provide management of our household activities while I completed my work. My heartfelt thanks.

February-2021

Kadir AKCAN

## TABLE OF CONTENTS

ACKNOWLEDGEMENTS .....	i
TABLE OF CONTENTS .....	ii
LIST OF FIGURES .....	iv
LIST OF TABLES .....	vi
MARKS AND ABBREVIATIONS .....	vii
ABSTRACT .....	viii
ÖZET .....	ix
INTRODUCTION .....	1
1. CLASSIFICATION OF AUTOMOTIVE STEELS .....	3
2. METAL FORMING PROCESS .....	6
2.1. Deep Drawing Operation .....	6
2.1.1. Stripping process .....	8
2.1.2. Force effect on deep drawing process .....	9
2.1.3. Redraw operation .....	11
2.1.4. Ironing operation .....	11
2.1.5. Stress conditions during deep drawing .....	12
2.1.6. Thickness change in deep drawn sheet .....	13
2.1.7. Effect of material properties .....	14
2.1.8. Effect of mold geometry .....	14
2.1.9. Effect of processing conditions .....	16
2.2. Material Behavior in Metal Forming .....	17
2.3. Temperature in Metal Forming .....	19
2.4. Other Sheet Metal Process .....	20
2.4.1. Cutting in metals .....	21
2.4.2. Piercing operation .....	24
2.4.3. Bending operation for sheet metals .....	27
2.4.4. Bending in V die .....	29
2.5. Sheet Metal Properties for Forming Process .....	31
2.5.1. Low carbon HS steel grades .....	33
2.5.2. Bake hardenable (BH) steels .....	33
2.5.3. Steels that do not contain intermediate atoms (IF) .....	34
2.5.4. High Strength Low Alloy (HSLA) Steels .....	35
2.5.5. First generation AHS steel grades .....	35
2.5.6. In ferritic / bainitic (FB) steels .....	36
2.5.7. Transformation induced plasticity (TRIP) .....	36
2.5.8. Martensitic (MART) Steels .....	38
3. HEAT GENERATION IN SHEET METAL WORKING .....	39
3.1. Heat Transfer Methods .....	39
3.1.1. Conduction .....	39
3.1.2. Convection .....	39
3.1.3. Radiation .....	40
3.2. Plastic Deformation Effect .....	40
3.3. Heat Transfer Mechanism During Draw Operation .....	45
3.4. Thermomechanical FE Model .....	45
4. TEMPERATURE VALIDATION OF FE SIMULATION RESULTS .....	49
4.1. Background, Problem Statement and Motivation .....	49
4.2. Validation of Thermomechanical Condition .....	55

4.3.Results of The Validation.....	60
5.SINGLE STROKE FORMING EFFECT .....	63
5.1.FE Simulation Models for Single Stroke .....	63
5.2.Analyses of Variance (ANOVA) for Deep Draw Operation.....	67
5.3.Results of Single Stroke .....	69
6. MULTI STROKE FORMING EFFECT .....	72
6.1.FE Simulation Models for Multi Stroke.....	72
6.2.Results .....	74
7.COOLING SYSTEM FOR COLD STAMPING DIES.....	82
7.1.Cooling Channel.....	83
7.2.Laminar or Turbulent Flow.....	84
7.3.Cooling Channel Design.....	86
7.4.Mathematical Model of Cooling Channel .....	90
7.4.1.Cooling channel formula .....	92
7.4.2.Cooling channel quantity.....	93
7.4.3.Cooling channel distance from contact surface .....	94
7.4.4.Cooling channel optimization .....	94
7.5.Results of Cooling System in Multi Stroke .....	96
7.6.Cooling System Design and Construction .....	103
8.CONCLUSIONS AND FUTURE WORK.....	106
REFERENCES .....	108
APPENDIX .....	112
PERSONAL PUBLICATIONS AND WORKS .....	133
VITA .....	134

## LIST OF FIGURES

Figure 1. 1.	Banana Curve .....	3
Figure 1. 2.	AHSS Using Increasing for Years .....	4
Figure 1. 3.	The use of HSS and AHSS from 2007 to 2015.....	5
Figure 2. 1.	Deep Draw Operation Steps .....	7
Figure 2. 2.	Examples of the Deep Drawing Die.....	8
Figure 2. 3.	Radial Pull and Circumferential Compression Forces.....	9
Figure 2. 4.	Drawn Shell Results.....	10
Figure 2. 5.	Redraw Operation Examples .....	11
Figure 2. 6.	An Example of the Ironing Method .....	12
Figure 2. 7.	Stress Condition.....	12
Figure 2. 8.	Thickness of Parts .....	13
Figure 2. 9.	Examples of the Shaping Process of a Spherical Part.....	16
Figure 2. 10.	Stress-Strain Plot.....	18
Figure 2. 11.	Sheet Metal Cutting Operation .....	22
Figure 2. 12.	Cutting Operations .....	24
Figure 2. 13.	Plastic Deformation .....	25
Figure 2. 14.	Beginning of Cutting Process .....	25
Figure 2. 15.	Cutting Progress .....	26
Figure 2. 16.	Cutting Deformations .....	26
Figure 2. 17.	After Cutting Operation .....	27
Figure 2. 18.	Tensile and Compression Elongation in Metal During Bending .....	28
Figure 2. 19.	Bending by V Shape Die .....	29
Figure 2. 20.	Springback Condition in Bending Operation.....	30
Figure 2. 21.	Die Neck Length .....	30
Figure 2. 22.	Steel Type for Cars .....	32
Figure 3. 1.	Deep Drawing Tool .....	43
Figure 3. 2.	Cup Drawing Schematic View .....	44
Figure 3. 3.	Temperature Distribution of FE Results of Cup Drawing Test .....	44
Figure 3. 4.	Heat Transfer of Stamping Die .....	45
Figure 3. 5.	Drawn Cup Thermomechanical Result Example .....	46
Figure 3. 6.	Draw Height-Temperature Relation Example in Draw Operation.....	47
Figure 4. 1.	Stress Strain Curve of Mild Steel, HSS and DP800.....	49
Figure 4. 2.	Ford Focus HB Model .....	50
Figure 4. 3.	Experiments Results .....	51
Figure 4. 4.	Flow Curves of 20°C .....	53
Figure 4. 5.	Flow Curves of 40°C .....	53
Figure 4. 6.	Flow Curves of 40°C .....	53
Figure 4. 7.	Flow Curves of 40°C .....	54
Figure 4. 8.	Forming Limit Curve of 1.6 mm thick DP800 .....	54
Figure 4. 9.	Stamping Tool from Previous Publication by Pereira and Rolfe.....	55
Figure 4. 10.	Blank View of FE Simulation 150mmx26mm .....	57
Figure 4. 11.	Drawn Part After Forming Operaiton .....	57
Figure 4. 12.	Before Starting the Operation.....	58
Figure 4. 13.	Blank Forming.....	58
Figure 4. 14.	Formed Blank Picture.....	59
Figure 4. 15.	Example Bead Form .....	59
Figure 4. 16.	Punch Force vs. Press Stroke, Experiments from .....	60

Figure 4. 17.	Temperature Increase in the Blank .....	60
Figure 4. 18.	Temperature Increase of the Tools .....	61
Figure 5. 1.	Cup Draw Model Similar to Reference .....	63
Figure 5. 2.	Schematic of the New Die Design .....	64
Figure 5. 3.	Draw Height 160mm Temperature Distribution.....	65
Figure 5. 4.	Temperature Distribution on Part Surface Before Split .....	66
Figure 5. 5.	Split Part .....	67
Figure 5. 6.	Minitab Software Deviation Results.....	68
Figure 5. 7.	Pareto Analyses Result.....	69
Figure 5. 8.	Draw Die Pipe System Estimation.....	69
Figure 5. 9.	Constant Die Temperature Drawability Effect .....	70
Figure 6. 1.	Press Stroke-Time Curves a)Link-Motion b)Mechanical Press.....	73
Figure 6. 2.	Condition 8M: Failure at 43rd Part with Over.....	74
Figure 6. 3.	Condition 8L: Failure at 22 <sup>nd</sup> Part with Over .....	74
Figure 6. 4.	Condition 22M: Failure at 83 <sup>rd</sup> Part with Over.....	75
Figure 6. 5.	Condition 22L: Failure at 45 <sup>th</sup> Part with Over.....	75
Figure 6. 6.	Tool Temperature Comparing 8 and 22 SPM for Link Press .....	77
Figure 6. 7.	FC Comparing for 8SPM and 22 SPM for Link Press .....	77
Figure 6. 8.	Wall Split Issue in Mass Production in 12 SPM .....	78
Figure 6. 9.	Maximum Blank Temperature in All 4 Conditions .....	79
Figure 6. 10.	Friction Coefficient a)1st stroke b)22th stroke .....	79
Figure 6. 11.	Multi Stroke and Single Stroke Friction Effect .....	80
Figure 6. 12.	Akcan Dead Loop .....	81
Figure 7. 1.	Conventional Die Design Picture.....	82
Figure 7. 2.	Hot Stamping System .....	83
Figure 7. 3.	Heat Transfer Condition In Case of Cooling Pipe .....	84
Figure 7. 4.	Heat Transfer in Pipe Process .....	85
Figure 7. 5.	Sheet Metal Inner Part Split Issue .....	87
Figure 7. 6.	Sheet Metal Split Issue .....	87
Figure 7. 7.	Big Dimension Sheet Metal Part Split Issue .....	88
Figure 7. 8.	Cup Drawing Model with Cooling Pipes .....	89
Figure 7. 9.	Upper Die Pipe Route .....	89
Figure 7. 10.	Punch (Lower Die) Cooling Route.....	90
Figure 7. 11.	Cooled Die Design Flow.....	91
Figure 7. 12.	Simple Model .....	92
Figure 7. 13.	Temperature Distribution After 8 Stroke .....	95
Figure 7. 14.	Pipe Optimisation for Hot Stamping .....	96
Figure 7. 15.	Temperature Condition 8 SPM Link Press .....	97
Figure 7. 16.	FC Condition 8SPM Link Press.....	98
Figure 7. 17.	Temperature Condition 8 SPM Mechanical Press .....	99
Figure 7. 18.	FC Condition 8SPM Mechanical Press .....	99
Figure 7. 19.	Tool Temperature Condition 22 SPM Link Press.....	100
Figure 7. 20.	FC Condition 22SPM Link Press.....	101
Figure 7. 21.	Tool Temperature Condition 22 SPM Mechanical Press .....	102
Figure 7. 22.	FC Condition 22SPM Mechanic Press .....	102
Figure 7. 23.	Cooling Pipe System in Hot Stamping.....	103
Figure 7. 24.	Drilling Method Implementation Example .....	104
Figure 7. 25.	Pre-Embedded Pipes .....	104
Figure 7. 26.	Standard Hot Stamping Test System .....	105

## LIST OF TABLES

Table 2. 1.	Strength Coefficient and Strain Hardening Exponent .....	18
Table 2. 2.	Cutting Space Defined for Three Different Metal Type .....	22
Table 2. 3.	Steel Types in Automotive Industry .....	33
Table 2. 4.	Low Carbon Steels Properties.....	33
Table 2. 5.	Bake Hardenable Steel Types.....	34
Table 2. 6.	IF Steels.....	35
Table 2. 7.	HSLA Steels .....	35
Table 2. 8.	DP Steels.....	36
Table 2. 9.	Trip Steels.....	37
Table 2. 10.	CP Steels.....	37
Table 3. 1.	Friction Coefficient Effects of Friction.....	42
Table 3. 2.	Contact Pressure HTC Scaling Relatio.....	47
Table 4. 1.	DP800 Has Different Name Standards.....	52
Table 4. 2.	Simulation Parameters .....	56
Table 5. 1.	Thermal Properties Used by Pereira and Rolfe.....	65
Table 5. 2.	Process Conditions.....	66
Table 5. 3.	Design of Experiment Model.....	68
Table 5. 4.	Die Temperature and Drawability Relation.....	70
Table 6. 1.	Simulation Parameters and Failure Criteria After First Hit.....	73



## MARKS AND ABBREVIATIONS

AHSS	:Advanced High Strength Steel
BH	:Bake Hardenable
COF	:Coefficient of Friction
CP	:Complex Phase
DDR	:Deep Drawing Ratio
DDRL	:Deep Drawing Ratio Limit
DP	:Dual Phase
FB	:Ferritic Bainitic
FE	:Finite Element
FC	:Failure Criterion
FSV	:Future Steel Vehicle (Program)
FEM	:Finite Element Method
HF	:Hot Formed (and Quenched)
HSLA	:High Strength Low Alloy (Steels)
HSS	:High Strength Steels
HTC	:Heat Transfer Coefficient
IF	:Interstitial Free
Mild	:Mild Steel
MS	:Martensitic (MART) Steel
SPM	:Strokes Per Minute
TRIP	:Transformation Induced Plasticity
TWIP	:Twinning Induced Plasticity

## **THERMOMECHANICAL MODELING OF STAMPING OF ADVANCED HIGH STRENGTH STEELS**

### **ABSTRACT**

As advanced high strength steels (AHSS) find more use in automotive industry to meet crashworthiness and light weighting targets, concurrently. AHSS typically have higher strength, but lower formability; often limiting a part's dimensions and geometric complexity.

Several studies have clearly shown that, in sheet metal forming, significant portion of the work done to overcome friction and to plastically deform a sheet is converted into heat. In this study, a thermomechanical finite element model has been developed to calculate the temperature rise in forming DP800 (AHSS). The model was validated with experiments from literature.

First cup drawing model developed as limit height before split issue in a single-cycle model. Some parameters defined variables in order to understand effect to model. The most effected parameter found as temperature.

A multi-cycle model is developed to find out possible problems due to tool heating. The process and material are selected to speed up the heating. Under different realistic press conditions, failures are observed after 20 to 80 hits.

Finally cooling system developed in multi-cycle process and shown, that improve the process conditions.

Although this study includes AHSS, the results may also help to improve mild steels and others, in deep draw operation because today randomly split issue is seen in mass production frequently. Because of that; new inspection systems developed in order to catch defected part before sending to next station in factory. After this study, these systems can be removed if implemented cold stamping dies properly.

**Keywords:** Cooling, Forming, Heat, Stamping.

## YÜKSEK MUKAVEMETLİ ÇELİKLERİN ŞEKİLLENDİRİLMESİNDE TERMOMEKANİK MODELLEME

### ÖZET

Yüksek mukavemetli çelikler, hafiflik ve çarpma esnasındaki yüksek dayanım gibi, özellikle otomotiv endüstrisindeki isterleri karşılarken; büyük boyutlu ve kompleks parçaların şekillendirme esnasında yaşanan zorlukları sebebiyle kısıtlı noktalarda kullanılabilir. Bu çalışmada, DP800 (AHSS) sacının şekillendirilmesi esnasında oluşan sıcaklık artışını hesaplamak için bir termomekanik sonlu eleman modeli geliştirildi. Bu model, literatürden deneylerle doğrulandı.

Sac metalinin şekillendirme esnasında; sürtünme ve plastik deformasyonun ısıya dönüştüğü, şuana kadar yapılan çalışmalarda açıkça ortaya koyulabilmiştir. Bu çalışmada, DP800 (AHSS) sacının şekillendirilmesi esnasında oluşan sıcaklık artışını hesaplamak için bir termomekanik sonlu eleman modeli geliştirildi. Bu model, literatürden deneylerle doğrulandı.

Çalışmanın ilk adımında, tek bir pres çevirimi esnasında sac parçanın belirlenen modele göre yükseklik limiti tespit edildi. Modele etkisini anlamak için bazı parametreler değişken olarak tanımlandı. En çok etkilenen parametrenin sıcaklık olduğu tespit edildi.

Sac metalinin ve onunla birlikte kalıbın ısınmasına bağlı olası sorunları bulmak için çok döngülü bir model geliştirildi. Farklı özelliklerdeki, gerçekçi pres koşulları altında, 20 ila 80 pres vuruşundan sonra, derin çekme yapılan sac parçada yırtılma eğilimi tespit edildi.

Son olarak soğutma sistemi, çok döngülü süreçte geliştirildi ve kalıptaki proses koşullarının iyileştiği tespit edildi.

Bu çalışma; tamamen yüksek mukavemetli çeliklerin verdiği yanıtları içermesine rağmen; benzer çıktılar seri imalatta yumuşak çelikler için; arada bir gözükten yırtılma probleminin yaşanmaması için kullanılabilir bilgiler içermektedir. Çalışmalar bu bağlamda kullanılabilir ise; yırtılmış sac parçanın bir sonraki istasyona gidişini engelleyen kontrol sistemlerinin kurulumuna ve bakımına ihtiyaç olmayacak, tam otomasyonlu bir pres hattında, ilk seferde doğru üretim garanti altına alınabilecektir.

**Anahtar Kelimeler:** Soğutma, Çekme, Isı, Sac Şekillendirme.

## INTRODUCTION

Sheet metal forming technology is an essential part of modern industry, which allows for the production of high quality products with complex geometries at low manufacturing costs. Nowadays, in the automotive and aerospace industries increasing demand has emerged for low cost, high strength and fast manufacturing volume. Mild steel does not provide high durability, so its using area is limited. Highly possibility to supply advanced high strength parts like Manganese-Boron Steel with complex geometry by hot stamping operation but this process cost high and increasing vehicle prices. Advanced High Strength Steels (AHSS) have high durability with high tensile strength, typically lower than Manganese-Boron steel. However, AHSS usage is limited for complex geometries in high production rates. Especially die temperature increased in deep draw operation so effecting draw operation parameters negatively.

If more AHSS could be used, it would be possible to reduce vehicle weight, because AHSS materials may provide longer durability, compared to mild steels or High Strength Steels (HSS). That means; engineers can reduce sheet thicknesses that will effect vehicle weight, fuel consumption and exhaust emissions. In the recent past, developed high strength material used in vehicles and weight reduced about %19 [1].

Even though vehicle design engineers want use more AHSS for parts, high yield strength make hard to work these steels with conventional stamping methods.

Automotive industry needs larger dimensions and more complex shape parts made with AHSS for lower weight and more safer vehicles. For instance, bodyside inner panels of vehicles has large dimensions and deep draw operation. Currently it is not possible to stamp stamp these with high strength steels, neither cold nor hot. Dual phase steels are not used in conventional cold stamping process, because they may crack before the part is fully drawn. Even though hot stamping is an alternative method for Boron materials that has higher strength, the process has restricted part dimensions and typically higher manufacturing cost that increasing the automotive part costs. Studies showed that sheet metal temperature increase in deep draw

operations with AHSS steels up to 150°C even starting to process in room temperature especially in radius points of parts [7] .

In this study; conventional cold stamping system was revised with a cooler based stamping system that is innovative and with the motivation to get more complex parts in draw die with high accuracy. Sheet metal and die parts temperature will not be increasing in draw operation via cooling system design so most of the die surface should have close-to-uniform temperature distribution with very limited scatter.



## 1. CLASSIFICATION OF AUTOMOTIVE STEELS

Steels is the most important material for automotive industry. There are number of applications in a vehicle, such as chassis, engine, wheels and body. That effects directly cost, fuel economy, emission, durability. Also need to possible to recycling for efficiency and environment. Today, steel manufacturer can supply different mechanical and chemical properties steels according to car manufacturers' requirements. Some steels have advantages for especially defined parts so car engineering department have to make steel selection according steel properties [2].

Manufacturing side is also very important for steel selection in design phase. Because some processes like hot stamping is slower than cold stamping so that selection affects cost of vehicle directly. Steels can be classified according to their strength level and yield strength range as; low-strength steels have less than 210MPa yield strength (interstitial-free and mild steels); HSS (carbon-manganese, bake hardenable and high-strength, low-alloy steels) that has yield strength 210-550MPa; and the new Advanced High Strength Steel (AHSS) (dual phase, transformation-induced plasticity, twinning-induced plasticity, ferritic-bainitic, complex phase and martensitic steels) has yield strength greater than 550 MPa [3].

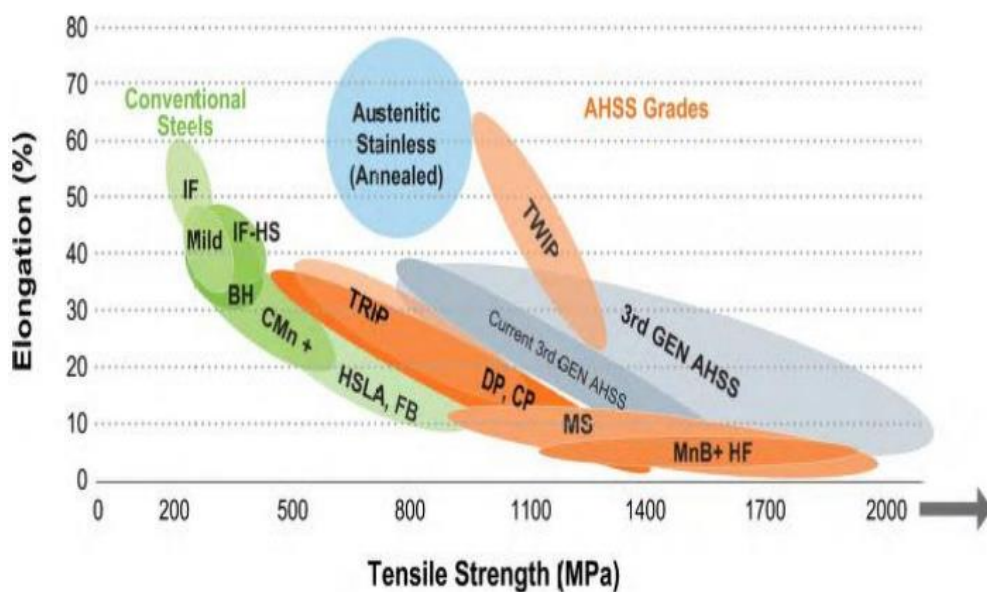


Figure 1. 1.Banana Curve [3]

Mild Steels, Interstitial-Free (IF) Steels (Low Strength and High Strength), Bake Hardenable (BH) Steels, High Strength Low Alloy (HSLA) Steels called as

Conventional Low and High Automotive Steels minimum yield point is 180 MPa and thickness between 0,5mm-1,5mm in automotive applications. These sheet metals can be shaped conventional stamping methods and possible to simulate via Finite Element Method (FEM) simulations [4].

AHSS group occurs from Dual Phase (DP), Complex Phase (CP), Ferritic-Bainitic (FB), Martensitic (MS), Transformation-Induced Plasticity (TRIP), Hot-Formed (HF), and Twinning-Induced Plasticity (TWIP). AHSS steels have important functional performance for automotive parts. If need to energy absorption in the crash zone; DP and TRIP steels preferred by design engineers. AHSS has two or more phases that multiple phase make their strength higher and elongation ability better [3] [4].

Today; AHSS called as 3th generation steel can be used roof outer, door outer, body side outer, package tray, floor panel, hood outer, body side outer, cowl, fender, floor reinforcements, Body side inner, quarter panel inner, rear rails, rear shock reinforcements wanted to used more but just flat parts can be manufactured because of high yield strength. B-Pillar and other complex parts can be manufactured by Hot-Formed (HF) Steel but that is expensive for automotive manufacturer companies. [5]

Figure 1.2 shows that; AHSS using increasing excessively and that helps to understand future better. Finding better shaping methods of AHSS possible to increasing more effort next years.



Figure 1. 2. AHSS Using Increasing for Years [3]

Automotive companies and steel manufacturers try to increase lighter part for vehicles in order to reduce fuel consumption. Especially HSS and AHSS using increasing in Figure 1.3 while comparing 2007 and 2015.

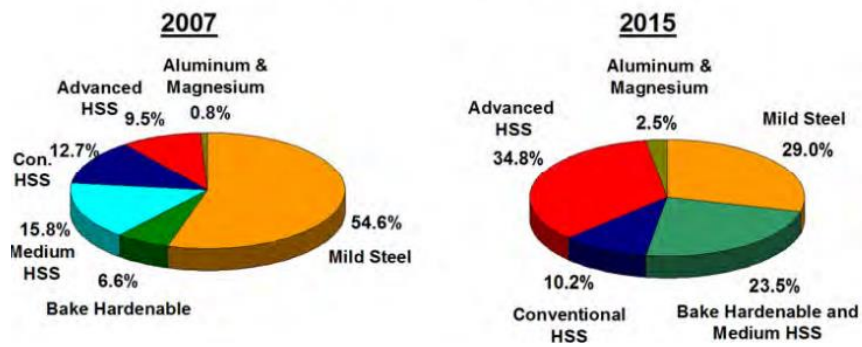


Figure 1. 3 The use of HSS and AHSS from 2007 to 2015 [3]

These graphs give information about future for next generation steels. Lighter and more durable parts market increasing for years.

In HSS, microstructure was ferritic and strengthening mechanisms were: (1) alloying with interstitials or (2) solid solution, (3) bake hardening effect (only valid for bake hardening steels in HSS), (4) carbide-forming and (5) grain refinement [6].



## **2. METAL FORMING PROCESS**

Today, the rapid development of technology leads researchers to intensive research on the use and evaluation of narrow and limited material resources in a more efficient and optimum way. As advancing technology requires us to make more conscious use of existing materials, many new interesting materials are being developed.

Sheet metal forming is of great importance as it finds many application areas today. Since the sheets are very sensitive materials, we need to know the shapeability of the sheets we will shape well and choose the material accordingly. In this project, the shapeability properties of metallic materials by deep drawing method will be examined.

### **2.1. Deep Drawing Operation**

In this study, especially focus on deep drawing operation parameters, so better to explain deep drawing operation. Deep drawing can be defined as a method of obtaining a three-dimensional deep cup from a flat metallic sheet. The most important method used to obtain cylindrical containers from sheet metal is deep drawing. When the depth of the part is greater than its diameter, the process is called deep drawing. Deep drawing processes can be applied one or more times on a part. A single processed part is called Shallow Drawn Part, and a larger number of drawn parts are called Deep Drawn Part. It is applied to various materials such as steel and aluminum. [8]

As can be understood Figure 2. 1 from, good deep drawing requires the wall of the container to be strong, in other words, resistant to thinning, and the collar to be as soft as possible. This is a matter to be considered in terms of material selection. The sheet should be able to flow in its own plane without losing its thickness under the applied force and take the desired three-dimensional shape [9].

Deep drawing is a manufacturing method and help to shape sheet metal according to die form. Today some vessels parts, vehicle body panels such as hood, floor, door, tailgate, sliding doors, airplane components, spoon, etc. can be manufactured by deep draw operation.

Deep draw operation occurred from three different tools. These are die, binder and punch. Die and binder hold the sheet metal parts according to defined force. These forces given by press machine or mechanical org as spring in order to prevent wrinkles during process. After holding whole sheet metal, punch make axial movement to the blank metal and continue movement to die cavity that helps to get same shape of punch and die surfaces. Binder mission just hold to sheet metal parts, so binder forces is important before process starting.

The four steps shows below;

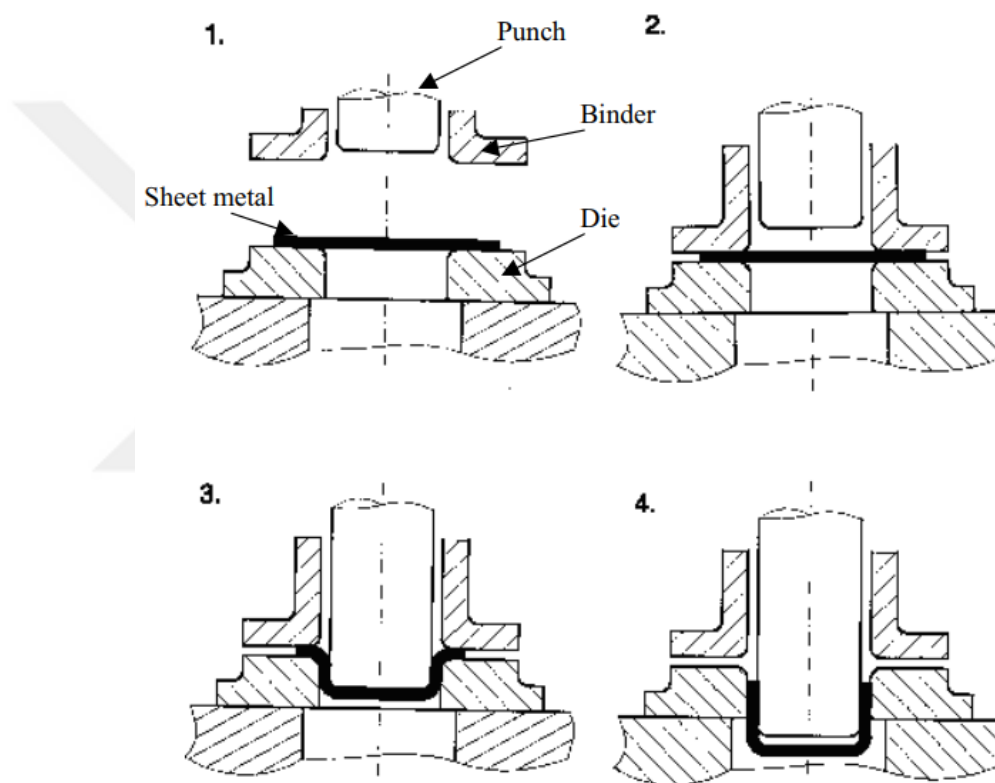


Figure 2. 1. Deep Draw Operation Steps [8]

1. All system is opened position and possible to put sheet metal part (or workpiece) between tools. Binder waiting uplifted position.

2. The binder move to down and hold the sheet metal part, it is mean workpiece not move to anywhere because defined holding pressure applied on the sheet metal part by springs. Punch ready to touch workpiece after step two.

3. The punch contact to sheet metal parts and shaping the parts while continue its movements. Workpiece formed through stretching. Movement distance is important in this step.

4. After to get completed parts step three, punch move to back and formed parts can be receive from die. [8]

Punch and die corners should have specific radii of curvature (RZ and RK) to prevent metal from snagging and tearing. The shaped part should be stripped from the punch after the process. For this, it is seen in Figure 2. 1 that the diameters of the molds expand after a certain depth. The widening of the diameter both reduces the friction surfaces between the mold and the side walls of the part and helps the stripping process. [10]

### 2.1.1.Stripping process

The upper parts of the part, after passing through the narrow zone of the mold, expand a little by the spring back effect. While the punch is withdrawn, the part is stripped from the punch by attaching to the recess where the mold's cross-sectional change is located. In some mold designs, the compression mold also acts as a stripping mold. There is very little space between the punch and the compression die. As the punch is withdrawn, the shaped piece is attached to the lower surface of the compression mold and stripped from the punch. To facilitate the stripping process, a hole is sometimes drilled in the center of the punch, extending to the base. During the stripping process, compressed air is sent to the base of the part through this hole, making the stripping process easier. In some cases, special stripping molds that are activated by a mechanical system are used. Standard die system shown in Figure 2 .2.

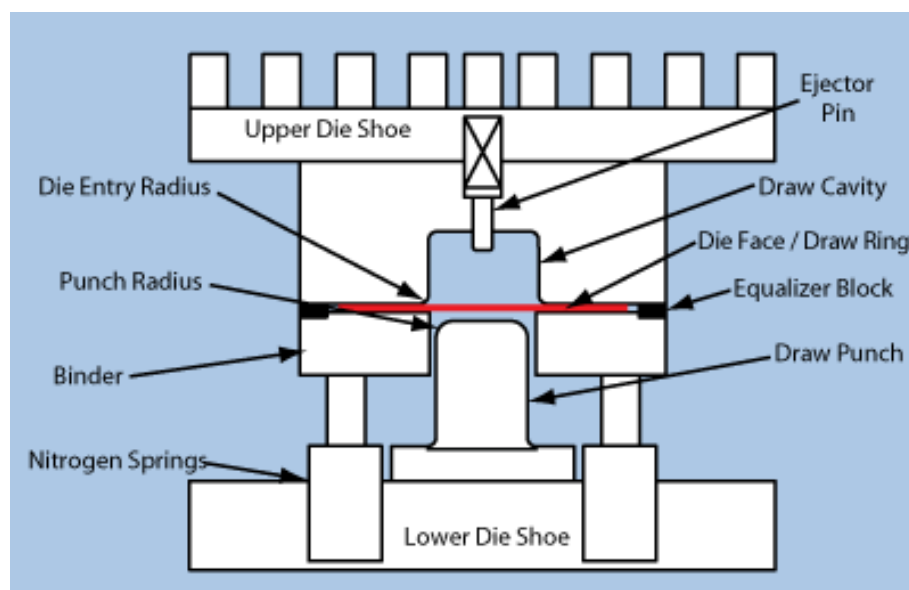


Figure 2. 2.Examples of the Deep Drawing Die [46]

### 2.1.2. Force effect on deep drawing process

There are no big changes in the nominal thickness of the material during deep drawing. As seen in Figure 2.3, the draft with a large diameter is pushed into the mold with a smaller diameter with the help of a punch and shaped.

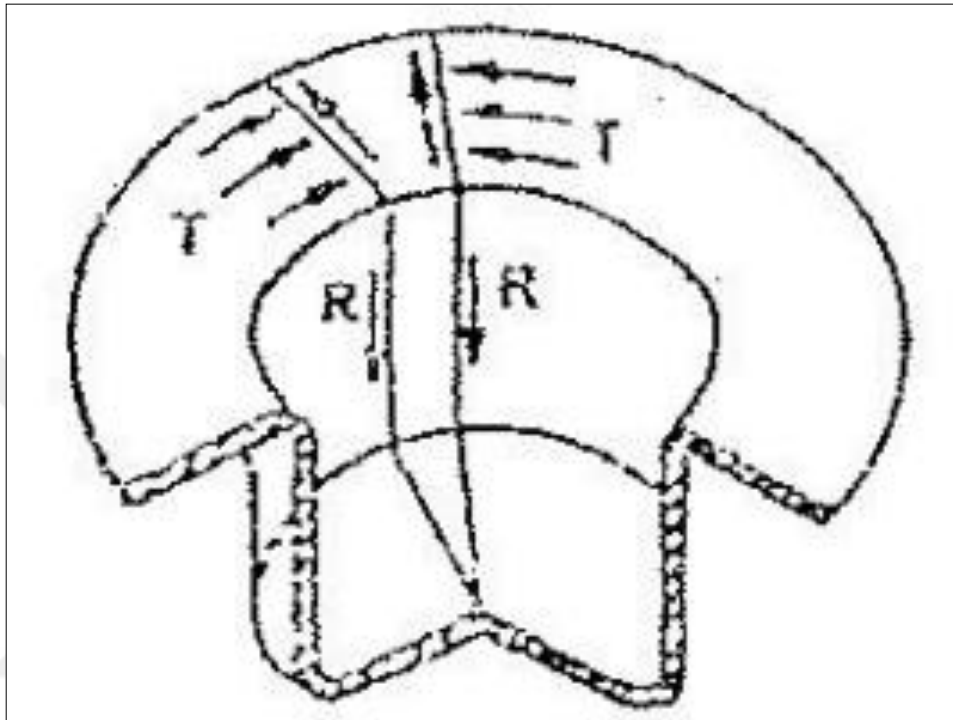


Figure 2.3. Radial Pull and Circumferential Compression Forces [9]

In the deep drawing process, while the material is pulled into the mold by radial pulling forces, peripheral compression forces occur in the region of the draft that has not yet entered the mold.

Environmental compression forces cause the material to shrink and thicken and if no measures are taken, the material wrinkles. Wrinkling is prevented by compressing the parts of the draft that have not yet entered the mold with the help of a suitable mold. Depending on the die geometry, a compression die may not be required if the blank is thick enough.

Except for these limit conditions, pre-compression process should generally be applied to the draft in deep draw in Figure 2.2. The clamping force should be applied in such a way that there should be no wrinkles on the draft circumference or part sidewalls in Figure 2.4.



Figure 2. 4. Drawn Shell Results

In cases where the clamping force is applied too much, the material cannot move between the molds and the thickness decreases rapidly with the effect of radial tensile forces and early damage is observed. In order to prevent this, it is benefited from the initial tables and trials. As the compression pressure, the pressure selected from the auxiliary table and relations is applied according to the material type. Then, the appropriate pressure is determined by the method of test and error.

In deep drawing process,  $d_0 / dz$  is defined as deep drawing ratio (DDR). The main purpose of this shaping method is to obtain the deepest container as possible.

However, the draft diameter cannot be increased unlimitedly in order to increase the depth. The maximum draft diameter to be used is determined by the deep drawing ratio limit (DDRS).

$d_0$  = draft diameter

$dz$  = punch diameter (average product diameter)

$DDRS = d_0 \text{ (max)} / dz$

The maximum value of this limit in ideal conditions is 2.7. It depends on material properties and process conditions in DDRS.

### 2.1.3.Redraw operation

In order to obtain deep cups, it is necessary to repeat the deep drawing process on the same piece. These processes are defined as re-deep drawing operations shown in Figure 2. 5 .

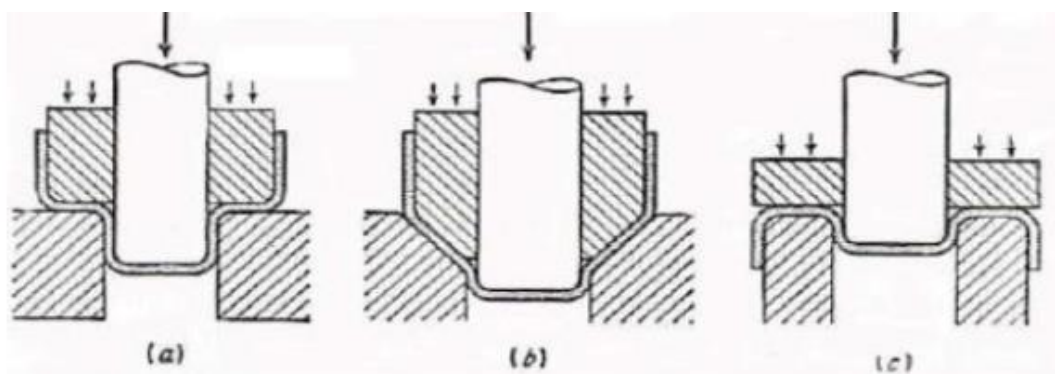


Figure 2. 5.Redraw Operation Examples [11]

In the "direct re-deep drawing" process, the bending and straightening processes are repeated twice and deformation hardening or deformation hardening occurs to a large extent. Mold design can be modified to reduce strain hardening. For example, in the case of (b) in Figure 2. 5, the bending straightening processes are less than the option (a), so the strain hardening is less. In the reverse re-deep drawing process, bending is always in the same direction in Figure 2. 5 c, so the strain hardening is less. If the cold deformed material deformation direction is changed, the material ductility increases. This phenomenon, which is defined as deformation softening or deformation softening, is seen in the reverse deep drawing process. Because of these features, reverse deep drawing is preferred in re-deep drawing processes.

### 2.1.4.Ironing operation

Another method applied to increase the depth of a deep drawn mold is a process called 'Ironing' in Figure 2. 6. In this process, the base thickness of the container remains constant, the depth is increased by thinning the thickness of the side walls. In the ironing process, the force calculation can be approximated by analogy with the wire drawing process.

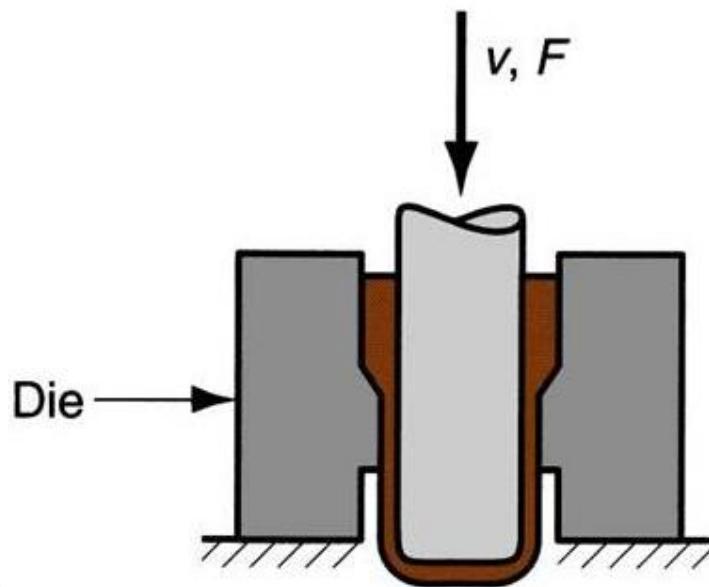


Figure 2. 6.An Example of the Ironing Method

In the deep drawing process, the deformation rate is reduced for each stage. Without the need for intermediate annealing, the material can be deformed by 50-80% of plastic in total. If necessary, intermediate annealing process is applied.

### 2.1.5.Stress conditions during deep drawing

In the deep drawing process, as can be seen in Figure 2 .7, the material is under the effect of different stress and plastic deformation in three separate regions.

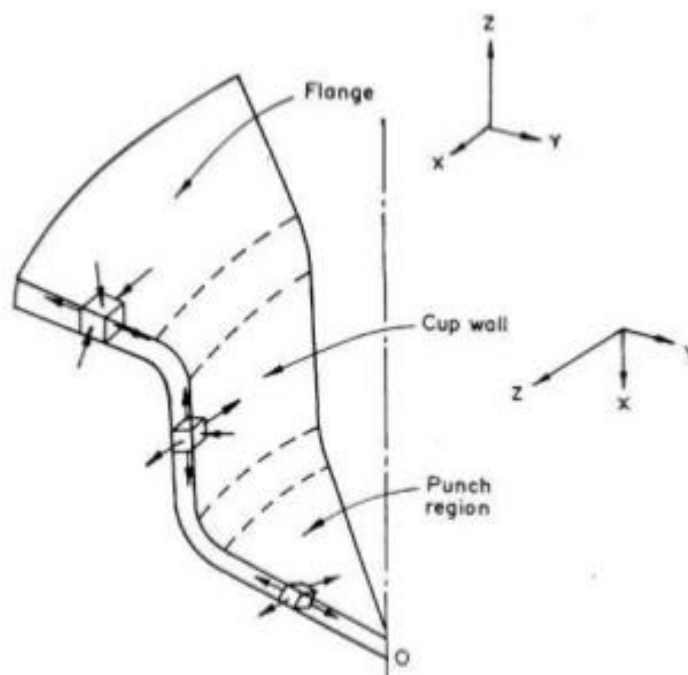


Figure 2. 7.Stress Condition [12]

The central region of the blank, which contacts the bottom of the staple, is bent along the perimeter of the staple towards the top of the staple. The thickness decreases a little in this area due to the bending. There is a biaxial tensile stress at the base of the part due to the action of the punch. The outer periphery of the blank is drawn radially into the mold at the mold entrance. As the material is drawn into the mold, the draft circumference decreases from  $\pi d_0$  to  $\pi d_z$ . Thus, the material is under the effect of compression stresses circumferentially and tensile stresses radially. In addition, the compression mold applies pressure perpendicular to the plane of the draft. As the material is drawn into the mold, its thickness increases due to environmental shrinkage. The material undergoes a bending and straightening process as it passes over the die radius. Meanwhile, its thickness decreases with the effect of radial pulling force. This thickness reduction somewhat compensates for the previous thickness increase. There is only biaxial tensile stress on the sidewall of the part. If the distance between the punch and die is less than the increased thickness of the material, the material will undergo ironing under the effect of pressure. In general, the distance between the die and the punch is kept larger than the material thickness to reduce friction forces and to prevent the die and punch from abrasion. Only in cases where a homogeneous material thickness is desired, the said distance is kept smaller than the material thickness.

### 2.1.6. Thickness change in deep drawn sheet

Thickness changes in different regions in deep drawing process are given in Figure 2 .8. The force applied by the punch is equal to the ideal deformation force, the friction forces and, if any, the forces consumed for the ironing process. The ideal strain force constantly increases throughout the process, as plastic stress will constantly increase due to strain hardening. Most of the friction forces occur on the surface of the compression mold. These force components increase rapidly initially.

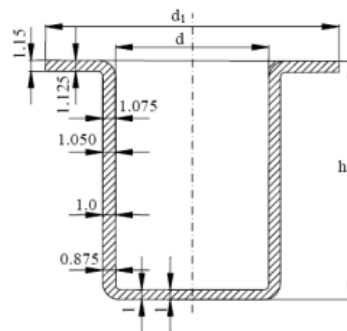


Figure 2. 8.Thickness of Parts



As the process progresses, the friction force decreases as the surface of the draft in contact with the compression die decreases. The ironing starts towards the end of the deep drawing process. The deep drawing force is applied to the base of the part to be produced via the punch. This force is indirectly transmitted to the side walls. The breakage phenomenon usually occurs in the region just above the punch curvature radius. In this region, the material undergoes only the tensile unit deformation without bending or radial tension. The strain in this region is in the form of planar plastic strain and causes thickness to thin. Damage occurs in the form of necking first and then tearing. [13]

### **2.1.7.Effect of material properties**

Thickness of the material has an increasing effect on the shrinkage ratio, as the excess thickness will allow it to thin. The fine grain structure of the material, being single-phase as much as possible and free from non-metallic residues affect the deep drawing capability positively.

The chemical composition has a significant effect on low carbon steels used in deep drawing. In these steels, elements such as P, S, N, Sb, As, Cr, Si act in the direction of reducing the deep drawing ability. It is desirable that carbon should be less than %0.8, manganese %0.35, silicon less than %0.01.

High deformation (strain) hardening base (n) and deformation velocity sensitivity base (m) values have positive effects on deep drawing process, while their efficiency is low.

The most important mechanical property affecting the deep drawing capability is R is the vertical anisotropy coefficient. The vertical anisotropy coefficient depends on the crystallographic structure and crystallographic orientation of the material. Increasing the R coefficient in the volume centered cubic system is achieved by appropriate crystallographic orientation. Proper crystallographic orientation is achieved by controlling the rolling conditions and the resulting soft annealing regime. [10]

### **2.1.8.Effect of mold geometry**

Its most important parameters are the mold curvature radius  $R_k$  and the distance ( $e$ ) between the punch and the die. In the process, the area most susceptible to cracking is the area of the wall near the part close to the base. The stress in this area is directly dependent on the force applied by the punch. [10]

Increasing the  $R_k$  value for certain deep drawing conditions decreases the deep drawing force, thus decreasing the deep drawing rate. However,  $R_k$  cannot be increased unlimitedly. Because, in extreme cases, the area of effect of the compression mold will decrease, and wrinkles and early damage are seen around the draft or on the side walls of the product. According to this:

In steel materials;

$$R = 0.8 [(d_0 + d_z) \cdot t_0]^{(1/2)} \quad (2. 1)$$

In Al and its alloys;

$$R = 0.9 [(d_0 + d_z) \cdot t_0]^{(1/2)} \quad (2. 2)$$

In the second and subsequent deep drawing processes;

$$R = (d_{n-1} - d_n) / 2 \quad (2. 3)$$

$T_0$ : original thickness of the material

$d_n$ : End diameter of the part

$d_{n-1}$ : Diameter of the part in the previous re-deep drawing process

The base edge of the punch should be rounded so that the sheet metal is not damaged by the punch. Increasing the  $R_z$  diameter decreases the deep drawing force and increases the deep drawing rate.

If the base of the part is desired to have a sharp corner or a small radius of curvature, the material is first formed with a punch with a large radius of curvature, then it is brought to the desired dimensions with the appropriate punch. The  $R_z$  value should not exceed 10 times the thickness of the material, otherwise wrinkles will appear on the side walls of the product obtained. Deep drawing and stretching methods are applied together in the forming process of spherical shaped parts. In this case, the measures shown in Figure 2 .9 are taken to prevent the material from wrinkling. [8]

Mold surface should be clean and uniform conditions for all process. That means; if oil accumulate in one surface or hardness are different in different locations of die, that effect negatively to part accuracy in drawing operation.

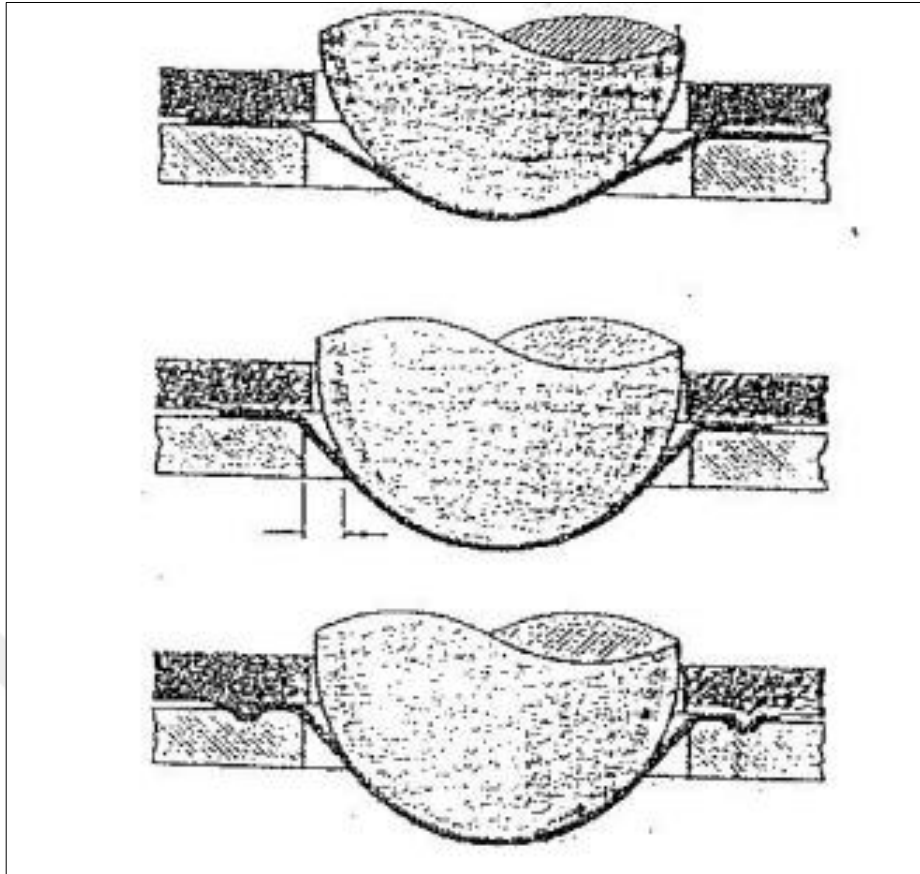


Figure 2. 9.Examples of the Shaping Process of a Spherical Part [11]

The material is prevented from moving by squeezing thoroughly along the circumference as seen in the top figure. In the meantime, the thickness is thinned by 10-15% by stretching and the part is preformed. Then, as the punch advances, the compression force should decrease and the material should be allowed to move into the mold, as shown in the middle figure. However, in this case, the material will be freed in the area indicated by the arrows and it may wrinkle. To prevent wrinkling, the material should be stretched well while moving into the mold. In this stretching process, changes are made in the molds, allowing the material to enter the mold in a controlled manner by making certain curves. [10]

### 2.1.9.Effect of processing conditions

As stated earlier, proper selection of compression pressure is an important factor in successfully continuing deep drawing. Meanwhile, lubricating some parts of the draft with a suitable oil will significantly reduce the friction forces, preventing early damage and increasing the deep drawing ratio. Only the surfaces of the draft in contact with the compression die and the forming die should be oiled. [10]

Lubrication of the surface of the staple in contact with the base will have a negative effect. The formation of friction force between the material and the punch surface in the base area of the punch increases the deep drawing capability. Only the surfaces of the draft in contact with the compression die and the forming die should be oiled. Lubrication of the surface in contact with the base of the staple will have a negative effect. It has a negative effect if the staple base is oiled. If the staple base is oiled, the force applied by the staple to the base of the part is transmitted to the side walls of the part. In this case, premature damage may occur on the side wall of the part. The formation of friction forces between the material and the punch surface in the base area of the punch has a positive effect on the deep drawing capability. [8]

Because the force applied by the punch to the base of the part is partially transmitted back to the punch with the effect of friction. In order to increase the friction between the inner surface of the part in the base region and the punch surface, the punch surface is roughened to be harmless.

In cold forming processes, brittleness can be created by increasing the temperature of the material to around 80 ° C with the effect of friction forces. For this reason, it is necessary to take cooling measures that can keep the process at room temperature continuously.

The hydrostatic pressure forces applied to the base of the part to be produced during the deep drawing process will delay the cracking event in the material and thus positively affects the deep drawing capability. Hydrostatic pressure forces can be applied with the help of a rubber block to be placed on the mold base or a rubber diaphragm filled with liquid during the process.

## **2.2. Material Behavior in Metal Forming**

Stress-strain curve considerable point for metal behavior during deep draw process. Stress-strain curves occurs from two important area as elastic region and plastic region. Plastic region is more important for deep draw forming operation. Figure 2 .10 that example stress-stain curves that occurs from elastic and plastic region. [8]

This section especially important for draw operation because during process, should be access to yield stress.

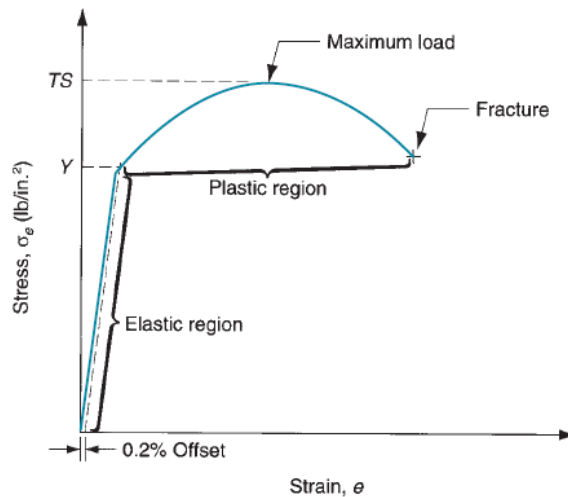


Figure 2. 10.Stress-Strain Plot [9]

The typical stress–strain relationship for a metal exhibits elasticity below the yield point and strain hardening above it. In the plastic region, the metal’s behavior is expressed by the flow curve:

Below the plastic region shows the elastic area and boundary is yield point in stress-strain curve and above of the plastic region is hardening area. Flow curve is significant term that is about material behavior:

$$\sigma = K \epsilon^n \quad (2. 4)$$

where K= the strength coefficient, MPa (lb/in<sup>2</sup>); and n is the strain-hardening exponent. The stress s and strain e in the flow curve are true stress and true strain. Flow curve show information about material plastic behavior in cold deep drawing or other process. K and n values listed in Table 2 .1 below [8].

Table 2. 1.Strength Coefficient and Strain Hardening Exponent(6)

Material	Strength Coefficient, <i>K</i>		Strain Hardening Exponent, <i>n</i>
	MPa	lb/in <sup>2</sup>	
Aluminum, pure, annealed	175	25,000	0.20
Aluminum alloy, annealed <sup>a</sup>	240	35,000	0.15
Aluminum alloy, heat treated	400	60,000	0.10
Copper, pure, annealed	300	45,000	0.50
Copper alloy: brass <sup>a</sup>	700	100,000	0.35
Steel, low C, annealed <sup>a</sup>	500	75,000	0.25
Steel, high C, annealed <sup>a</sup>	850	125,000	0.15
Steel, alloy, annealed <sup>a</sup>	700	100,000	0.15
Steel, stainless, austenitic, annealed	1200	175,000	0.40

Strain hardening occurs in deep draw operation for materials that seen in lower temperatures. In that case; elasticity decreases and the hardness increases. While

trying to change material shape; crystals moving faster and materials produce against force that is resistance to deformation and called strain hardening in cold working. Strain hardening can be reduced with high temperature process but that changed part shape negatively so not always prepared.

Sometimes strain hardening requires by part designers because hardened surface will be necessary for parts. Today all FEM simulation softwares can calculate the strain hardening effects to parts. Strain hardening increases the tensile strength and hardness of metal parts and ductility is reduced. [11]

### **2.3. Temperature in Metal Forming**

In cold working forming operation; flow curve has important role in plastic deformation.  $K$  and  $n$  values depend on temperature so that shows that; changed temperature helps to get different yield strength and tensile strength value of materials. Strength and strain hardening reduces at higher temperatures. While increasing temperature during forming operation; need lower forces. However ductility is increased higher temperatures. Three different temperature forming method implanted as cold, warm and hot working. [8]

Cold working meaning forming sheet metal at room temperature. Cold working advantages like below;

- Better accuracy, better tolerances
- Part surface obtained clear
- Higher strength due to strain hardening
- Cheap operation

Because of these results, cold forming using mass production so much and manufacturer desires to change hot forming process to cold forming process especially because of cheaper. Cold forming disadvantage point is that need greater forces while forming sheet metals. Because of that, today engineers try to reduce forming forces because that increase also sheet metal temperature during forming [8] [11].

Warm working is process between hot forming and cold forming operations. This process implemented above the room temperature however below the recrystallization temperature. Often  $0,3T_m$ , that is melting point heating of material

implemented in this process. That helps to reduce forming forces but increase manufacturing cost by heating process. [8]

Hot working have important role in stamping world because today lots of durability safety zone parts such as B-pillar, dash pillar or reinforcement parts manufactured by this method. This process make material softer by heating before forming the parts between  $0,5T_m$  and  $0,75T_m$ . While increasing forming temperature, the strain hardening exponent is zero and ductility of the material increased. The advantages given as below;

- Material shape will be changed by temperature effect
- Required press forces can be decreased
- Metals fracture level is lower than cold working parts
- Material mechanical properties isotropic

Above advantages shows powerful hot forming workings but that have some disadvantages points like below;

- Dimensional tolerances must be higher
- Energy requirements are bigger because of heating process
- Surface oxidation is not preferred
- Surface quality is not good
- Tool life is shorter
- Longer manufacturing time
- Higher manufacturing and investment costs

These parts cost increase the vehicle prices directly, so especially automotive manufacturer companies prefer to get parts by cold working if possible. [8]

#### **2.4.Other Sheet Metal Process**

Forming processes are processes that cause significant shape changes in metal parts whose initial shape is mass rather than sheet metal. Starting shapes include cylindrical bars and logs, rectangular logs and slabs, and similar geometries.

Forming operations work in the form of giving enough tension to the metal to take the desired shape. Sheet metal forming processes require in-plane tensile forces

and lower forces than mass forming. The tensile strength of the material is very important in deciding which forming process is appropriate.

Sheet metal is generally anisotropic. Their properties change with direction and direction. The majority of defects that occur while shaping are caused by thinning or tearing. Unit strain analysis is performed when deciding on the most appropriate direction for shaping. When pressure is applied to a fluid, pressure is transmitted exactly to every point of the fluid. In hydraulic systems, different forces are transmitted by using pistons with different surface areas. Thus, the desired force can be obtained by changing the surface areas to which the fluid is transmitted [8].

Sheet metal operations involve cutting and forming relatively thin sheets. Typical sheet metal thicknesses are between 0.4 mm and 0.6 mm. Even though the thickness exceeds 6 mm, the term plate is used instead of sheet metal. Sheet and plate stocks used in sheet metal processes are produced by straight rolling. The most commonly used sheet metal is low carbon steel (Typically 0.006% - 0.15% C) [9].

Sheet metal processing is usually done at room temperature (cold working). There are exceptions where the material is thick, brittle and high deformation is required. Many sheet metal processes are carried out on machines called presses. The term sheet pressing is used to distinguish extrusion and forging processes. Sets of sheet metal processes are called punches and dies. In addition, the name sheet press mold is also used [8].

Sheet metal processes are divided into 3 basic categories: deep drawing, cutting, bending. Drawing operation explained above. Cutting; It is used for cutting large sheet material into small pieces, perimeter cutting of part and drilling holes. Bending allow to bring the sheet metal to the desired shape [14].

#### **2.4.1.Cutting in metals**

The cutting process of sheet metal is shearing between two edges. The cutting movement is realized in four stages by moving towards the fixed edge as shown in Figure 2. 12. First, the punch presses against the surface to be cut and creates plastic deformation on the surface of the sheet. The punch continues its downward movement and enters the sheet metal and divides the metal into two parts. The thickness at which the punch penetrates the sheet is usually one third of the



thickness of the sheet. The punch continues to move into the sheet metal and a break occurs between the two cutting edges. If the gap between the punch and the die is at appropriate values, the two breaking lines match each other and a clean cut is obtained [8].

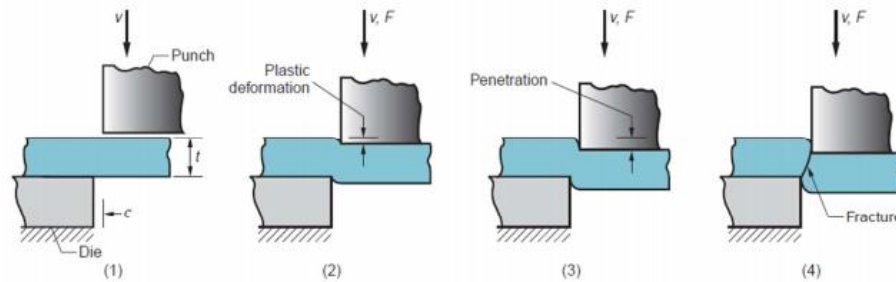


Figure 2. 11. Sheet Metal Cutting Operation [8]

Process parameters in sheet metal cutting; the gap between the punch and die is the sheet thickness, material type, strength and cutting length. Let's define these parameters and their relationship to each other [12] [8].

Space in cutting process; It is the distance between the punch and die as shown in Figure 2 .12. If there is an unsuitable gap, a faulty product may occur. If the gap is too small, the lines of break tend to cross each other. This situation causes double-sided glossy surface formation and high cutting force. If the gap is too big; metal gets stuck at the cutting edges and causes very high burr. The optimal clearance depends on the type of sheet metal. The recommended gap in the literature is obtained by the formula given below [8].

$$c = A_c t \quad (2. 5)$$

In the equation,  $c$  is the space in mm, and  $A_c$  is the allowable space,  $t$  is the sheet thickness in mm. The permissible gap is determined according to the type of material. The permissible gap values are given in Table 2. 2.

Table 2. 2. Cutting Space Defined for Three Different Metal Type

Metal Type	$A_c$
1100S and 505S aluminum alloys, all tempers	0.045
2024ST and 6061ST aluminum alloys; brass, all tempers	0.060
Cooled-rolled steel, half hard; stainless steel, half-hard and full hard	0.075

The total resistance of the piece against the separation of the strip material during the molding is called the shear force. It is important to anticipate the cutting force that will be needed. The shear force in sheet metal processes is calculated by the following formulas.

$$F=StL \quad (2. 6)$$

S defines sharing resistance of metal, t is thickness and L is length of metal. Sharing resistance occurred by material tensile strength. That is about 0,7 times smaller than material tensile strength. In that case formula can changed as below;

$$F=0.7TStL \quad (2. 7)$$

Each material has different tensile strength value.

Cutting can be done in different ways;

- a. Part cutting: It is the process of cutting the part in the desired shape along a closed line.
- b. Straight cutting: It is the process of cutting the part in the desired shape along a non-closed line.
- c. Splitting: It is the process of partially separating the device.
- d. Hole cutting: It is the process of cutting the part of the desired shape and size and dropping it from the material strip.
- e. Final cut: It is the process of cutting the part in the opposite direction of the cut. In this way, cutting edges are sharper and cutting surfaces are smoother.
- f. Difference cutting: Discarding the edge that occurs when drawing or bending (removing the difference piece).
- g. Burr cutting: It is the process of debarring the pressed or cast parts.
- h. Inlay: The tool is torn with a properly shaped punch, the piece is not cut and dropped.

Cutting operation called as trimming operation in some literature. Today even companies try to implement all trim operation in one operation in order to complete all operation efficiency, that is not easy method for all operation.

Especially Aluminum operation, sheet metal deformation seen in edges if wanted to cut all operation in one process and that is effect the panel quality.

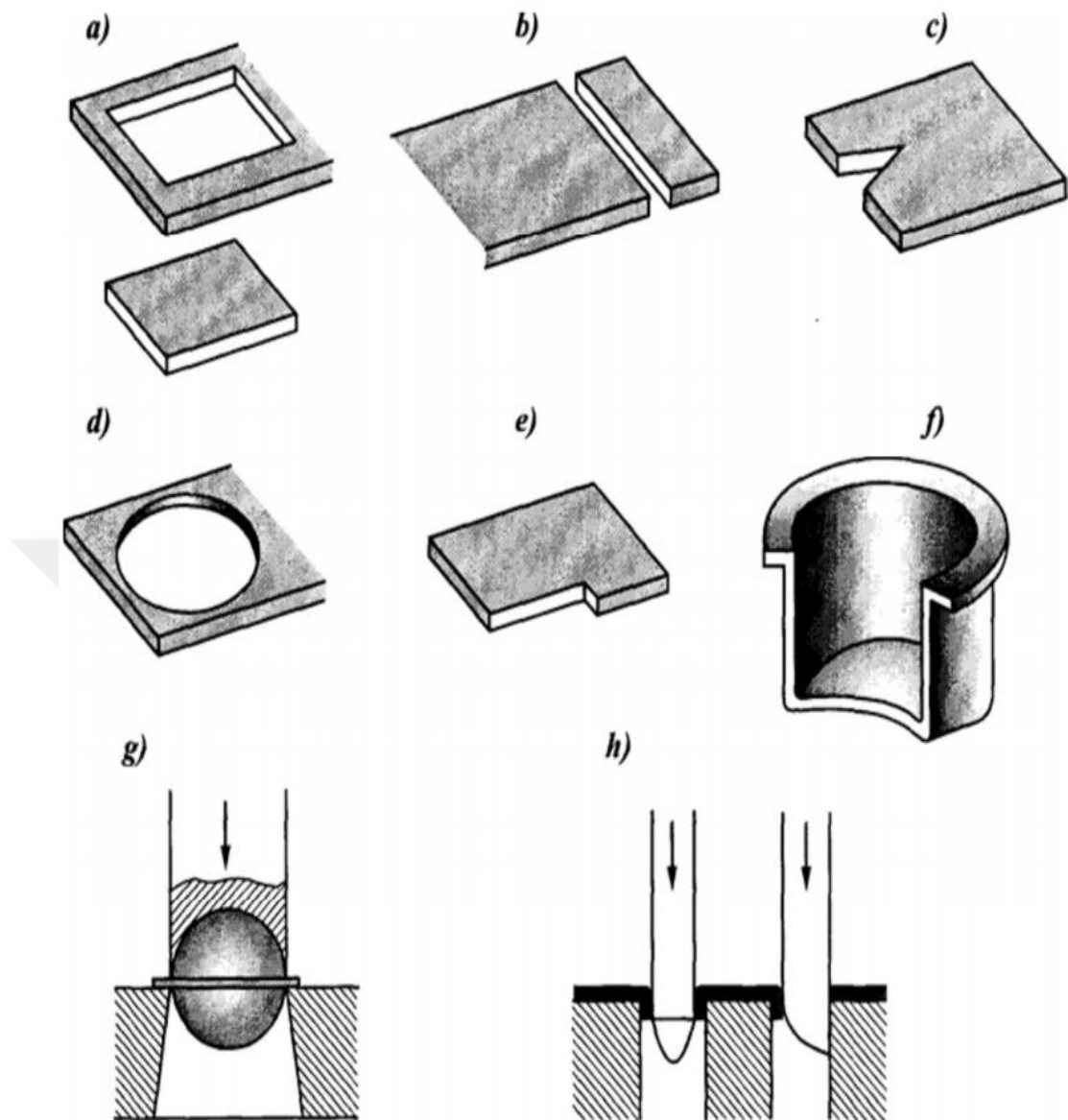


Figure 2. 12.Cutting Operations [11]

#### 2.4.2.Piercing operation

Piercing operation occurs from steps, the first step called as Plastic Deformation and the second one is Sinking, third step of operation is Cutting Step.

##### a.Plastic Deformation

When the material is placed on the die and the press head is first activated, the punch comes into contact with the material and creates a pressure effect on the material. Plastic deformation occurs when the elasticity limit of the material is exceeded. First step showed in Figure 2.13.

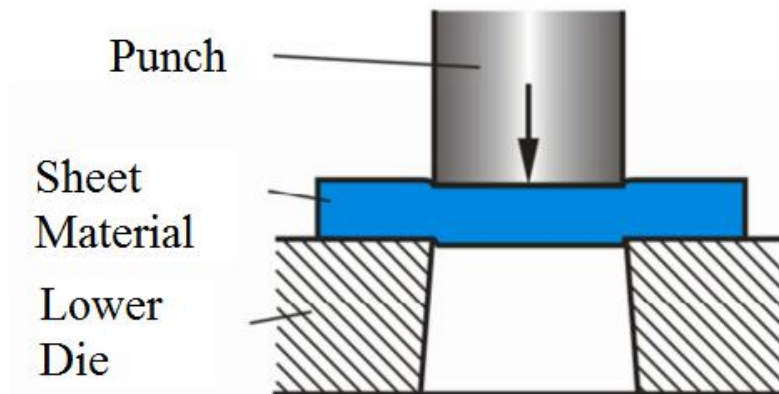


Figure 2. 13. Plastic Deformation [8]

b. Sinking

While the driving force of the press head continues, the punch forces the material to pile up shown in Figure 2.13 and Figure 2.14. The desired shape material is pushed into the mold cavity. At this stage, the actual shearing (slip cutting) event occurs.

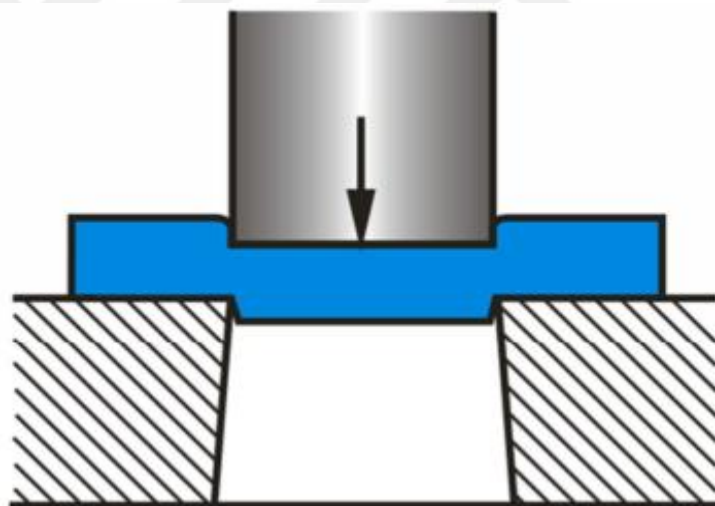


Figure 2. 14. Beginning of Cutting Process [8]

c. Cutting

Continued punch pressure causes material breakage to begin at die and punch cutter blades. These are the points where the greatest stress concentrations occur. Under normal cutting conditions, the fractures extend towards each other and meet. When this happens, the breaking is completed and the material is cut from the material strip as desired. The formation of cutting is shown in Figure 2.15.

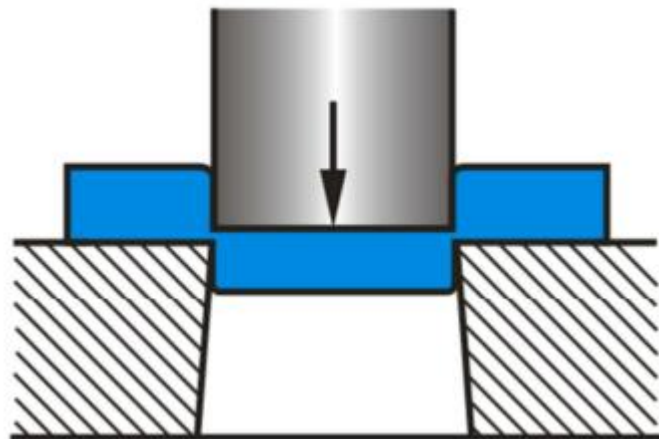


Figure 2. 15.Cutting Progress [8]

Parts cut (molded) from strip materials cannot be cut exactly between the female die and punch. The part to be cut from strip material between the female die and punch shows maximum shear resistance between the two cutting edges. At the same time, the punch sinks into the material a little and cuts until the material reaches the flow limit. After the maximum resistance, the material loses its strength and starts to flow. When it exceeds the flow limit, the part breaks. It is seen that a tension stress occurs on the upper surface of the strip material and the lower surface of the molded part, and a compression stress on the punch touch surface of the molded part. That is shown in Figure 2.16.

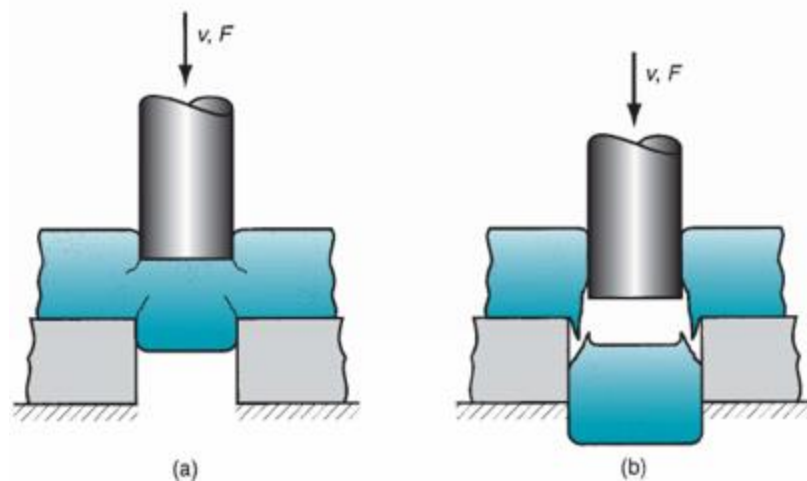


Figure 2. 16.Cutting Deformations [8]

When a circular hole is made in the sheet metal, the outer size of the part removed from the sheet will be larger than the hole size due to the geometry of the sheared edges shown in Figure 2.17. Thus, the punch and die dimensions of a round sheet metal workpiece with a diameter of  $D_b$  are as follows.

$$\text{Punch diameter of sheet workpiece} = D_b - 2c \quad (2.8)$$

$$\text{Die diameter of sheet workpiece} = D_b \quad (2.9)$$

For a round hole with diameter  $D_h$ , the punch and die dimensions can be determined as follows.

$$\text{Hole punch diameter} = D_h \quad (2.10)$$

$$\text{Hole die diameter} = D_h + 2c \quad (2.11)$$

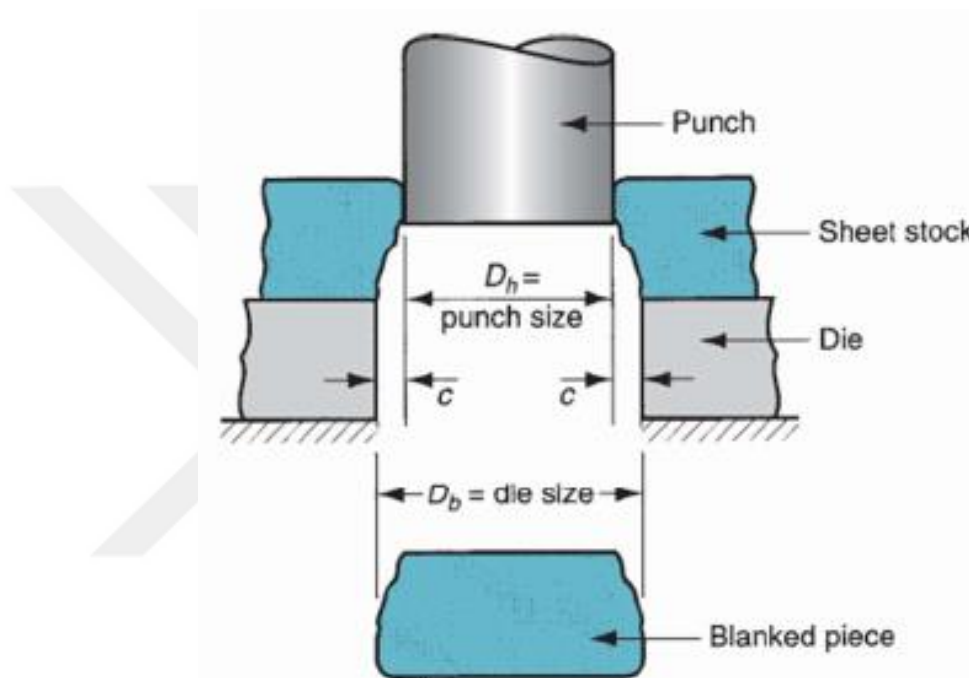


Figure 2. 17.After Cutting Operation [8]

The angular gap on both sides of the die cavity must be from  $0.25^\circ$  to  $1.5^\circ$  in order for the sheet metal workpiece or scrap to come out of the mold easily.

#### 2.4.3.Bending operation for sheet metals

Bending is the plastic deformation of metal that occurs around a linear axis with little or no change in surface area. The bending process is carried out with punch and die sets. The punch and die should have proper alignment and clearance. It is defined as the bending process around a straight axis (neutral axis) as shown in Figure 2. 18a. During bending, compression occurs in the area below the neutral axis, and in the region above the neutral axis. These strain cases can be seen in Figure 2. 18.

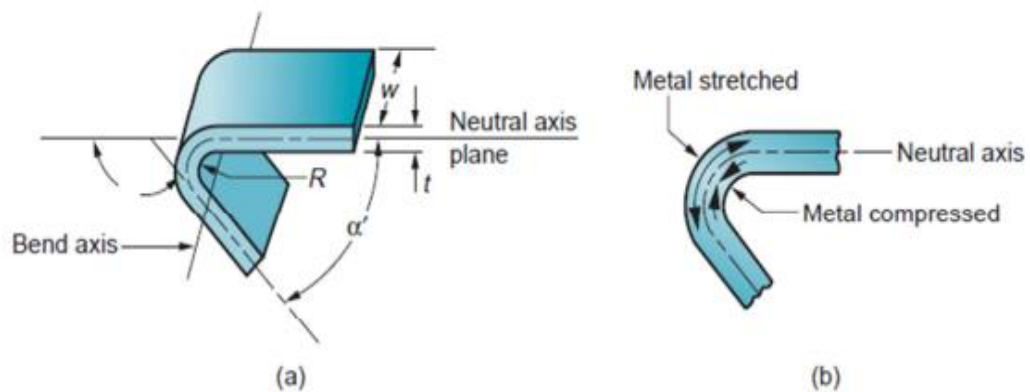


Figure 2. 18. Tensile and Compression Elongation in Metal During Bending[8]

The following factors are important in defining the bending process:

- The smallest bending diameter that can be given without breaking the metal should be determined.
- Metal softness should be known.
- The thickness of the material should be determined.

The dimensions of the part to be bent should be decided in order to obtain a bend with the desired precision. Because the bent metals get thinner.

Bending Dies has important role in sheet metal area. The process of forming the material along an axis with or without the aid of heat is called bending, and the molds that perform this process are called bending molds. In the bending process, a part of the material passes in a different direction either by keeping its cross-section as much as possible or by changing it slightly. The force applied in the bending process should be greater than the resistance of the material, but smaller than the resistance shown by the mold. The changes in the cross section of the bent material generally depend on:

- a. The quality of the material
- b. The thickness of the material
- c. The bending angle
- d. The bending radius
- e. The bending force

#### 2.4.4. Bending in V die

Sheet metal is bent between the V shaped die and the punch shown in Figure 2. 19. With the V die, both very narrow and very wide bending angles can be obtained. V-die bending is generally used for low-number production. Molds are relatively cheap and simple.

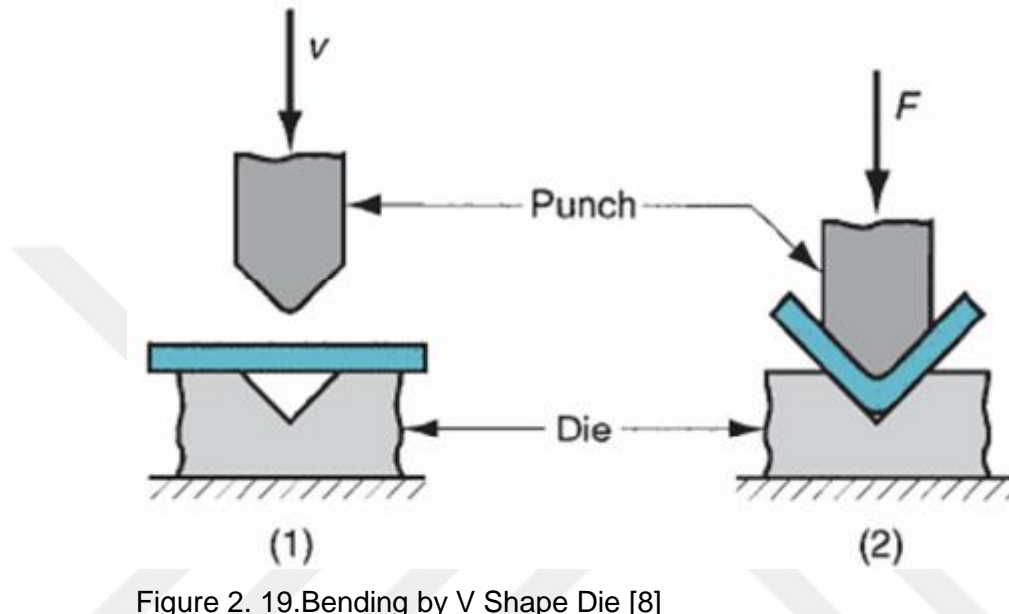


Figure 2. 19. Bending by V Shape Die [8]

Metal thickness  $t$  in sheet metal bending; It is bent at the angle called the bending angle. This angle is calculated as  $\alpha'$  in sheet metal parts, where  $\alpha' + \alpha = 180^\circ$ . The bending radius is normally specified from the inside of the part as opposed to the neutral axis. This value is determined from the radius of the tool required to perform the operation. Bending is usually done in the width  $w$  of the workpiece.

#### Bending Back (Springback)

After the shaping process, when the bending pressure is removed, the elastic energy remaining in the bent part tries to bring the part to its original position. This elastic recovery process is called spring-back (springing). Its effect shows in Figure 2. 20. It is defined as the increase in the angle of the bent piece when the forming tool is lifted. It can be expressed by the formula below;

$$SB = \frac{(\alpha' + \alpha't)}{\alpha't} \quad (2. 12)$$

Equality SB; spring-back,  $\alpha'$  is the angle of the sheet metal part in degrees,  $\alpha't$  is the tool angle in degrees. The amount of springback increases with increasing elasticity



modulus  $E$  and yield strength  $Y$ . Excessive bending or excessive load is applied to remove spring-back. In excessive bending, the punch angle and radius are made slightly smaller than the desired angle. With this process, the desired length of the sheet comes after the spring back. In the compensation process performed by applying excessive load, the piece is compressed at the end of each process. Thus, plastic deformation occurs in the compressed area. [10] [8]

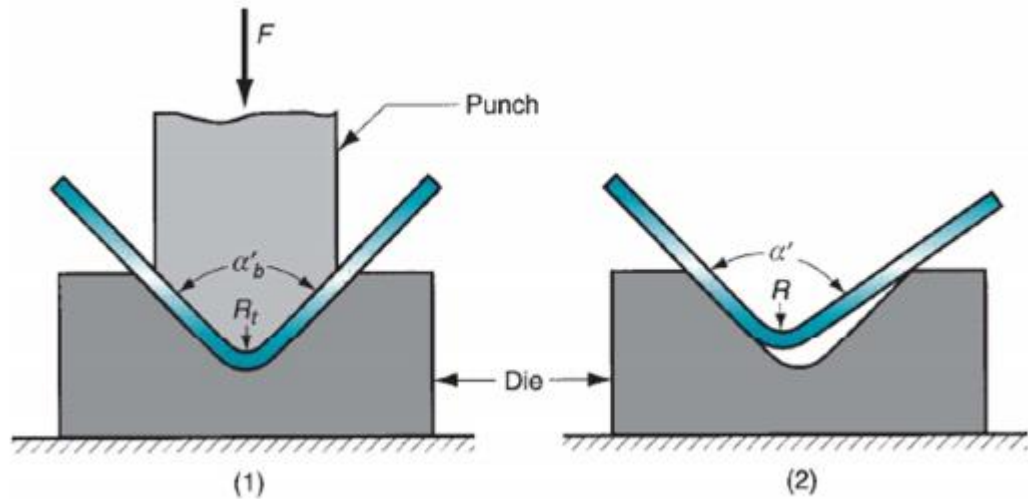


Figure 2. 20.Springback Condition in Bending Operation [8]

Bending force calculation is important before start to define die force sources. The force required for bending to occur; The geometry of the punch and die depends on the strength, thickness and length of the sheet. Bending force is found with the following formula [8].

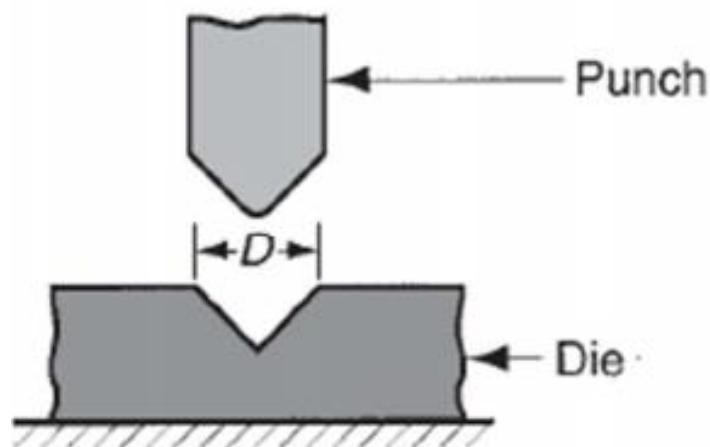


Figure 2. 21.Die Neck Length

Equation F; Bending force in N, TS; The tensile strength of sheet metal in MPa, w; The width of the sheet in the direction of the bending axis in mm, t; sheet thickness in mm and D; It is the mold opening length shown in Figure 2 .21 as mm. Kbf is a fixed value and  $K_{bf} = 1.33$  for V mold. [8]

## **2.5. Sheet Metal Properties for Forming Process**

Cutting, bending, drawing, etc. The first condition to be sought in sheets to be selected for chipless forming processes should be compliance with the anticipated pressing process. Undesirable situations such as cracking, tearing, rupture should not occur during pressing on the selected material. In addition, the shapes of the parts intended for pressing should be determined in accordance with the pressing method chosen. The type of steel sheet to be selected for the parts to be produced by the "cutting" method in pressing is of little importance. These materials must be suitable for surface treatments after manufacturing [15].

The sheet metal to be selected is of great importance for the parts to be produced by methods such as bending-drawing-plastering. Because the shape change is in question in this manufacturing method, the material should be able to enter without cracking, tearing, rupture if the operation method suitable for the anticipated form is selected [15].

Pressed sheets are manufactured from soft non-alloy steels by hot or cold rolling method according to their intended use. The sheets under 2 (mm) used in press works are manufactured by cold rolling method. The scales formed on the surface after the processing of hot rolled sheets are removed with acid and then released to the market. The choice between hot or cold rolled sheets is more of a problem of obtaining the desired thickness of material rather than a quality preference. It is difficult to obtain thick sheets as cold and thin sheets as hot rolled. In medium-thick sheets, the surface condition of the part to be produced will be a factor determining the preference, if the surface condition is not important, hot rolled sheets can be preferred because they will be cheaper. Cold rolled sheets are superior to hot rolled sheets in terms of precision in dimensional tolerances. [9]

Important parameters such as safety, fuel saving, environmentalism, predictability, durability and quality in the automotive sector are effective in starting the work on material selection. In the automotive sector where competition takes place in line with these parameters, Advanced High Strength Steel (AHSS) containing different

qualities is widely used. While high strength (HS) steel generally has a ferritic microstructure; Thanks to its more complex microstructure, AHS steel has come to the fore in terms of high strength and ductility properties. In addition, its high shaping ability provides great convenience in automobile production. Steel qualities used in automobile construction are shown in Figure 2. 22.[5]

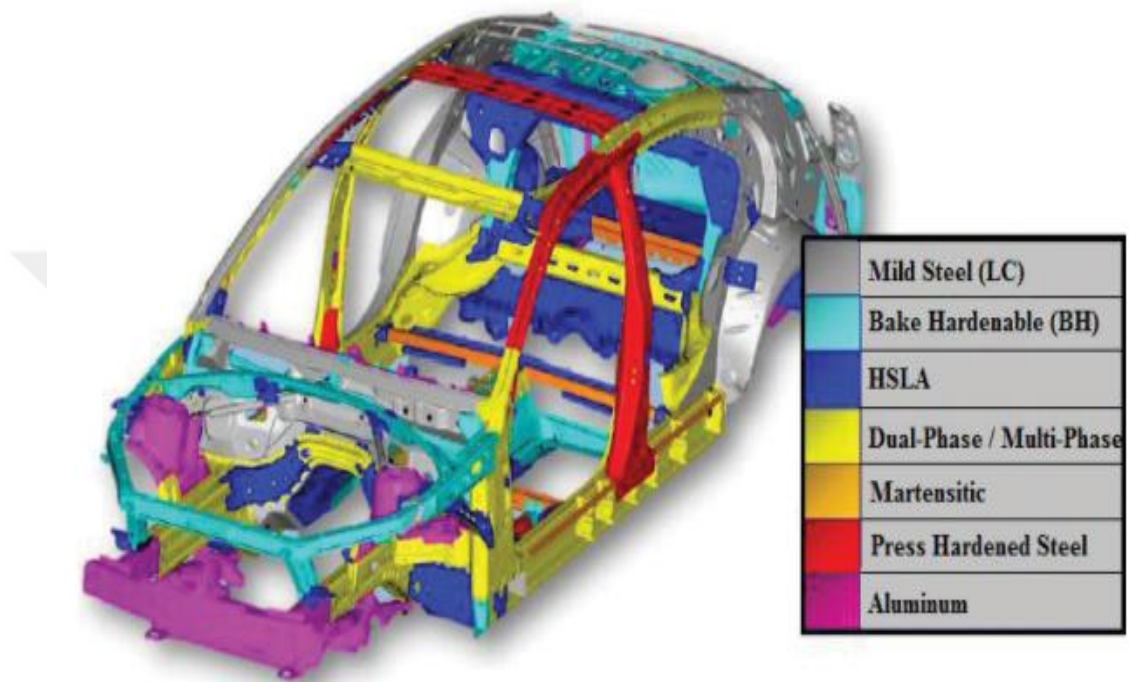


Figure 2. 22. Steel Type for Cars [3]

Steel grades used in the automobile industry are generally divided into three basic categories depending on the material microstructure. The first category, low-carbon (C ratio 0.13% and lower), high strength (HS) steels are the backbone of automotive steel grades. The second category is the development of HS steels, which is known as the first generation of AHS steels. The third category consists of the second generation of AHS steels. Although these three categories contain different steel classes from each other, they have common physical and metallurgical properties. Automotive steel types are shown in Table 2 .3. In addition to metallurgical comparison, these steel grades are also classified according to their strength. Figure 1.1 shows the steel qualities used in the automotive industry according to their strength. [3] [5] [12]

These materials changing for years according to customer requirements, cost and safety factors.

Table 2. 3. Steel Types in Automotive Industry

<b>Low Carbon HS Steels</b>
Low Carbon (LC) Steels
Bake Hardenable (BH) Steels
Interstitial-Free (IF) Steels
High-Strength Low-Alloy (HSLA) Steels
<b>First Generation AHS Steels</b>
The AHSS family includes Dual Phase (DP)
Complex-Phase (CP)
Ferritic-Bainitic (FB)
Martensitic (MS)
<b>Second Generation AHS Steels</b>
Twinning-Induced Plasticity (TWIP)

### 2.5.1. Low carbon HS steel grades

Low-carbon (LC) steels and extra-low-carbon (ELC) steels were initially developed due to their low cost and easy shaping properties. LC steel with large polygonal ferritic grain microstructure is formed as a result of the heat treatment cycle. LC steel is used in many automotive parts, from small parts to large deep drawn parts. Thanks to its low carbon content, it is also suitable for use in common automotive welding technology. However, due to its low yield strength, its impact resistance is low and therefore its use is limited. In order to eliminate this problem, furnace hardenable (BH) steels have been developed. Low carbon steel grades used in cold forming are given in Table 2.4. [1] [3] [12]

Table 2. 4. Low Carbon Steels Properties [17]

Steel grade	C % by mass max.	0.2% Yield point [MPa]	Tensile strength [MPa]	Fracture elongation [%] min.	Vertical anisotropy r min.	Work hardening exponent n min.	Zinc coating group
DX51D	0.18	-	270-500	22	-	-	Z 70 - Z 600
DX52D	0.12	140-300	270-420	26	-	-	Z 70 - Z 600
DX53D	0.12	140-260	270-380	30	-	-	Z 70 - Z 600
DX54D	0.12	120-220	260-350	36	1.6	0.18	Z 70 - Z 275
DX56D	0.12	120-180	260-350	39	1.9	0.21	Z 70 - Z 275
DX57D	0.12	120-170	260-350	41	2.1	0.22	Z 70 - Z 275

### 2.5.2. Bake hardenable (BH) steels

Bake hardenable steels have a basic ferritic structure and are formed as a result of solid solution hardening. In this process, which is based on the deformation aging mechanism, the steel is first given shape (pre-stressing); then the steel is painted

and the painted steel is heat treated. Thus, an increase in yield strength is achieved thanks to the cooking in the oven. During the formation of these steels, when carbon is preserved in solution and given to the furnace in painted form or kept at room temperature for a few weeks, carbon is discharged from the solution. Thanks to this step, the yield strength is increased in order to increase the impact resistance without decreasing the ductility. BH steel is widely used in automobile exterior panels where the creep resistance must be high. The BH mechanism realized as a result of uniaxial stretching after pre-stressing is given. In galvanized BH steel, the increase in strength is provided at a higher rate and the shaping ability of this material is higher. For this purpose, it is widely used in body in white (BIW) in automobile construction. BH steel grades are given in Table 2 .5. [1] [3] [5]

Table 2. 5.Bake Hardenable Steel Types [17]

Steel grade	Mn % by mass max.	0.2% Yield point [MPa]	Tensile strength [MPa]	Fracture elongation [%] min.	Vertical anisotropy r min.	Work hardening exponent n min.	Bake- hardening value BH <sub>2</sub> [MPa] min.	Zinc coating group
HX180BD	0.7	180-240	290-360	34	1.5	0.16	35	Z 70 - Z 200
HX220BD	0.7	220-280	320-400	32	1.2	0.15	35	Z 70 - Z 200
HX260BD	0.8	260-320	360-440	28	-	-	35	Z 70 - Z 200
HX300BD	0.8	300-360	400-480	26	-	-	35	Z 70 - Z 200

### 2.5.3.Steels that do not contain intermediate atoms (IF)

These steels have a microstructure lacking the N and C spacer atoms. In order to keep the spacer atoms constant, alloying elements such as Nb and Ti are added. The high ductility of IF steel is ensured by the lack of a constant intercalating atom. Compared to other steels with the same strength, the anisotropy coefficient (r) value is quite high. Thanks to this feature, it is ideal for deep drawing product, which is sometimes referred to as extra deep drawing steel (EDDS). It has low yield strength and high strain hardening exponent (n). Elongation rates are higher than low carbon steels. Typical IF steel is not aged; For this reason, it is suitable for hot dip galvanizing process. Widely used in automobile construction, fender, side panels that are difficult to shape, and the floor panel. IF steel grades are shown in Table 2 .6. In IF steel, strength increase is provided by the combination of solid solution hardening, carbide and / or nitride precipitation and grain reduction methods. Strength increase is also achieved with phosphorus, another solid solution hardener. [3] [5] [12]

Table 2. 6.IF Steels [17]

Steel grade	Ti % by mass max.	0.2% Yield point [MPa]	Tensile strength [MPa]	Fracture elongation [%] min.	Vertical anisotropy r min.	Work hardening exponent n min.	Zinc coating group
HX160YD	0.12	160-220	300-360	37	1.9	0.20	Z 70 - Z 200
HX180YD	0.12	180-240	330-390	34	1.7	0.18	Z 70 - Z 200
HX220YD	0.12	220-280	340-420	32	1.5	0.17	Z 70 - Z 200
HX260YD	0.12	260-320	380-440	30	1.4	0.16	Z 70 - Z 200
HX300YD	0.12	300-360	390-470	27	1.3	0.15	Z 70 - Z 200

#### 2.5.4.High Strength Low Alloy (HSLA) Steels

These steels are formed by precipitation hardening and grain size reduction processes. In HSLA steel, there is no softening in the weld area and the grain size does not increase; Thanks to these features, it can be easily welded. In addition, coating options (such as galvanized) are wide in this steel. In galvanized HSLA steel, mechanical parameters in the direction of elongation can be changed in an alternative way, depending on customer request. Accordingly, the yield strength can be reduced to 20 MPa and the tensile strength to a lower range of 10 MPa. The elongation rate can be increased by 1%. HSLA steel is mostly used in suspension systems, chassis and durability increasing parts. It has high fatigue and impact resistance. HSLA steel grades are as in Table 2 .7. [4] [3].

Table 2. 7.HSLA Steels [17]

Steel grade	Mn % by mass max.	0.2% Yield point [MPa]	Tensile strength [MPa]	Fracture elongation [%] min.
HX260LAD	0.6	260-330	350-430	26
HX300LAD	1.0	300-380	380-480	23
HX340LAD	1.0	340-420	410-510	21
HX380LAD	1.4	380-480	440-560	19
HX420LAD	1.4	420-520	470-590	17
HX460LAD	1.7	460-560	500-640	15
HX500LAD	1.7	500-620	530-690	13

#### 2.5.5.First generation AHS steel grades

Two-phase (DP) steels have a martensite dispersed ferritic microstructure. While ferritic structure provides ductility, strength ratio is controlled with martensite structure ratio. Besides high strength and elongation, DP steel does not show discontinuous flow. However, there is a high level of GH effect, which is gained as a result of martensitic transformation. With the use of martensite dispersion DP steel



in automobile production, the impact resistance of this steel increases thanks to its high dynamic absorption energy. In addition, DP steel has high tensile strength; Accordingly, the elongation rate and deformation hardening base (n) value are also high. It is used in parts subject to collision such as automobile side panels, axle fittings and reinforcement parts. DP steel provides safety in the car and is effective in vehicle lightness. DP steel grades are given in Table 2. 8. [3] [12]. DP steels are typically named after their tensile strength levels. For example, DP800 means a dual phase steel with approximately 800 MPa tensile strength. A recent study by Ford of Europe showed that replacing mild steel with DP800 could save 35% weight in crash components. DP800 could be used both in axial crush regions (such as front or rear rails) and 3-point bending regions (such as rocker reinforcement and B-pillar) [18] [19].

Table 2. 8. DP Steels [17]

Steel grade	Mn % by mass max.	0.2% Yield point [MPa]	Tensile strength [MPa]	Fracture elongation [%] min.	Work hardening exponent [n] min	Bake hardening value BH <sub>2</sub> [MPa] min.	Zinc coating group
HCT450X	2.0	260-340	450	27	0.16	30	Z 70 - Z 200
HCT500X	2.0	300-380	500	23	0.15	30	Z 70 - Z 200
HCT600X	2.2	340-420	600	20	0.14	30	Z 70 - Z 200
HCT780X	2.5	450-560	780	14	-	30	Z 70 - Z 200
HCT980X	2.5	600-750	980	10	-	30	Z 70 - Z 200

### 2.5.6. In ferritic / bainitic (FB) steels

The strength increase is achieved by thinning the ferrite and bainite grains in their microstructure and second phase hardening with bainite. The most important features of HSLA and DP steels are good stretchability in the cutting edges measured by hole expansion test. Compared to HSLA steel with the same strength, the n value and total elongation amount are higher. It has the feature of easy welding.

It has high resistance against impact and fatigue. FB steel examples and application areas used in the automotive industry. [4]

### 2.5.7. Transformation induced plasticity (TRIP)

Residual austenite is formed from austenite with slow cooling and then rapid cooling in steels with Transformation Induced Plasticity (TRIP), that is, plasticity with transformation additives. Hardness in the material as a result of the transformation of a certain part of the residual austenite to martensite during deformation by stress

or deformation; The ductility increase is also achieved with the remaining residual austenite. During the transformation, there is a transition from austenite to the bainite phase. The distribution of phases in the microstructure is as follows: Ferrite (0.50-0.55), bainite (0.30-0.35), residual austenite (0.07-0.15) and martensite (0.01-0.05). The greatest property of TRIP steel is that it contains residual austenite in its microstructure. In order to obtain the best mechanical properties in this steel quality, the carbon content and its distribution in the microstructure must be very good so that the C content in austenite is maintained at 15-25 ° C in the cooling process. The amount of C is limited up to 0.20-0.25% by weight in order to maintain its weldability. To achieve a potential weight reduction, the BH mechanism can be implemented by heat treatment. It is used in anti-crash applications and safety parts in the automobile industry. TRIP steel grades are shown in Table 2 .9. [3] [12].

Table 2. 9.Trip Steels [17]

Steel grade	Mn % by mass max.	0.2% Yield point [MPa]	Tensile strength [MPa]	Fracture elongation [%] min.	Work hardening exponent [n] min	Bake hardening value BH <sub>2</sub> [MPa] min.	Zinc coating group
HCT600T	2.5	400-520	600	25	-	40	Z 70 - Z 200
HCT690T	2.5	430-550	690	23	0.18	40	Z 70 - Z 200
HCT780T	2.5	470-600	780	21	0.16	40	Z 70 - Z 200

### 2.5.8.Multiphase (CP) steels

These steels are similar to TRIP steel microstructure; it only contains no residual austenite. Thanks to the hard phases obtained by martensite, bainite and precipitation hardening, the strength value of CP steel varies between approximately 800 and 1000 MPa. Thanks to this feature, it is used in areas resistant to impact, such as bumpers in automobiles. Its formability feature is better than DP steel. Grain reduction is achieved by adding Ti, V and Nb. It is suitable for the zinc plating method and is suitable for spot welding. CP steel grades are given in Table 2 10. [4] [3]

Table 2. 10.CP Steels [17]

Steel grade	Mn % by mass max.	0.2% Yield point [MPa]	Tensile strength [MPa]	Fracture elongation [%] min.	Bake hardening value BH <sub>2</sub> [MPa] min.	Zinc coating group
HCT780C	2.2	600-750	780	10	30	Z 70 - Z 200
HCT980C	2.2	800-950	980	6	30	Z 70 - Z 200



### **2.5.8.Martensitic (MART) Steels**

100% martensitic steel is obtained by quenching after the continuous annealing process. Although it has lower ductility compared to other AHS steels, it is a very high strength steel. The strength hardness depends on the amount of C in the steel structure and the austenitizing temperature. The mechanical properties of steel vary according to fast or slow cooling. Slow cooling is important in order to increase ductility in terms of forming the steel. [8] [12]



### 3.HEAT GENERATION IN SHEET METAL WORKING

#### 3.1.Heat Transfer Methods

In drawing operation; temperature changing occurred during process, some part temperature increasing and some dropping in system. Heat transfer is important item during process. Heat transfer called as energy transfer from higher one to lower one and all system tries to reach same temperature level. While all system part have same temperature; heat transfer stops. Heat transferred as three methods: conduction, convection, radiation.

##### 3.1.1.Conduction

If minimum two different parts, that can be solid, liquids or gases, touching to each other directly and they have different temperatures, higher temperature can be transferred to lower temperature.

Fourier's Law have important role about conduction. High temperature gap increasing rate of heat transfer (Q), and high length of wall(DX), reduced rate of heat transfer. That is shown as below;

$$\dot{Q}_{\text{cond}} = kA \frac{T_1 - T_2}{\Delta x} = -kA \frac{\Delta T}{\Delta x} \quad (\text{W}) \quad (3. 1)$$

In this formula; k is called thermal conductivity of the materials. That is changing from material to material according to material chemical and mechanical properties.

##### 3.1.2.Convection

Convection is the second energy transfer method from solid surface to fluent or gas materials. Fluent material movement velocity is important for this method. If fluid motion is faster, convection transfer is greater.

Forced convection is a option of convection system mean that; fluid is forced to change position by pump, wind or fan. The other option is called natural convection that's mean is fluid change position without force, its density help to energy transfer. That is shown as below;

$$\dot{Q} = hA_s(T_s - T_\infty) \text{ (W)} \quad (3.2)$$

### 3.1.3.Radiation

Radiation is completely different energy transfer method from conduction and convection. This heat transfer method occurs by electromagnetic changing of material atoms and molecules. This heat transfer method not needs any medium for transfer. That is shown as below;

$$\dot{Q}_{\text{emit,max}} = \sigma A_s T_s^4 \text{ (W)} \quad (3.3)$$

Stefan Boltzman coefficient is constant value for all calculation. In this study radiation heat transfer method is not be used because die dimension is big and especially focus on high level heat transfer by conduction and convection. Additionally during draw operation heat transfer is not constant, that is changed depend on time so steady versus heat transfer is better to get correct results. [20]

### 3.2.Plastic Deformation Effect

Deep drawing operation change the material shape by exceeds yield strength of material and being plastic zone. In that zone need to energy to change. It is mean according the thermodynamic law-one energy is not disappear but that is changing from one form to other form.

Press velocity and kinetic energy try to change material shape and that kinetic energy converted into heat about 90 percent of kinetic energy changed to heat. The rest of 10 percent energy changed to material inside energy. However, not possible to measure or not have any formula to get this information that get via experimental method. Farren and Taylor experimental studies show these important results. Higher temperature effect the material flow stress data and need to implement more force in order to be shaped material. Additionally increased temperature of material negatively effects to die material and friction coefficient is increase.

Even today; computer simulation softwares can be predicted to temperature effects during draw operation, some experimental studies checked simulation software reliability [21] [22] [23].

Material internal energy is important in this section because that receive 10 percent of material. Internal energy related to atoms a molecules movement so directly dependent to temperature.

Material total energy occurs from all energy types. U is called as internal energy [24]. That can be written as below;

$$E = U + KE + PE = U + m \frac{v^2}{2} + mgz \quad (\text{kJ}) \quad (3.4)$$

$$E = KE + U \quad (3.5)$$

$$E = 0,90Q + 0,10U \quad (3.6)$$

Equation 3.6. seen 0,90 and 0,10 coefficient obtained by Farron and Taylor experimental studies. [23]

### 3.3. Friction and Lubrication in Metal Forming

In deep drawing, lubrication is important in terms of reducing the punch force, increasing the deep drawing ratio limit, reducing tool wear and extending the life and preventing production defects. Only the surface of the shrinkage sheet in contact with the matrix should be oiled. As a lubricant, mineral oils, soap solutions, emulsions are used in general applications, and hard coatings, wax and solid lubricants are used. The lubrication process is very useful as it reduces the work consumed by controlling the external friction. On the other hand, the high friction on the cylinder surfaces of the stamp increases the tensile ability. With the tension of the wall, the material in the wall moves upward due to the stamp, causing shear stress between the walls and the stamp. Therefore, the lower parts of the wall are not affected by all the pulling force. This is very important because the walls below do not undergo as much deformation hardening as the upper walls. Thus, hardened stamps and lubricants are used to increase the pulling ability. With very low friction, the bottom of the container appears to become thinner. [8] [10] [16]

The main types of oil used in deep drawing are given below.

- Greases
- Mineral oils
- Molicot oils
- Waxed oils
- Soapy dry lubrication
- Teflon and P.T.F.E. lubrication with films
- Graphite oils
- Vegetable oils

- Animal oils

In mass production, these oils can be applied automatically or manually.

Friction in metal forming is due to the close contact between the tool and the work surface and the high pressures that bring the surfaces together during these processes. In most forming processes, friction is undesirable for the following reasons: (1) Metal flow in work is delayed, resulting in residual stresses and sometimes defects in the product. (2) The forces and forces required to perform the operation increase; and (3) Tool wear can cause dimensional accuracy loss, which may require defective parts and tool replacement. Tool wear is a big problem as tools in metal forming are often expensive. Friction and tool wear are higher when working hot due to the much harder environment. If temperature increase in draw operation, that highly available to effect lubrication coefficient and part quality in mass production. [8] [25]

Friction in metal forming differs from most mechanical systems such as gears, shafts and bearings, and other components that have relative motion between surfaces. These other conditions are generally characterized by low contact pressures, low to medium temperatures, and sufficient lubrication to minimize metal-to-metal contact. In contrast, the metal forming medium has high pressures between a hardened tool and a soft part, plastic deformation in the softer material, and high temperatures (at least during hot work). These conditions can lead to relatively high coefficients of friction in metalworking, even in the presence of lubricants. Typical values of the coefficient of friction for the three categories of metal forming are listed in Table 3 .1[8] [16].

Table 3. 1.Friction Coefficient Effects of Friction [8]

Category	Temperature Range	Strain-Rate Sensitivity Exponent	Coefficient of Friction
Cold working	$\leq 0.3T_m$	$0.000 \leq m \leq 0.05$	0.1
Warm working	$0.3T_m - 0.5T_m$	$0.05 \leq m \leq 0.1$	0.2
Hot working	$0.5T_m - 0.75T_m$	$0.05 \leq m \leq 0.4$	0.4-0.5

When the coefficient of friction becomes large enough, a condition known as sticking occurs. In metalworking, bonding (also known as static friction) is the tendency of two surfaces to stick together and not slip when moving relative to each other. This means that the frictional stress between the surfaces exceeds the shear flow stress of the working metal and, as a result, the metal is deformed by a shearing process

below the surface and does not slip on the surface. Adhesion occurs during forming processes and is a major problem during rolling. We will discuss this in this context in the next section. Many metal forming processes apply metalworking lubricants to the tool-work interface to reduce the adverse effects of friction. Benefits include less grip, strength, strength and wear on tools and better product surface quality. Lubricants also perform other functions, for example heat dissipation of the tool. Lubricants used for cold working operations include, mineral oils, greases and oily oils, water-based emulsions, soaps and other coatings. Hot forging is sometimes performed dry for certain processes and materials (e.g. hot steel and aluminum extrusion). When used for hot work, lubricants contain mineral oils, graphite and glass. Molten glass becomes an effective lubricant for the hot extrusion of steel alloys. Graphite in water or mineral oil is a common lubricant for hot forging of various working materials. Last research clearly shows that increased temperature in draw operation effect to panel quality negatively. [8] [25] [38] [16]

While temperature increasing during draw operation, that is effect to part quality so need to reduce temperature with some method. One and known method is using extra lubricant before draw operation. That is conventional method and works for years in mass production but not possible to use each lubricant to each process. Hoschouer C., Jeffery J., Kenny F., Infante D. D., Altan T. Implemented one experimental study and used 24 different lubricant to understand which has better performance, tool system shown in Figure 3. 1.

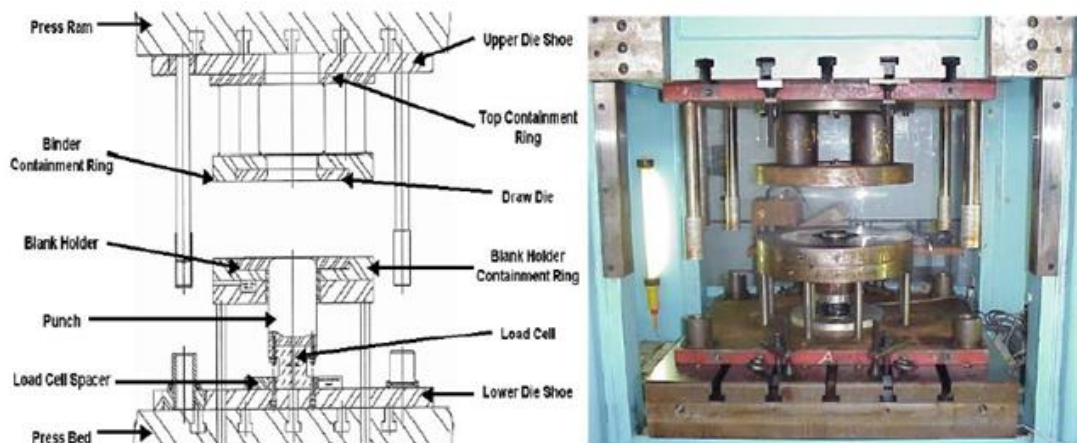


Figure 3. 1. Deep Drawing Tool [22]

As a first step finite element (FE) simulation set up and experimental die manufactured shown in Figure 3. 1. Same condition implemented for all lubricants such as draw height, blankholder force and sheet material seen in Figure 3. 2.

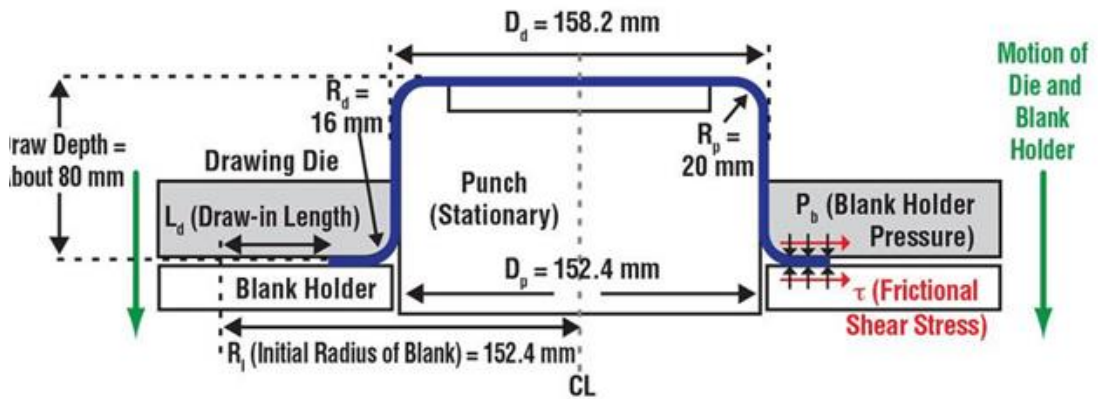


Figure 3. 2. Cup Drawing Schematic View [26]

Temperature effects investigated in that study and both FE and experimental results showed that sheet metal temperature increased up to  $101^\circ\text{C}$  shown in Figure 3. 3 and known that result effects to sheet friction coefficient. Because of that extra lubricant implementation is conventional method in order to increase friction coefficient and reduce sheet metal temperature [26].

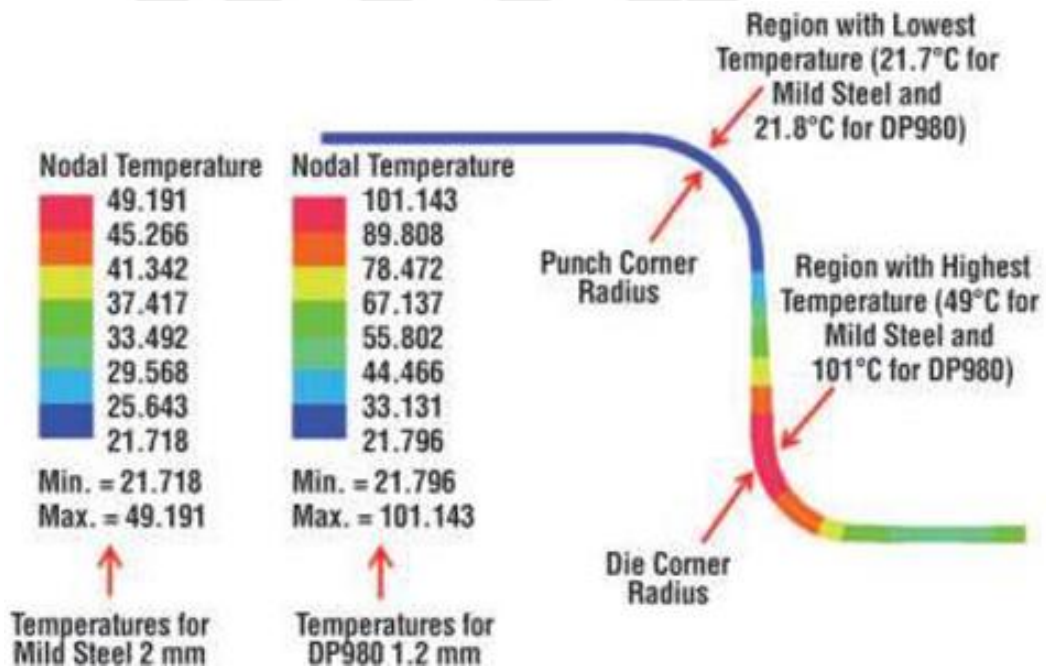


Figure 3. 3. Temperature Distribution of FE Results of Cup Drawing Test [26]

After getting experimental results, the best lubricants selected via test. If cup flange shorter, that's mean lubricant is better and coefficient of friction (COF) is better. Also lubricant properties have to be same even temperature increased over  $100^\circ\text{C}$ . Lubricant has two missions in conventional method; one is reduce the sheet metal temperature and the second is increasing the COF value. [26]

### 3.3.Heat Transfer Mechanism During Draw Operation

Sheet metal temperature increasing during draw operation over 100°C and die has lower temperature at room conditions [21]. Normally die heat transfer condition shown in Figure 3. 4.

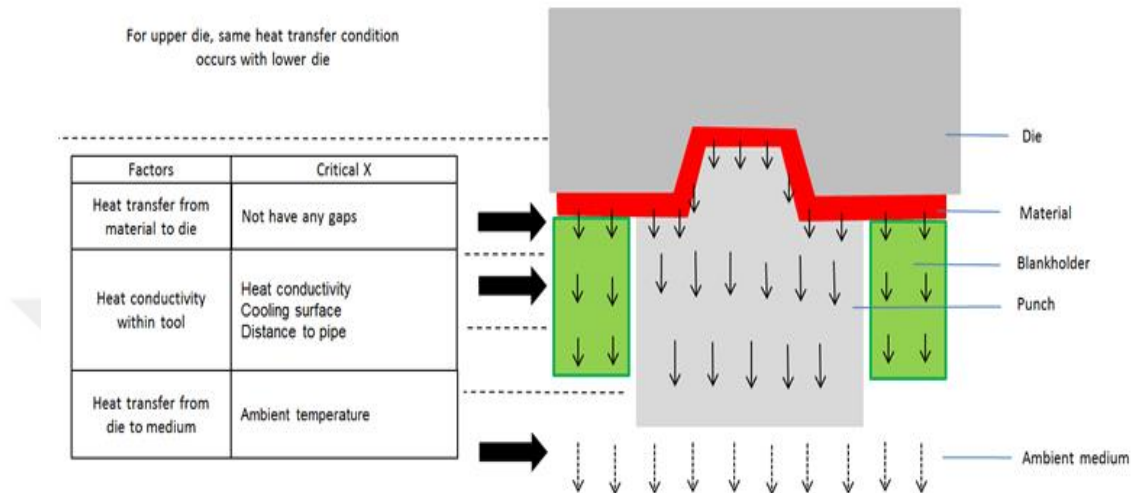


Figure 3. 4.Heat Transfer of Stamping Die

The temperature differences conditions create heat transfer conditions from sheet metal to die. Although this condition decrease the sheet metal temperature, not enough to get normal room temperature levels.

In this study; while sheet metal temperature increasing during draw operation, the temperature distribution to die and ambient and try to reduce temperature increasing negative effects by designing cooling pipes to die. This study occurs from two important points;

- 1- Negative effects of temperature increasing during draw die operation for AHSS
- 2- Reduce the negative effects of high die temperature by using cooling pipes

### 3.4.Thermomechanical FE Model

Although Autofom R8 Thermal developed for hot stamping dies, in this study, that is used for cold stamping dies.

Vehicle developing phase reducing via developed new simulation methods and softwares. If this phase long, vehicle unit price increase and that would effect market status of brands. Today each vehicle manufacturer company try to reduce develop phases.



Sheet metal feasibility is a vehicle development phase. In that phase; sheet metal parts manufacturable condition checked by engineering team and vehicle design changed by stamping team if necessary for manufacturing.

Autoform software tries to reduce stamping feasibility duration by developing simple software. Especially solver time is so much that effect the computer performances at the same time.

The most important point in Autoform software; calculating the sheet metal temperature during draw operation given in Figure 3 .5. Maximum temperature of 8SPM Schuler press line. Temperature distribution shown that is reached up to 188,3 °C after 170mm stroke.

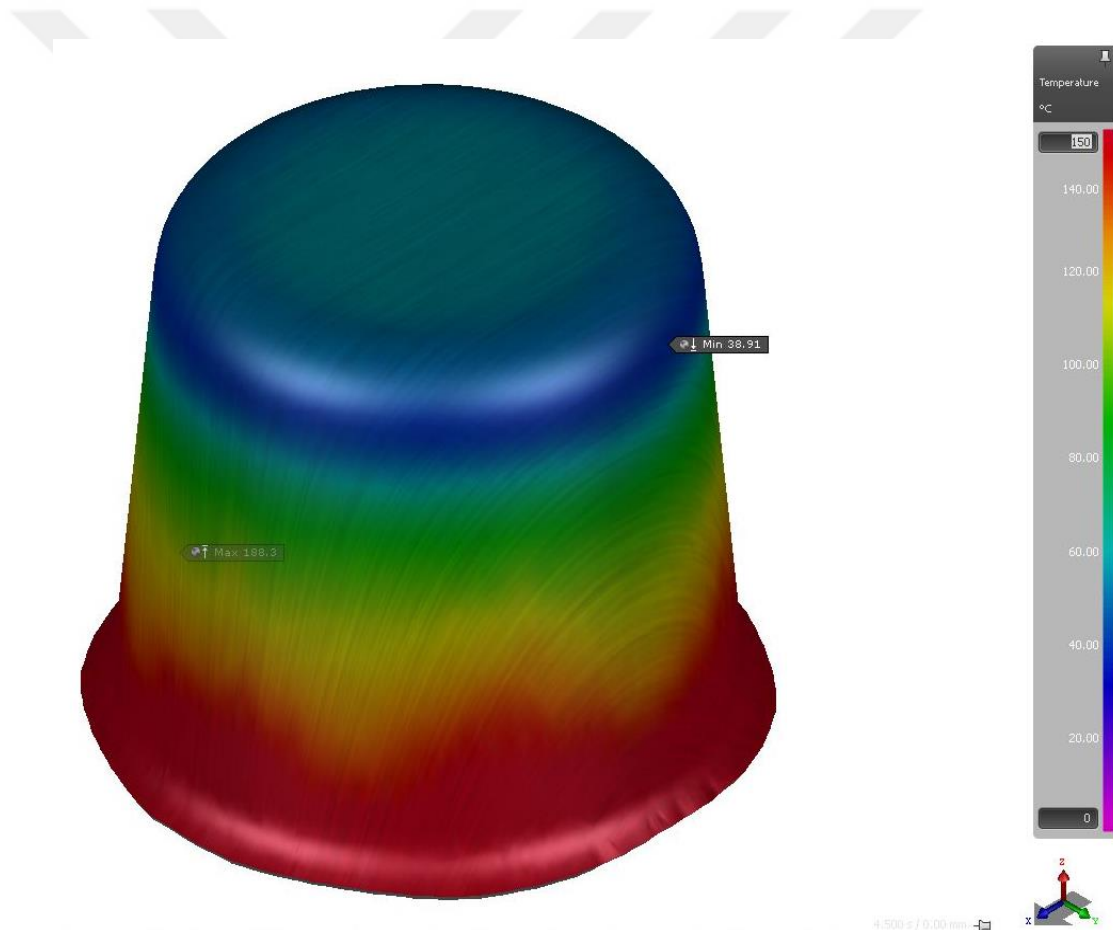


Figure 3. 5.Drawn Cup Thermomechanical Result Example

Stroke-temperature graph can be get from software given in Figure 3. 6. Stroke and time relation known from press curves, so time dependent temperature can be get from this graph.

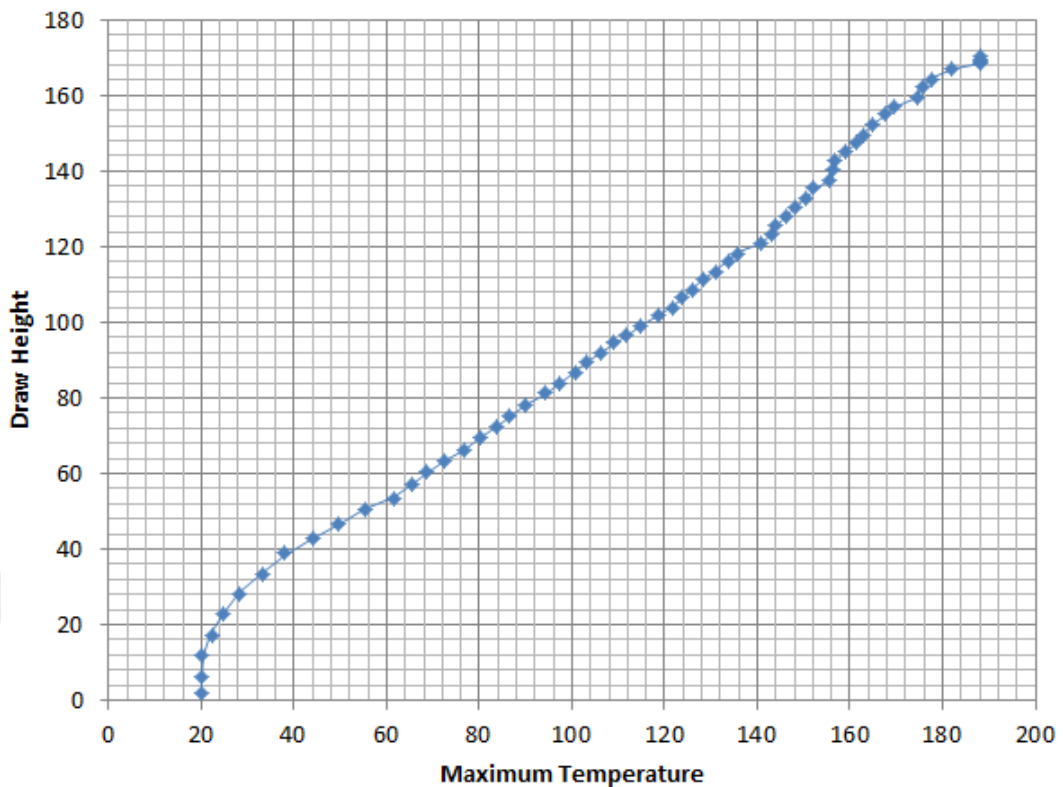


Figure 3. 6.Draw Height-Temperature Relation Example in Draw Operation

The second important point is oil effects to sheet metal forming and that is used in Triboform that embedded to Autoform software. This software tries to figure out oil distribution and oil effects in stamping operation. These friction models occurred and taught from real results and codes/formulas not shared by Autoform.

Even heat transfer coefficient (HTC) from sheet metal to tool can be entered in software, this coefficient effect changed during simulation according to contact pressure during draw operation. Contact pressure and HTC relation given in Table 3 .2. In draw operation between sheet metal and die have changeable contact. If sheet die touch to sheet metal with over 20 MPa pressure; HTC directly can be used but if die surface have zero contact to sheet metal part, heat is not transfered to die surfaces.

Table 3. 2.Contact Pressure HTC Scaling Relation

Pressure	Scaling Factor
0 Mpa	0,3
1 Mpa	0,7
2 Mpa	0,8
3 Mpa	0,9
20 Mpa	1,0

If heat transfer preferred from to die; contact condition is important. That must be more surface in order to increase heat transfer. HTC to tool defined as 2,75 Watt/m<sup>2</sup>K [27]. Ambient temperature defined as 20°C and HTC to ambient defined as 0,020 W/m<sup>2</sup>-K. Tool volumetric heat capacity defined 4,370 mJ/mm<sup>3</sup>K and tool conductivity defined 32 mW/(mmK).



#### 4. TEMPERATURE VALIDATION OF FE SIMULATION RESULTS

Using of Advanced High Strength Steel (AHSS) has increased day by day in industry. Especially automotive industry prefers because of high tensile strength values that helps to manufactured lighter and more safety vehicles. AHSS stronger than mild steels but has restriction for complex shapes and big dimensional parts.

##### 4.1. Background, Problem Statement and Motivation

In this study U-Channel drawing the thermomechanical FE model validated by comparing predictions with experimental results. After validation of FE simulation results same with experimental results, DP800 material has been compared in terms of temperature, thickness and press velocity in deep draw operation by taguchi method. According to that; eight different experiment combinations implemented and temperature has been affected more than others during deep draw operation in prediction FE model.

Reached temperature up to 130 degree has been affected drawability of sheet metal parts because that impacted coefficient of friction (COF). In case of constant temperature condition investigated by FE simulation in order to understand if using cooling pipe system in stamping dies. Constant die temperature and drawability graph obtained that show temperature effects during deep draw operation.

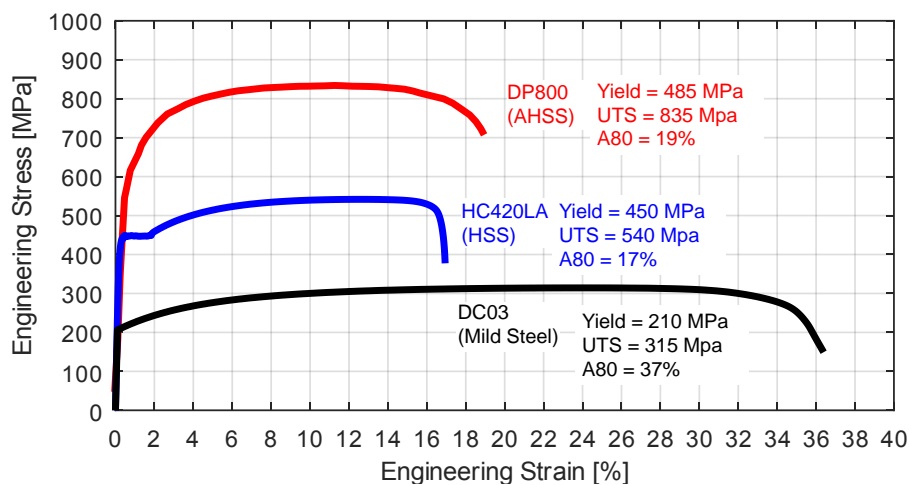


Figure 4. 1. Stress Strain Curve of Mild Steel, HSS and DP800

Figure 4 .1. Clearly shows of AHSS material effects by a graph. Automotive industry needs bigger dimensional and complex shape parts as AHSS for lower weight and more safety vehicles. Especially new vehicle models need to use lighter materials seen in Figure 4 .2. For instance bodyside inner panels of vehicles has big dimension and deep draw operation but not possible to get parts either cold or hot stamping process as AHSS. This dual phase materials not let to us for these items with conventional cold stamping process because to crack issue in draw operation. Even hot stamping is an alternative method for Boron materials that has higher strength, that have restricted part dimension and higher manufacturing cost that increasing the automotive part costs.

Studies showed that sheet metal temperature increasing in draw operation for AHSS steels up to 150°C even starting to process in room temperature especially in radius points of parts [7]. Especially DP steels consist of a soft ferrite matrix for formability and numerous martensitic islands for strength [28].

In press forming, there would be heat generation due to plastic deformation and also, due to the friction between the blank and the tools. Local high temperatures would be observed with: (a) deeper draws, (b) higher strength materials and (c) high press speeds [29].



Figure 4. 2.Ford Focus HB Model

In this study; conventional cold stamping system revised as cooler base stamping system that is innovative and motivated to get more complex parts in draw die with high accuracy. Sheet metal and die parts temperature not increasing in draw operation via cooling system design so die all surface have equal uniform temperature.

#### 4.1. Material Model

Previous publication by Fallahiazoodar, Peker and Altan has used constant room temperature mechanical properties for CP800 and DP600 and also by Preira and Rolfe used DP800, DP600, HSLA300 and HSLA400 even mechanical properties changed by temperature degree.

Another previous publication by Winkler, Thompson, Worswick, Riemsdijk and Mayer has verified temperature and velocity effect to material yield strength point and tensile strength points. In that study, above verification implemented for DQ, HSLA 350, DP 600, and DP 780 materials by uniaxial tensile tests were conducted at quasi-static (QS) (0.003 and 0.1 s<sup>-1</sup>), intermediate (30 and 100 s<sup>-1</sup>), and high (500, 1000, and 1500 s<sup>-1</sup>) strain rates using an Instron, instrumented falling weight impact tester and tensile split Hopkinson bar (TSHB) apparatus, respectively. Elevated temperature tests at 150 °C and 300 °C were also conducted at high strain rates. [30]

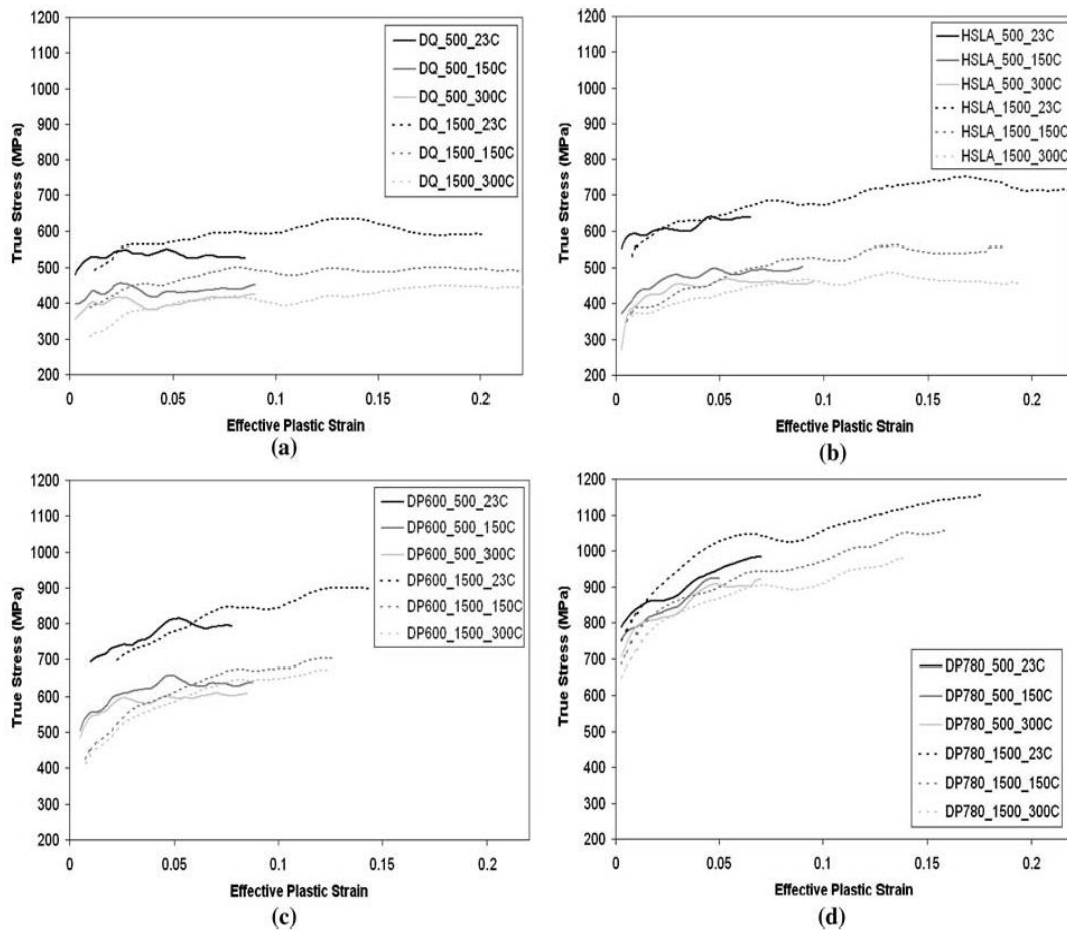


Figure 4. 3.Experiments Results [30]

Elevated temperature investigated strain rates of 500 and 1500 s<sup>-1</sup>, at 150°C and 300°C Figure 4 .3. shows the temperature effects on the true stress vs effective plastic strain response of the different type tubes. Strength reduces when increasing temperature for DP materials. Temperature increased from 23 °C to 300 °C. [30]

DP800 is selected, as this grade can be used in most applications in a car body. There are several standards in Europe which defines chemical and mechanical properties of DP800. Table 4 .1. Summarizes the mechanical properties of DP800 equivalents in the European Norm EN 10338, German Association of the Automotive Industry's VDA239-100 and Ford's internal standard WSS-M1A368. It is important to note that these steels also have bake-hardening effect.

Table 4. 1. DP800 Has Different Name Standards

<b>Standard</b>	<b>EN10338</b>	<b>VDA239-100</b>	<b>WSS-M1A368</b>
<b>Naming – Primary (Secondary)</b>	HCT780X (1.0943)	CR440Y780T-DP	CRDP800 (A14)
<b>Proof strength (R<sub>p0.2</sub>) [MPa]</b>	440-550	440-550	420-550
<b>Tensile strength (R<sub>m</sub>) [MPa]</b>	≥780	780-900	780-900
<b>Total elongation (A<sub>80</sub>) [%]</b>	≥14	≥14	≥14
<b>n<sub>4-6</sub> [-]</b>	-	≥0.15	≥0.15
<b>n<sub>10-20/Ag</sub> [-]</b>	≥0.11	≥0.11	≥0.11
<b>BH<sub>2</sub> [MPa]</b>	≥30	≥30	≥30

In this study, commercially available metal forming simulation software, AutoForm ® R8 with Thermo Plug-In was used for simulations. Material data was taken from AutoForm material library using Tata Steel's DP800 GI (Galvanized) Thermo model. There were 24 flow curves (4 temperature levels and a total of 6 strain rates), some of them are plotted in Figure 4 .4, Figure 4 .5, Figure 4 .6, Figure 4 .7[31].

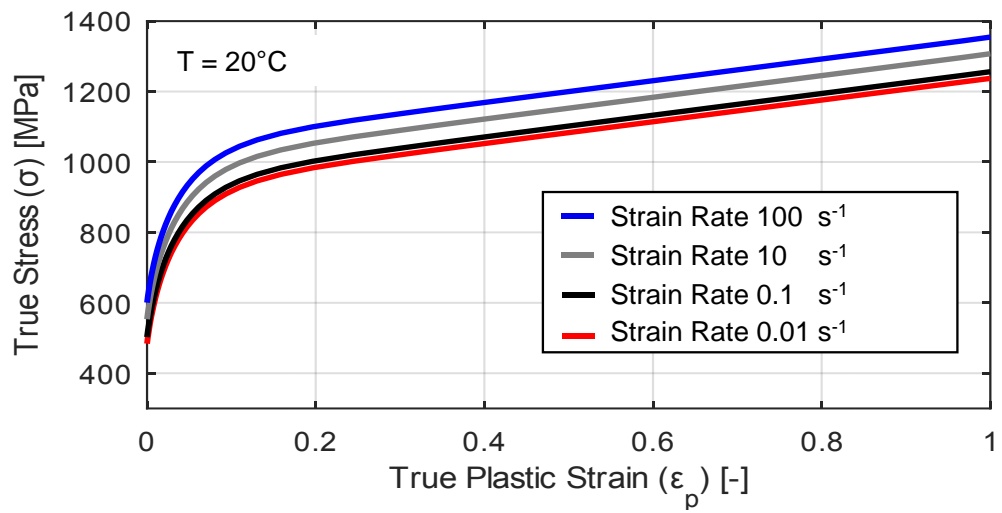


Figure 4. 4.Flow Curves of 20°C [31]

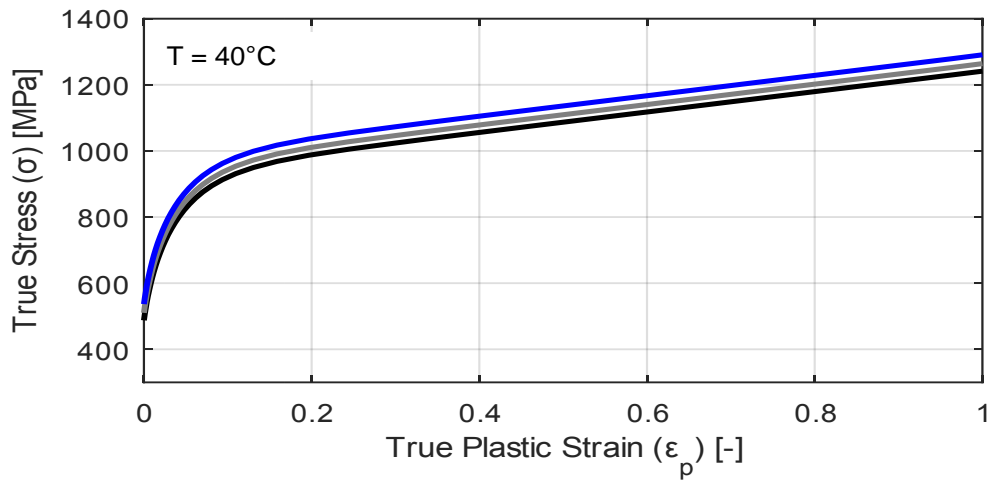


Figure 4. 5.Flow Curves of 40°C [31]

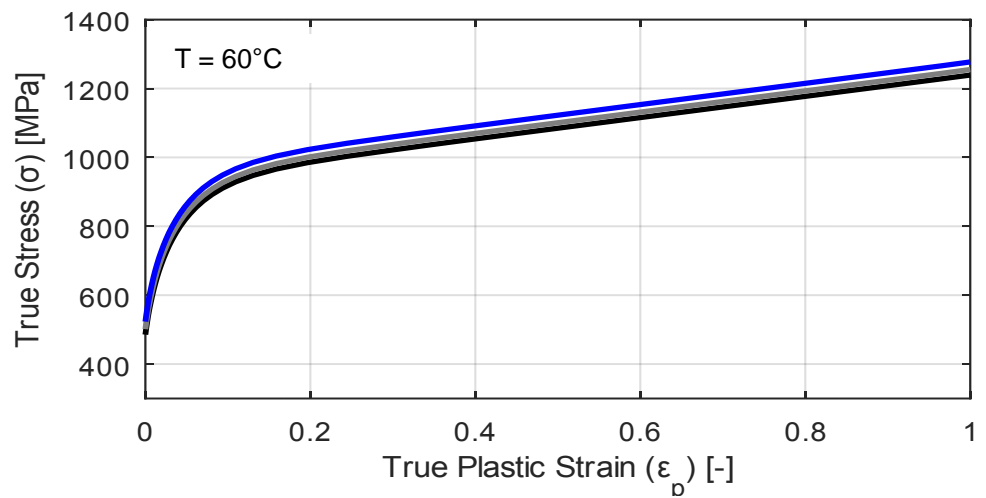


Figure 4. 6.Flow Curves of 40°C [31]



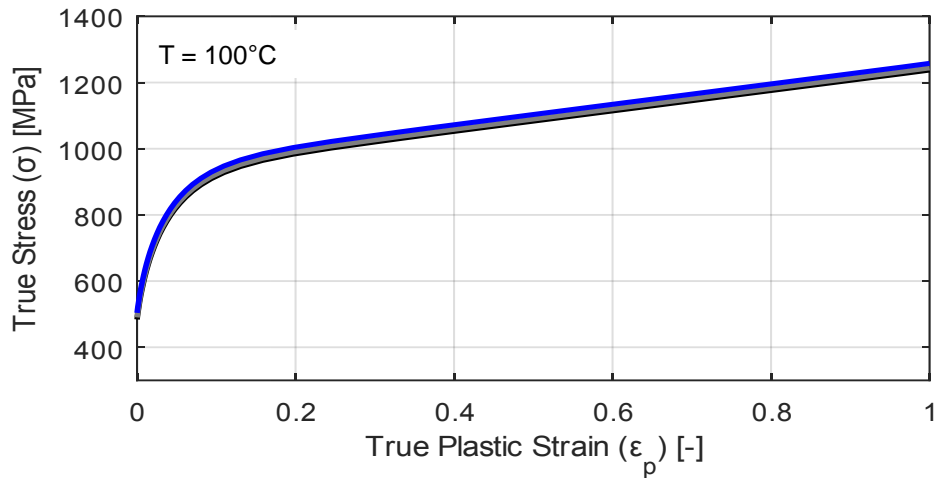


Figure 4. 7.Flow Curves of 40°C [31]

Lastly for the Forming Limit Curve, Abspoel 2012 model is used – commonly referred to as Tata Steel model. In this model,  $r$ -values and total elongation ( $A_{80}$ ) values for all 3 directions ( $0^\circ$ ,  $45^\circ$  and  $90^\circ$  to rolling direction) and thickness of the blank are required. The output will be similar to Marciniak FLC (i.e.,  $FLC_0$  coinciding with the y-axis) with only 4 data-points, as clearly indicated in Figure 4 .8. FLC is given for only  $20^\circ\text{C}$ . When the thickness is different than that of the FLC, Keeler approximation is used to calculate the new FLC. [32] In this study, Vegter 2006 (also known as Corus-Vegter or Vegter-Full) yield locus is used. [33] [34]

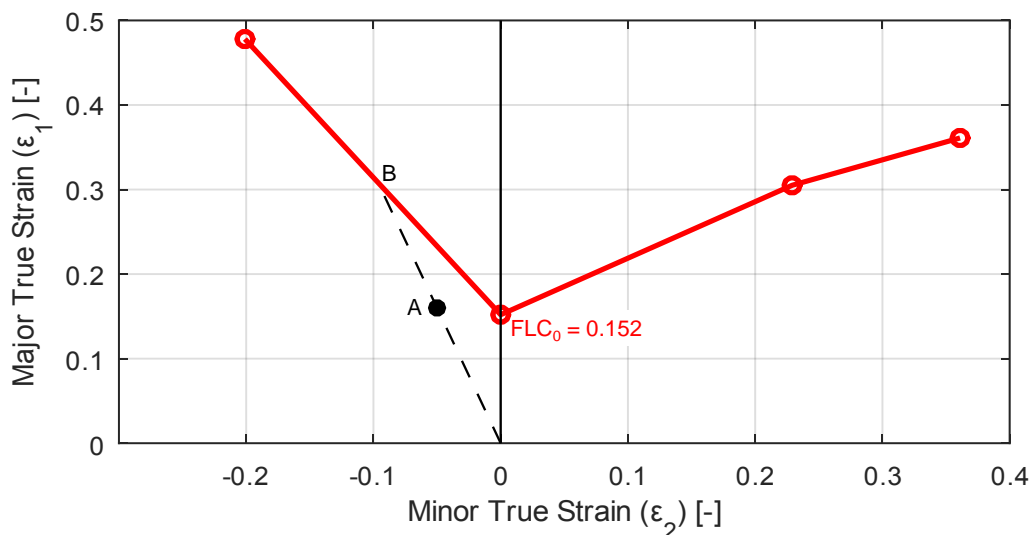


Figure 4. 8.Forming Limit Curve of 1.6 mm thick DP800 [31]

In the automotive industry, "failure criteria" are used when designing a simulated tool. Suppose, for a given element, the maximum distribution of small deformation during deformation is point in Figure 4 .8. The failure criterion is the linear distance

from the starting point to point a divided by the linear distance from the FLC. In Figure 4 .8., the failure criterion for point A is approximately 0.5. In theory, if the failure criterion is greater than or equal to 1.0, the piece will be split. In the tool design process, failure criteria are typically kept at 0.7-0.8 to achieve solid production.

#### 4.2.Validation of Thermomechanical Condition

The experimental work by Pereira and Rolfe [21] was repeated to verify the predictions of the thermomechanical model. The dimensions of the tools are given in Figure 4. 9. Pereire and Rolfe studied a number of different steel sheets. Only the 2.0 mm DP800 was copied in this study. Prior to forming, tools were considered 20 ° C uniform. The tools were modeled with 3D heat conduction and 100 mm tool height was added. This means the tools can get hot after piercing. Simulation parameters are summarized in Table 4 .2. In these simulations, mechanical pressure is simulated with a motion curve developed by one of the co-authors.

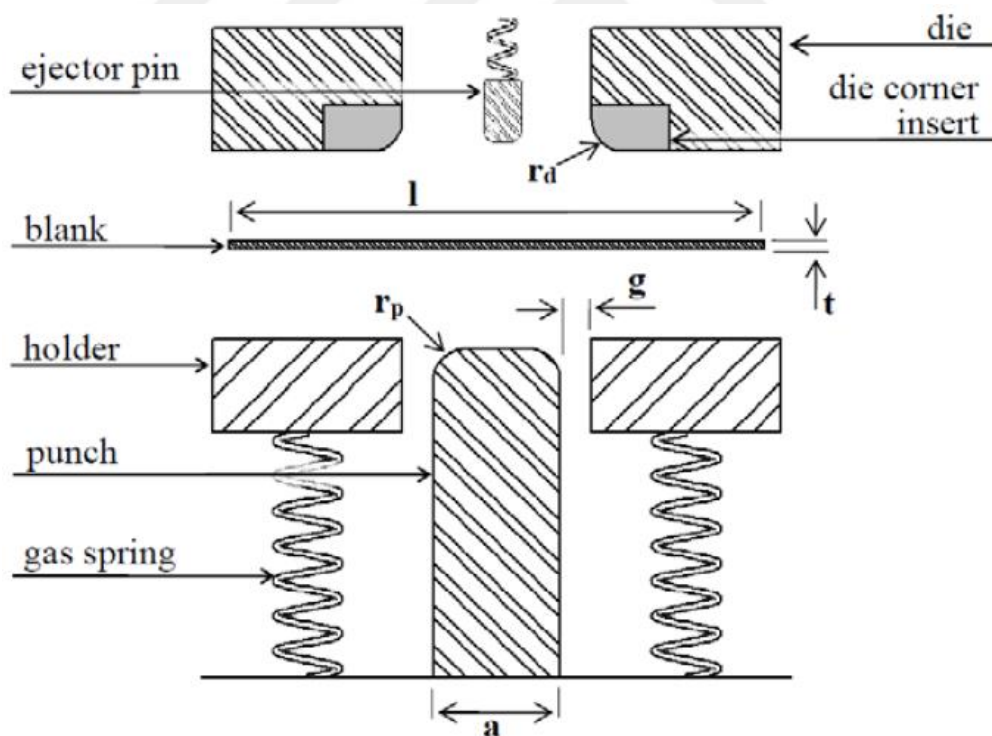


Figure 4. 9. Stamping Tool from Previous Publication by Pereira and Rolfe [1]

Autoform R8 allows to define heat capacity for temperature of sheet, Heat Transfer Coefficient (HTC) to ambient for heat transfer to ambient, HTC to tools (pressure dependent) and HTC to gaps (between tool and sheet) for heat transfer to tools,

conductivity for heat transfer in blank, expansion coefficient (thermal strain) and dilatation (due to phase transformation) for volume change.

Previous publication by Pereira and Rolfe has U Shape draw operation experiment in Figure 4. 9. Experimental inputs listed in Table 1 and outcome so before starting to base study in this publication, predicted simulation software to be tried to validate in order to take similar results.

Table 4. 2.Simulation Parameters [21]

<b>Friction coefficient [-]</b>	0.15	
<b>Blankholder force [kN]</b>	27.2	
<b>Draw depth [mm]</b>	40	
<b>Mechanical press stroke length [mm]</b>	203.2	
<b>Stroke rate [SPM]</b>	1	
<b>Thermal properties</b>	<b>Tools</b>	<b>Sheet</b>
<b>Initial Temperature [°C]</b>	20	20
<b>Heat Conductivity [W/m°K]</b>	22	52
<b>Volumetric Heat Capacity [mJ/mm<sup>3</sup>°K]</b>	3.588	3.564

Pereira and Rolfe conducted all experiments and measurements in five replicates. In this study, we digitized three of them to compare our simulation results. This method makes the numbers easier to read. Three data sets were selected as the highest scores, lowest scores and average. The first comparison is made between impact force and impact.

According to this experiment; blank dimension defined as 150mm length and 26mm width in Figure 4 .10. Sheet metals have little oil in order to protect them from corrosion and also helps to drawability limits. That is attends to sheet metal by Autoform software in FE simulation like real life.

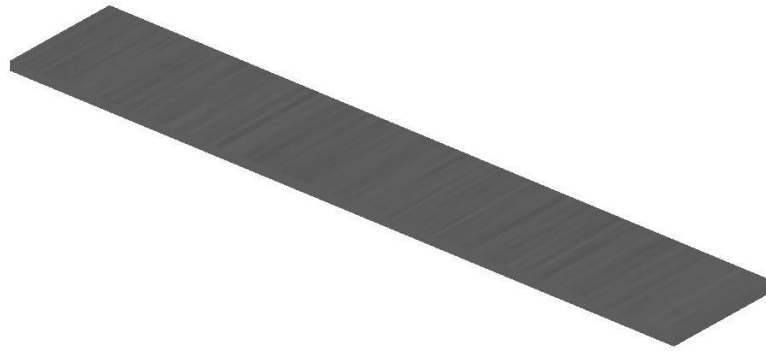


Figure 4. 10. Blank View of FE Simulation 150mmx26mm

After completing operation, Figure 4.11. Part obtained from the die. During process, lots of information can be obtained from the software but the most important point is to get the correct dimension part. Especially part thinning points are important. Although getting the part, thinning conditions affect part durability. These results are so important for automotive, aircraft and other businesses.

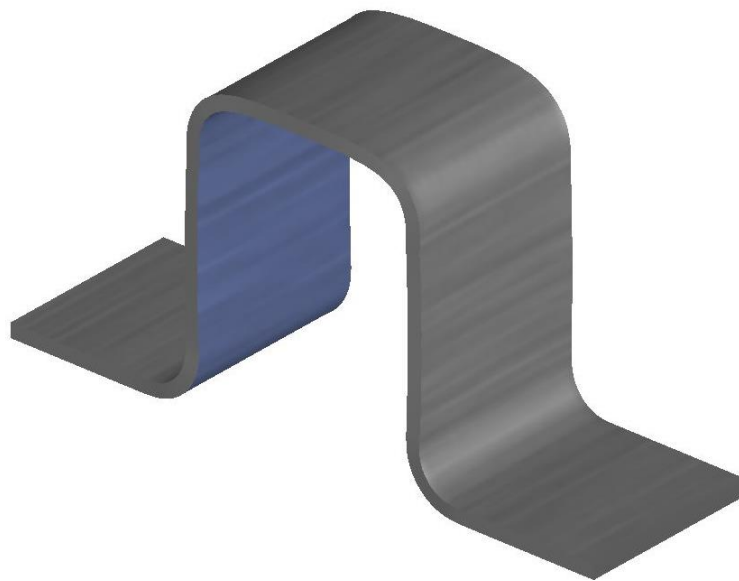


Figure 4. 11. Drawn Part After Forming Operation

In draw operation; blank (sheet metal parts) shown in Figure 4.10. is put to the blankholder and ready die to closing in Figure 4.12. The blank is located between the blankholder and the upper die, and the upper die closes up to touch the blank's upper surface.

The same die is modeled in Catia CAD software as a first step. The U-shape upper die surface, punch surface, and blank holder surface are modeled as seen in Figure 4.12. After that, the Autoform R8 software is used to simulate sheet metal forming conditions.

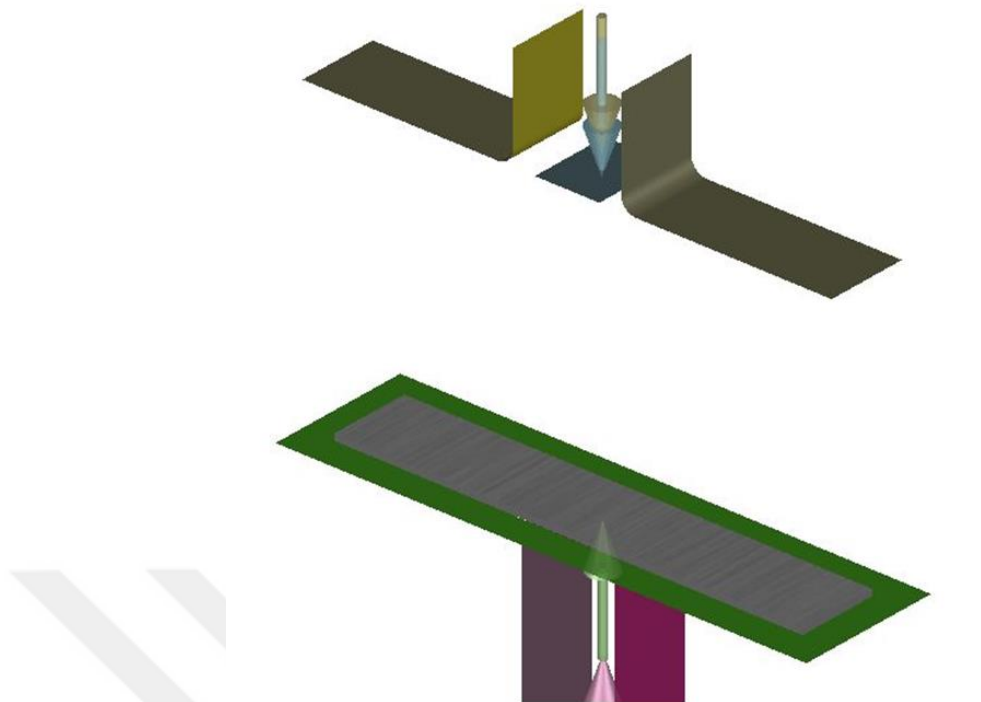


Figure 4. 12.Before Starting the Operation

While upper die touch to blank surface, blank can not move anywhere between die and blankholder. Punch ready to forming sheet metal and while moving, all form mirrored to sheet metal shown in Figure 4.13.

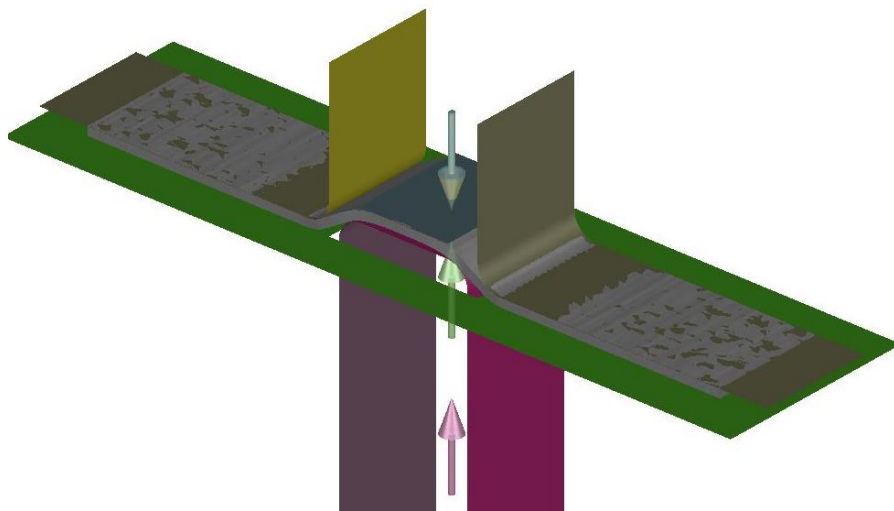


Figure 4. 13.Blank Forming

While upper die turn back to the upward position, operator or robots can take the formed part from punch surface. All operation must be fast during process because the part cost must be cheaper in order to sellable vehicles in the market. Today all engineering team works together while design the parts. Vehicle design engineers have restrictions before creating new vehicle.

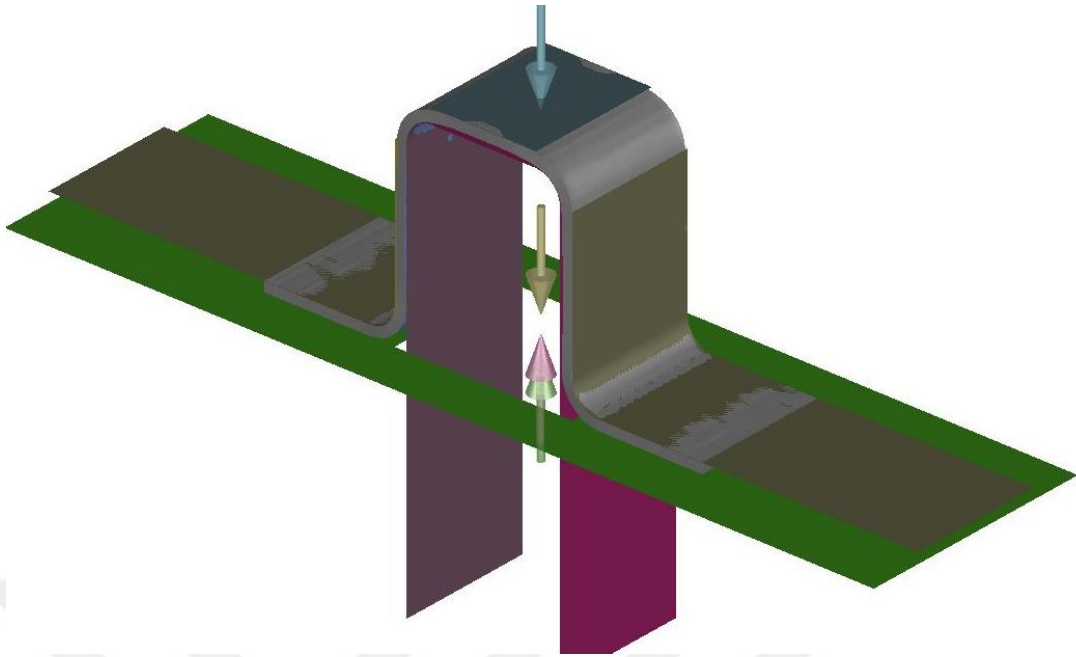


Figure 4. 14. Formed Blank Picture

Today, the most using method in draw operation using bead form to hold sheet metal better between upper die and blankholder shown in Figure 4.15. That help to hold sheet metal better but all geometry must be selected after some calculation and experience.

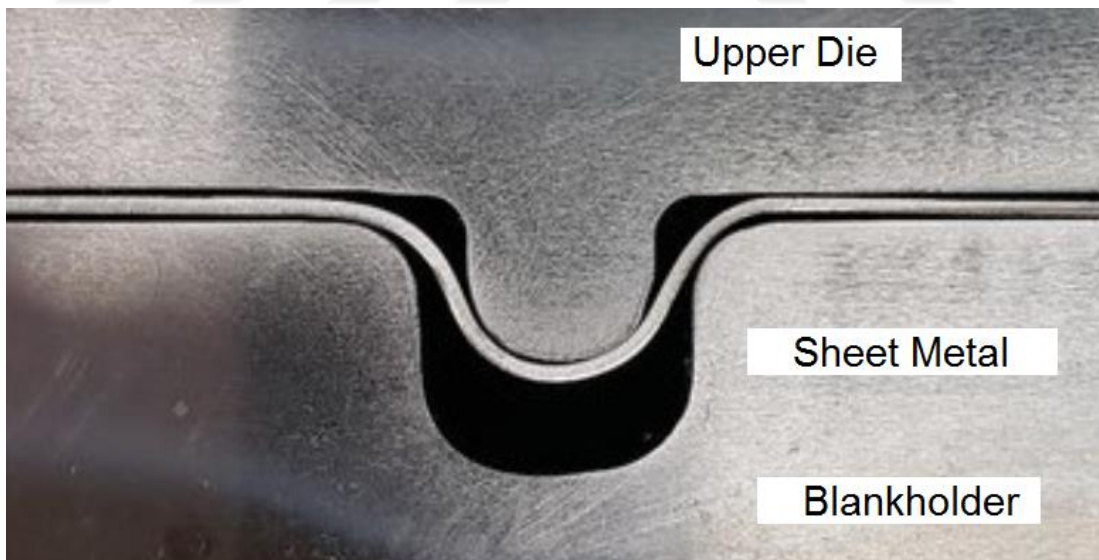


Figure 4. 15. Example Bead Form [35]

Automotive manufacturers or other sheet metal companies try to shape big and complex parts like door or fender. Harder to hold these sheet metal parts shaping in mass production conditions.

### 4.3. Results of The Validation

As can be seen in Figure 4.16, the curves were very narrow. The discrepancy under the impact may be due to the compression of the gas springs. Since the paper did not share the details of the gas springs but assumed an average force of 27.2 kN, the compression effect had to be neglected. The second comparison was made with the temperature of the raw material. As can be seen in Figure 4.17., the highest temperature calculated in the simulation only overestimated the experimental peak temperature by 0.15-1.84°C. On the other hand, die temperatures are estimated slightly lower, with 0.13 to 0.79°C. These can be explained by the heat transfer coefficient between the blank and the tool, the constant friction coefficient, the change in material properties between the material card and the tests. However, the results show that the thermomechanical model has a good correlation with experiments.

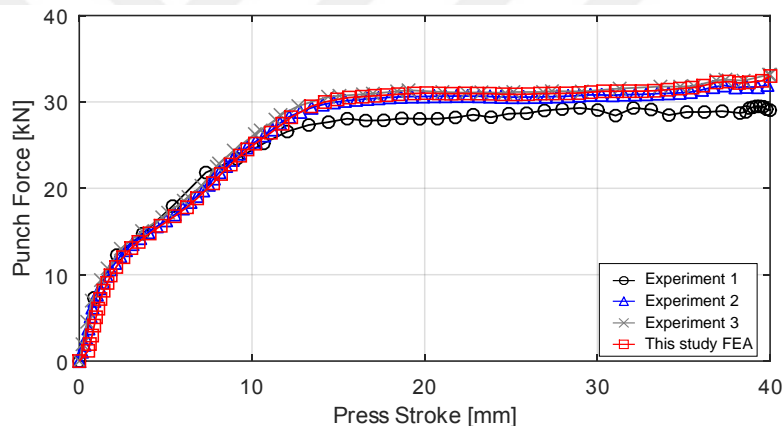


Figure 4. 16.Punch Forces vs. Press Strokes, Experiment from [21]

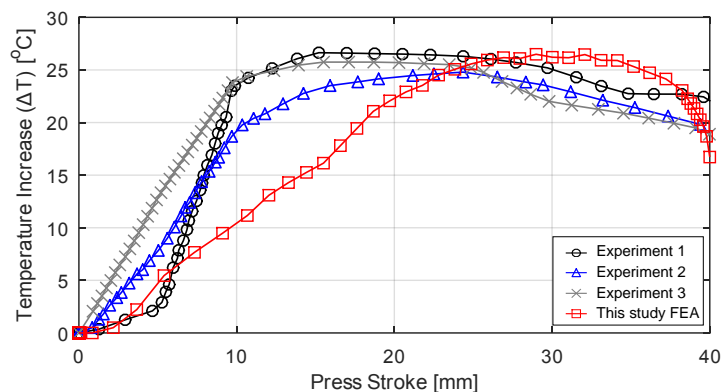


Figure 4. 17.Temperature Increase in the Blank [21]

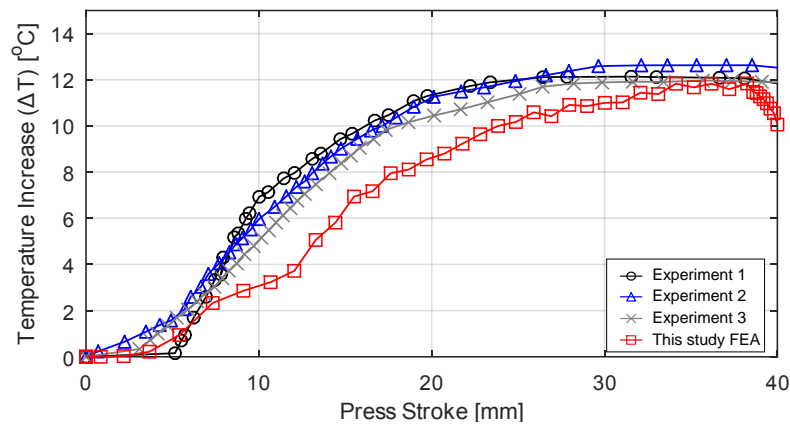


Figure 4. 18. Temperature Increase of the Tools

Some assumptions made in the simulations, explained below. These assumptions will effect the simulation results: (a) the properties of low-carbon steel were used from literature [21]; (b) the heat transfer coefficient which determines the amount of the heat transferred from sheet to the dies was considered as a constant value. However, as determined experimentally, this value is a function of the gap and pressure between the sheet and the die; (c) the sheet and the tools are simulated as surface elements and thermal integration points through the thickness were considered to analyze the heat conduction inside the tools (d) previous studies by Fallahiarezoodar, Peker and Altan has used constant COF and also by Preira and Rolfe used even COF changing with pressure and temperature changing during stamping. In this study; used different method by Autoform Triboform module used and just using mill oil that COF changing with pressure and temperature during draw operation. [7]

For 3 graphs have small deviation between two curves. That occurs from not being used thermal properties of low carbon steel in simulation. That accepted as negligible in software instead of the real values for the specific sheet metal. COF affected from process temperature and pressure during draw operation.

TriboForm is Autoform oil module and that used in this matching study. Since TriboForm software used in this study, COF received as variable according to pressure and temperature effects. So, Figure 4.16, Figure 4.17. and Figure 4.18. temperature distribution obtained that matching with real experiment results very well.

Same simulation method will be used for next studies after making acceptance of above thermal and mechanical properties.



In this section; especially tried to find same results with experimental model, implemented before by Pereira and Rolfe, and FE simulation model. After validation, FE and experimental results, next studies can be progressed.



## 5.SINGLE STROKE FORMING EFFECT

Environment is hard in mass production. Manufacturing time must be faster and material price must be cheaper. That is called more efficiency and that is necessary to reduce good prices. So each input is pushed to make more outputs. In this study; two main study driven in order to understand thermomechanical effects during forming operation. First step is single stroke effects to sheet metal parts and second is multi stroke effects to metal parts that is simulate real life.

### 5.1.FE Simulation Models for Single Stroke

The cup drawing test is an approach to understand drawability condition of process and available to compare some parameters such as press velocity, temperature, pressures etc. In this study, Figure 5 .1 cup dimension used and draw height given as H that is variable parameter.

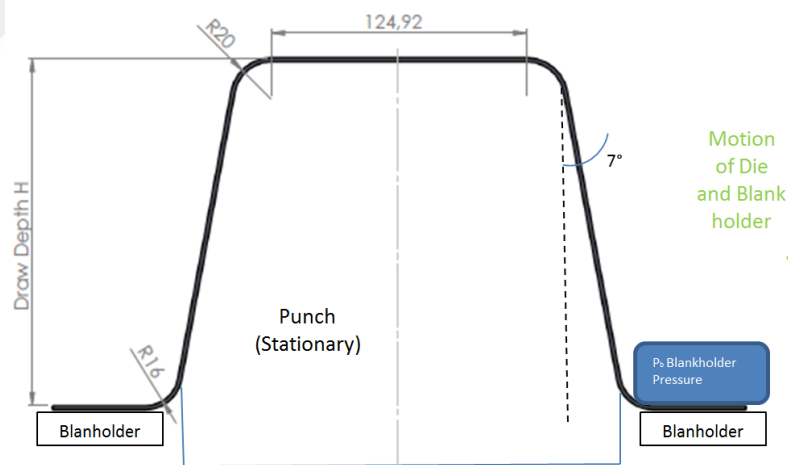


Figure 5. 1.Cup Draw Model Similar to Reference [26]

Similar cup dimensions used with previous publication by Hoschouer et. al., except draw height and wall angle. Previous publication draw height given as 80mm and wall angle is  $0^\circ$  its mean that vertical wall and DP800 part drawn properly [26]. However, in real mass production line and also automotive parts; especially need to wall angle and that preferred minimum  $7^\circ$  according to some vehicle parts investigation.

Same previous study especially focused the lubrication effect on die drawability and that measured by flange perimeter [7]. Extra lubrication affects the part costs, process timing and environment in manufacturing plants. In this study temperature effects especially investigated with regards to drawability without using extra lubrication so flange perimeter is not measured but; draw height measured before part split issue. Maximum drawn height will be shown that the which parameters effects to drawability more than other.

As a first step; die designed in Catia software. Draw die occurs from 3 important points such as; upper die, lower die and binder (blankholder). Blankholder take forces from the bottom side that is a single action draw die. Forces coming from the press machine and if press is not have ability to supply forces, gas spring can use in design phase. Totally 4 air cushion pin added to blankholder. Each cushion pin located actually 90° to each other shown in Figure 5. 2.Upper and lower die press connection points that are defined generally in standards books also related with press machine.

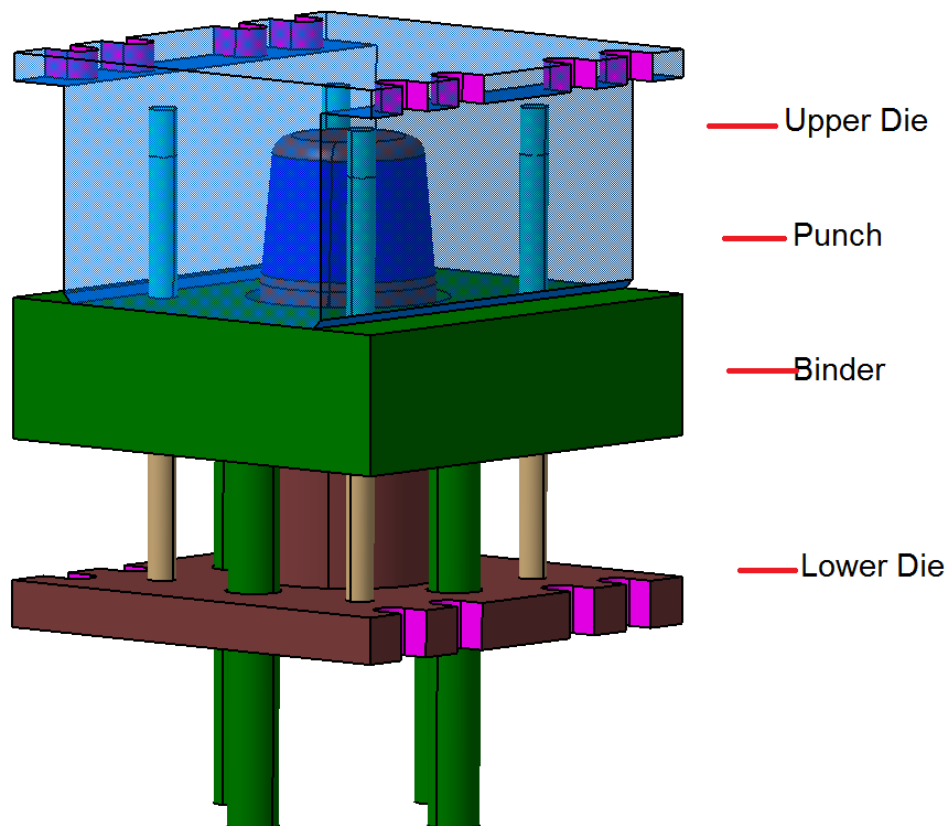


Figure 5. 2.Schematic of the New Die Design

In this design totally 4 guide pin used that helps to locate binder and upper die in same vertical position. If these tool parts are not used, not possible to get correct parts in die. Additionally wear plates using in generally die designs but our test system is small and guide post enough for location but for bigger draw dies, first guidance provided with wear plates and the fine guidance provided with wear plate with lower tolerances.

Table 5. 1. Thermal Properties Used by Pereira and Rolfe [26]

	Tools	Sheet
Density (kg/mm <sup>3</sup> )	$7.7 \times 10^{-6}$	$7.9 \times 10^{-6}$
Heat conductivity (J/s m °C)	22	52
Heat convection with air (W/m <sup>2</sup> °C)	50	—
Specific heat capacity (J/kg °C)	460	480
SHTC (J/s m <sup>2</sup> °C)	20	20
Expansion coefficient (1/°C)	$12 \times 10^{-6}$	$12 \times 10^{-6}$
Initial temperature (°C)	20	20

Proper drawn shell that mean not have split issue with optimum blank diameter, obtained as 80mm height properly issue by using Table 5 .1. process conditions. Draw die height increased from 80mm to 160mm in 10mm height increments and blank diameter as well. Proper drawn shell part obtained for 80mm, 90mm, 100mm, 110mm, 120mm,130mm, 140mm, 150mm and 160mm according to Table 5 .2. Proper drawn shell simulation shown in Figure 5 .3a that is formability results of Autoform.

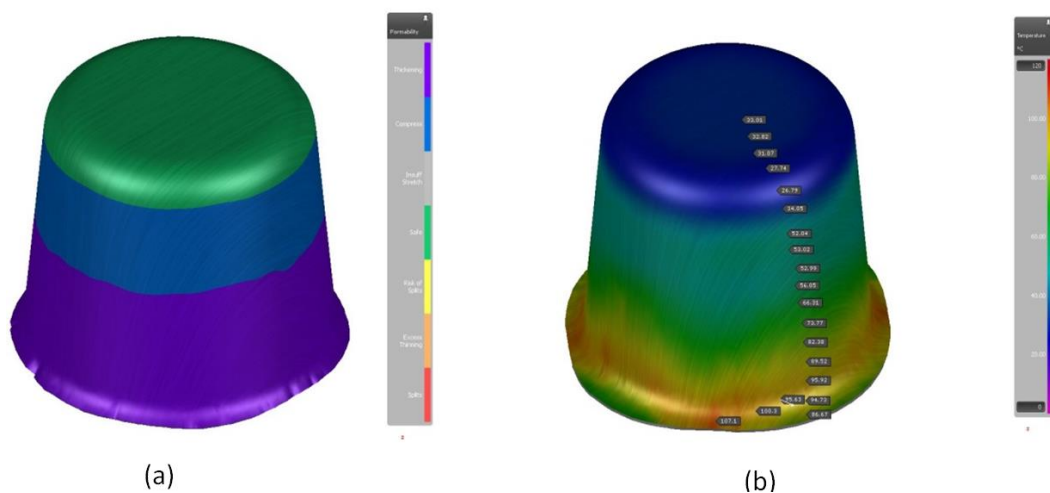


Figure 5. 3.Draw Height 160mm Temperature Distribution

Blank and die surface temperature increasing during draw operation and 160mm draw height condition seen like Figure 5 .3b. Temperature start as 33°C from flat surface and increasing gradually to 107°C in lower radius area. This temperature increasing excessively in case of splitting starting in process. Upper die lower radius reached to 55,12°C end of the operation, lower punch upper radius temperatures reached to 27°C and punch edge of binder temperature increased to 31°C during draw operation for 160mm draw height operation.

Table 5. 2.Process Conditions

	Value	Unit
<b>Material</b>	DP800	
<b>Mat. Thickness</b>	1.6	mm
<b>Blank Diameter</b>	380	mm
<b>Blankholder Force</b>	110	kN
<b>Press Motion</b>	79,35	mm/sn

Even optimized blank dimension and blankholder tonnage given as input to simulation, not obtained proper drawn shell part for 170mm punch height according to Table 5 .2 process condition. After blank sheet metal drawn 115mm of 170mm total punch height, blank splitting and deformed from the upper radius area. Before splitting issue; high temperature observed on the top area of blank. That reached up to 130°C seen in Figure 5. 4.

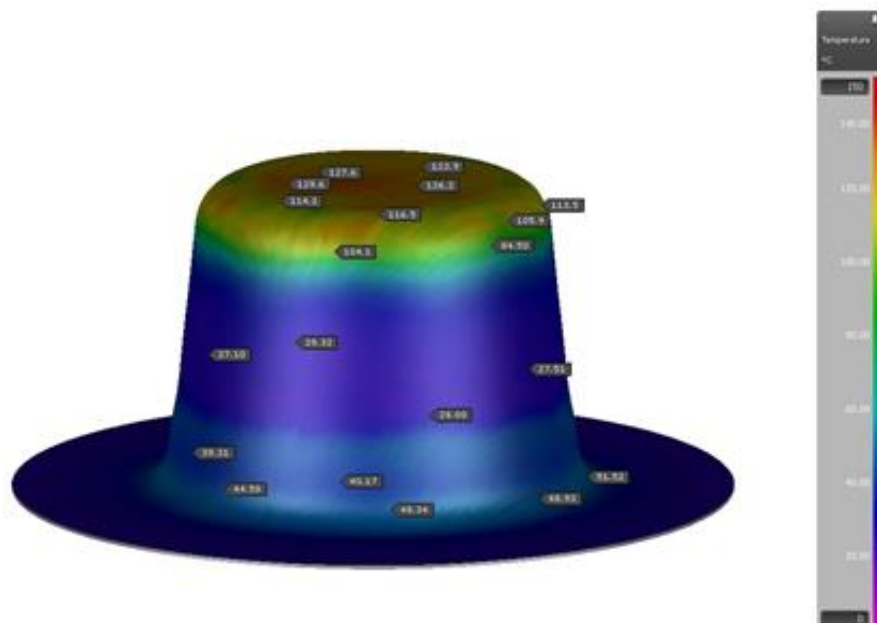


Figure 5. 4.Temperature Distribution on Part Surface Before Split

This prediction gives information about temperature increasing excessively before splitting issue on upper radius area. If continue draw operation even evaluated temperature degree splitting issue starting and punch surface seen in draw operation and sheet metal relaxing with this process shown in Figure 5. 5.

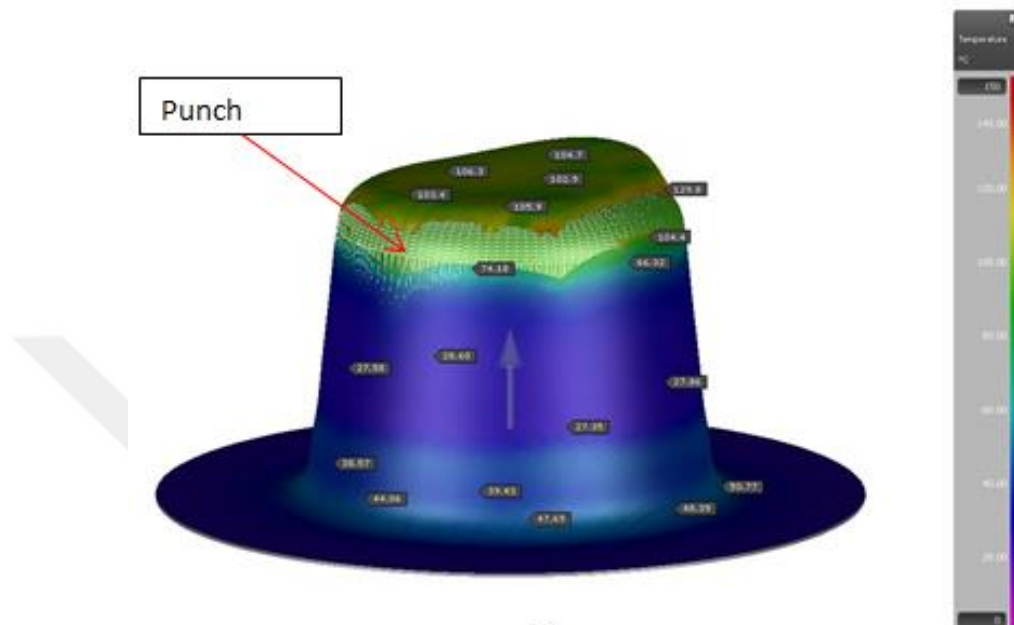


Figure 5. 5.Split Part

This issue showed that not proper to drawability situation in next side of this article and known that while temperature increasing COF increasing as well so to see split issue indisputable. Even adding lubricant will solve the issue since decrease COF before process that makes extra cost and dirty working area.

## 5.2. Analyses of Variance (ANOVA) for Deep Draw Operation

Drawability effected by some parameters such as; press velocity, press tonnage, friction coefficient, material properties, temperature,...etc. but not known which parameters effects more than others. In this study, especially focused on temperature effects for AHSS materials in draw operation. Die cooling, material thickness and press velocity selected as parameters for 170mm height cup draw operation. Cooling effect simulates the upper die and punch have constant temperature that is 20°C in this study. Die has not cooling mean, die own temperature obtained during draw operation. Blank diameter holds constant as 381mm but press tonnage changed. 60kN preload force implemented to 1,2mm thickness DP800 material and 90kN preload force implemented to 1,6mm thickness same material because that is known that material as long as thickness of material

increased, preload force should be increased in order to push to blank properly. In this design of experiment model (DoE) totally three parameters changed during simulation experiments and drawability results get as below. Drawability measured as drawn height before splitting. 170mm drawability results show that; draw operation completed clearly, in other words parts obtained in full stroke press deep draw operation given in Table 5 .3.In this section cooling meaning all die temperature figure out like same temperature. So cooling channel is not used, that is helps to understand temperature effects to die.

Table 5. 3.Design of Experiment Model

Experiment No	Cooling	Thickness (mm)	Press Velocity (mm/sn)	Drawability (mm)
1	No	1,6	79,35	144,66
2	Yes	1,6	79,35	170
3	No	1,2	79,35	141,75
4	No	1,2	11,7	98,27
5	No	1,6	11,7	142,78
6	Yes	1,6	11,7	170
7	Yes	1,2	11,7	170
8	Yes	1,2	79,35	170

The lowest drawability results obtained as 98,27mm. It is mean that after starting to draw operation, just 98,27mm draw height achieved without splitting. So not possible to get proper part according to that process condition. And draw operation completed properly for experiment-2, experiment-6, experiment-7 and experiment-8 and results received in Figure 5.6. by Minitab software.

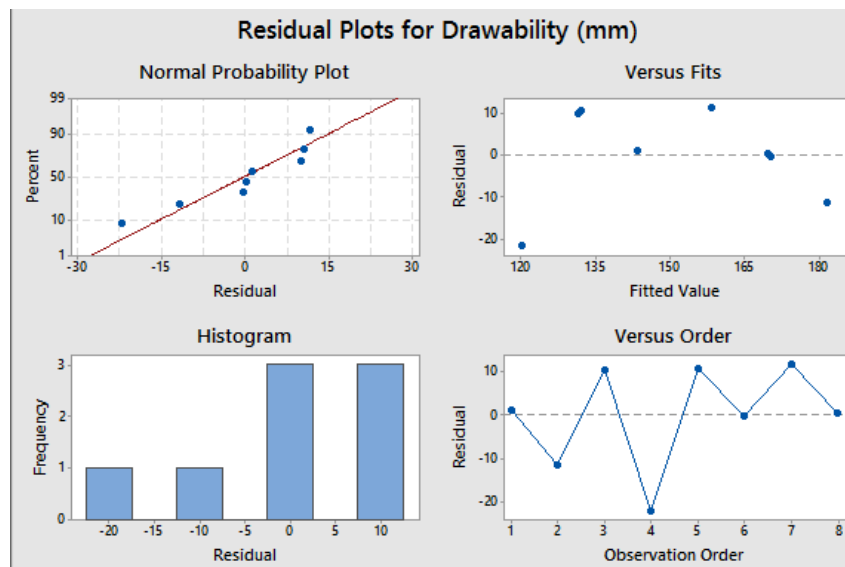


Figure 5. 6.Minitab Software Deviation Results

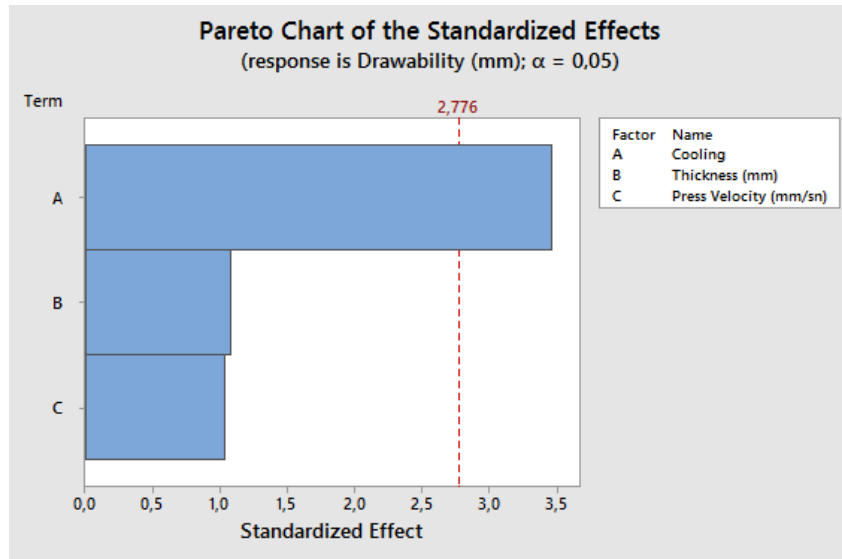


Figure 5. 7.Pareto Analyses Result

ANOVA shows that which factor affects the results more than others in Figure 5.7. In this study cooling effect drawability significantly but others not as much as it. Its mean even thickness or press velocity changed, not effect drawability significantly. Cooling draw operation dominant factor to improve draw operation according to ANOVA investigation.

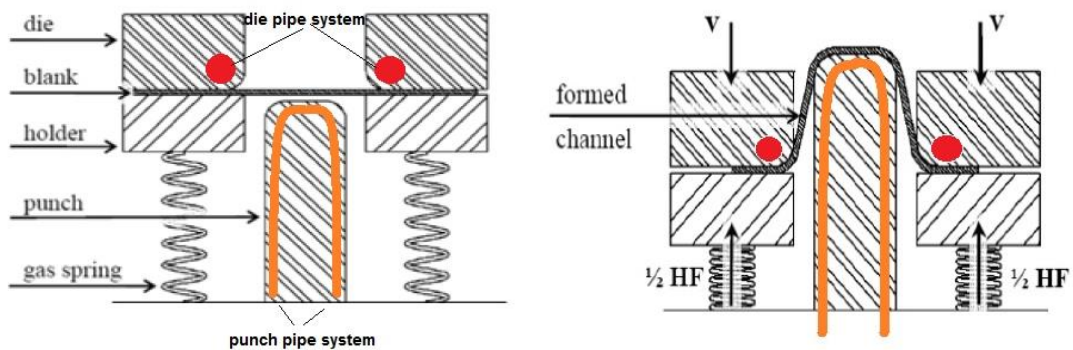


Figure 5. 8.Draw Die Pipe System Estimation

This study not includes if die surface have constant temperature by using piping system what drawability effects obtained. Figure 5 .8. showed to die pipe illustration for conventional draw. These cooling pipes using conventional hot stamping pipes and possible to use deep draw area of conventional stamping dies.

### 5.3.Results of Single Stroke

All result received after using FE simulation software and given in Table 5 .1. In this section die temperature completely put constant temperature that is mean that; all die surfaces have uniform temperature that makes the better quality part. After



understanding temperature effect with this study, next detail study can continue for next steps.

Table 5. 4.Die Temperature and Drawability Relation

Experiment No	Temperature	Drawability (mm)
1	20	170
2	30	155
3	40	153,98
4	50	152,5
5	60	151
6	70	150,23
7	80	147
8	90	146,76
9	100	146,76
10	110	146,76
11	120	146,76
12	130	146,76
13	140	146,76
14	150	146,76

Die constant temperature changed from 20°C to 150°C in 10°C increments in order to see drawn part quality effect by temperature in Figure 5 .9. That shows that high temperature have negative effect for drawability.

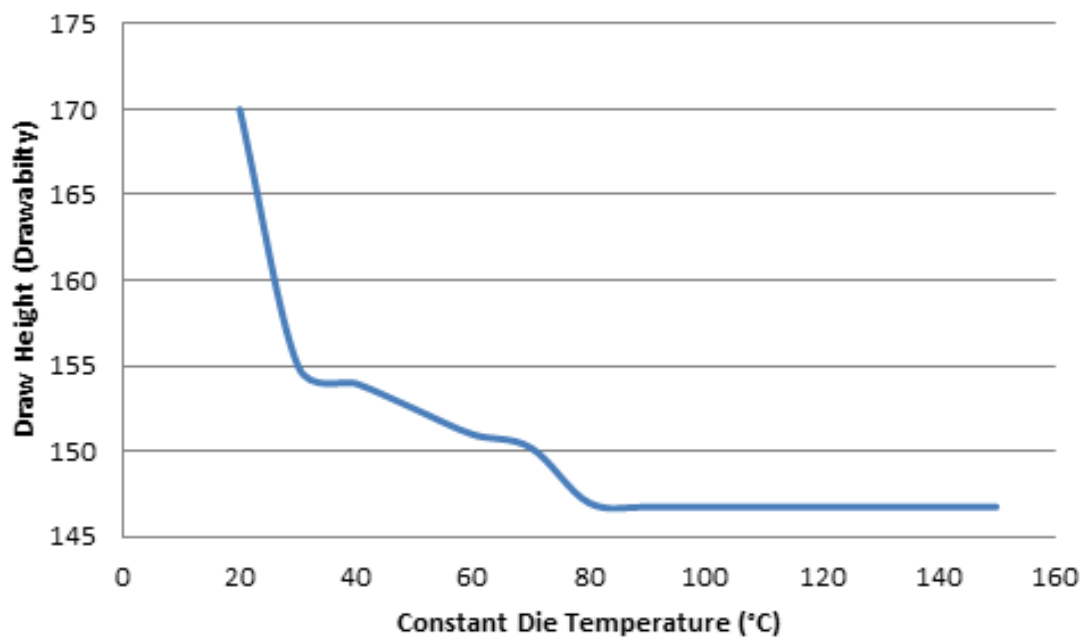


Figure 5. 9.Constant Die Temperature Drawability Effect

While temperature increased; mill oil friction coefficient increased and also mechanical properties of DP800 increased. That is effect to results negatively. If stamping die cooled especially radius areas, that will make positive effect for DP800 material results and will be easy to get drawn part for deep draw process. When die temperature fixed in constant temperature as 20°C, drawn shell can be obtained but if die temperature fized to 60°C, sheet metal just drawn up to 151 mm. While temperature increasing, effect panel drawability quality. Die temperature increasing stoke by stoke, so especially in mass production, die not have enough time for cooling because next sheet metal should pressed. Multi stroke effect will be investigated in Chapter-6.



## **6. MULTI STROKE FORMING EFFECT**

One stroke and multi stroke results should be different in sheet metal process, because while sheet metal temperature increasing during process, die cooling is not allowed because of production speed. So die temperature increased step by step during forming operation [7]. In this step especially multi stroke effect will be investigated.

### **6.1.FE Simulation Models for Multi Stroke**

In this study, the effect of tool temperature on the deep drawing of the DP800 was investigated. In order to measure the effect of die temperature [36] slightly modified. Ju et al. used a flat wall punch. In most automotive applications, the punch typically has a positive wall angle to make the part easier to pull and remove. A wall angle of  $7^\circ$  is quite common, although it varies from room to room. The die set shown in Figure 5 .1 is designed for workpieces up to 170mm deep.

Lubrication (or simulation of friction) affects deep stretch. Most studies use a variety of oil or water based lubricants. "Dry presses" are preferred in the automotive sector for environmental reasons. In the so-called "dry pressing" workshop, the cavities are made with grinding oil without any additional lubricant [37]. Grinding oil is an oil film on the spool to prevent corrosion, usually  $1.0\text{-}2.0\text{g} / \text{m}^2$  during transportation.

In this study, the simulations were made with mill oil only. The coefficient of friction was not chosen as a constant value throughout the part, but the TriboForm plugin was used. An oil of  $1.0 \text{ g} / \text{m}^2$  was selected and the GI Dual Phase friction model was imported from the TriboForm library.

In industrial production, a linked motion press is used for deep drawing. The press has an adjustable frequency converter from 8 to 22 strokes per minute (SPM). The actual stroke time curves of the stamping press in Otosan are shown in red in Figure 6. 1. To study the effect of pressing speed, a mechanical press with the same stroke length and SPM and no joint action was also modeled. The black curves in Figure 6. 1 illustrates these phantom mechanical pressure pulse width profiles.

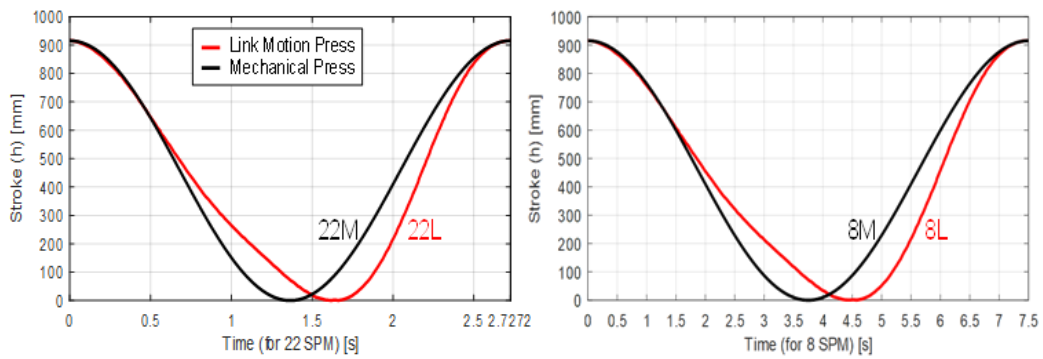


Figure 6. 1.Press Stroke-Time Curves a)Link-Motion b)Mechanical Press

Differences will be simulated between 4 different models:

- 1) Due to the reduced compression speed to 8 SPM, the yield strength will be slightly lower due to the lower strain rate.
- 2) Since the TriboForm plugin is used, the coefficient of friction increases with decreasing speed.
- 3) When using a thermal insert, heat is generated in the cavity (due to plastic deformation) and at the interface between the mold (due to friction). At higher speeds, there is less time to dissipate the heat. Higher local temperatures can occur and soften the steel. but increase the friction.

Due to all of these print speed interactions (SPM and tip), it was determined that there would be significant changes in formability if the spacing force was kept constant between 4 different models. To achieve comparable results, the power of the blank holder was changed to keep the "failure criterion" (FC) as close as possible after the first shot. Table 6.1 shows the parameters and HR values after the first hit. The incoming spaces for each stroke are assumed to be 20 °C. Tools had an equal temperature of 20 °C before the first stroke, but they can store heat after each stroke. Household appliances lose some of their heat to the environment through convection. [32]

Table 6.1.Simulation Parameters and Failure Criteria After First Hit

Short name	Press Speed (SPM)	Press Type	Blankholder Force (kN)	FC after first hit
8M	8	Mech.	78	0.677
8L	8	Link	77	0.675
22M	22	Mech.	80	0.676
22L	22	Link	87	0.679

## 6.2.Results

In the automotive industry, the process is designed to keep the FC value between 0.7 and 0.8 depending on the complexity of the parts. In this study, HR values were deliberately kept very close to 0.7 after the first stroke. Then further cycles are performed until the HR value exceeds 1.0. In this case, the fragment is assumed to be split (error). Figure 6. 2 through Figure 6 .5 summarize the change in FC values and die temperature. The maximum local temperature of each tool surface (punch, die or cavity) is displayed here.

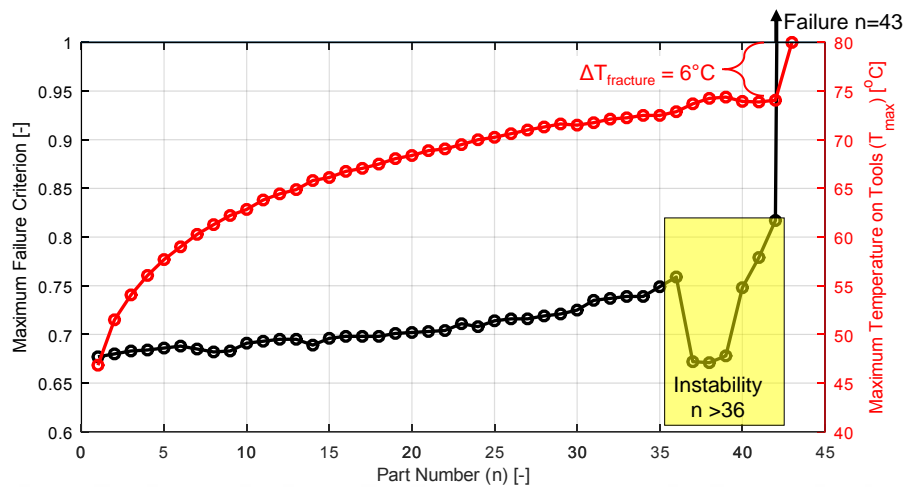


Figure 6. 2.Condition 8M: Failure at 43rd Part with Over

### Appendix-A

Table A shows that, failure criterion and tool temperature increasing during process, that is clearly shows that FC and temperature have relation. That is given also Figure 6.2.

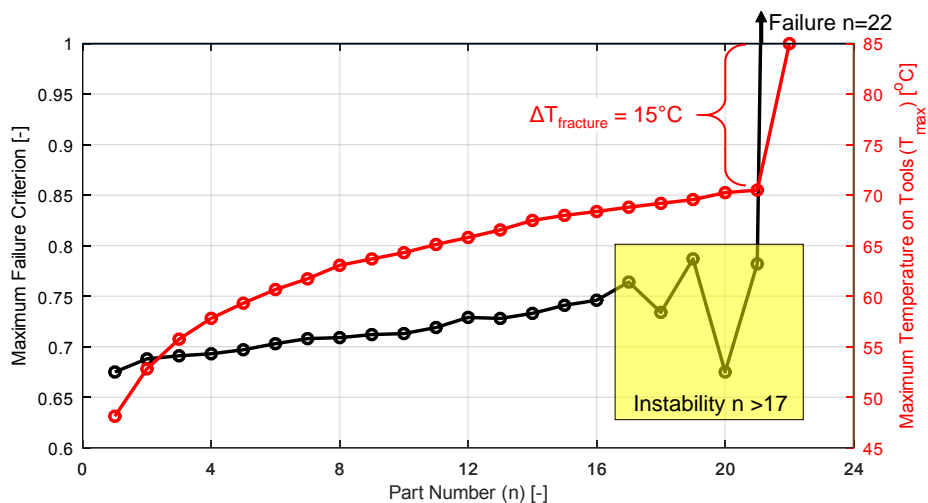


Figure 6. 3.Condition 8L: Failure at 22<sup>nd</sup> Part with Over

Link press results different while comparing mechanical and link press for same press speed that is 8 stroke per minute (SPM). Figure 6.3 contains results of Table B except sheet metal temperature that is seen constant.

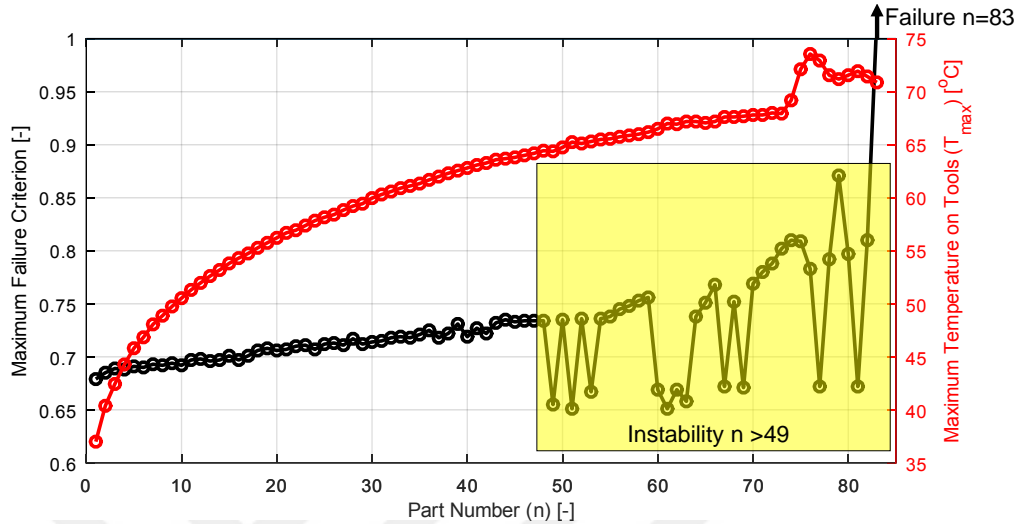


Figure 6. 4.Condition 22M: Failure at 83<sup>rd</sup> Part with Over

22 SPM mechanical press results show that; split of parts occurs after more hits than 8spm and tool temperature increased slower. One reason is, die have not lower time to increase temperature via heat transfer from sheet metal to die surface seen in Appendix-C That helps to reduce heat transfer duration and increase process steps without split issue shown in Figure 6.4.

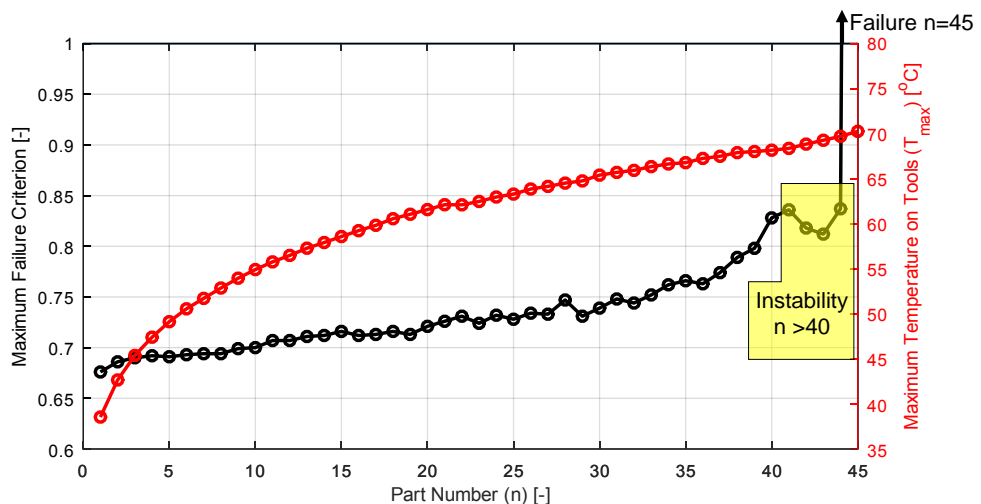


Figure 6. 5 Condition 22L: Failure at 45<sup>th</sup> Part with Over

Lastly Figure 6.5 clearly shows that mechanical press split issue seen earlier in link press according to Appendix-D.

In most punctures the first stroke has a much lower FC value and a heater failure takes much longer to occur (300-500 strokes [25] [39]). The use of extra deep drawing (170mm) and heavy duty steel (DP800) in this custom construction may have accelerated the failure due to die temperature. This was done to (1) reduce simulation time and (2) keep the error below the software limit of 100 cycles.

In any case, a few strokes before the error will lower the HR values. This is called "instability". This may be due to an error in the mathematical model and requires further investigation.

Typically, failure is observed as soon as the mold temperature exceeds 70°C. Waanders et al. At temperatures above 60°C, the coefficient of friction can increase by 40% [25].

Contrary to expectations, the coupling of action presses appeared to be disadvantageous in this study. This can be explained by the increased coefficient of friction due to the reduced sliding speed and the reduced time to dissipate thermal energy when engaging the flushing presses. In fact, the lower impact when building force improves lubrication conditions. Another problem was the downtime: the time of the last segment (hot) and the timeout (cold) that entered the tools. The mathematical model can be developed by measuring the actual dead times in a pressure line.

Sheet metal parts have thinning and crack issue in mass production. In this study especially simulated Ford Otosan Schüller press lines with two different speed as 8 SPM and 22 SPM. Two different press speed tool temperature especially compared shown in Figure 6. 6. That is show that 8 SPM tool temperature higher than 22 SPM from starting of first stroke and continue same gap for next step parallel. In 8 SPM, press velocity slower and heat occurs in sheet metal and transferred to die time-dependent. 8 SPM press motion have more time for transfer to sheet metal temperature to die surfaces than 22 SPM. That's why 8 SPM die temperature higher than 22 SPM.

In production line; especially higher SPM preferred if press allowed to it in order to use manufacturing plant efficiency. That have some limits such as; raw material supply duration or operator quantity. Besides all of them; to get high quality part in press important factor like others.

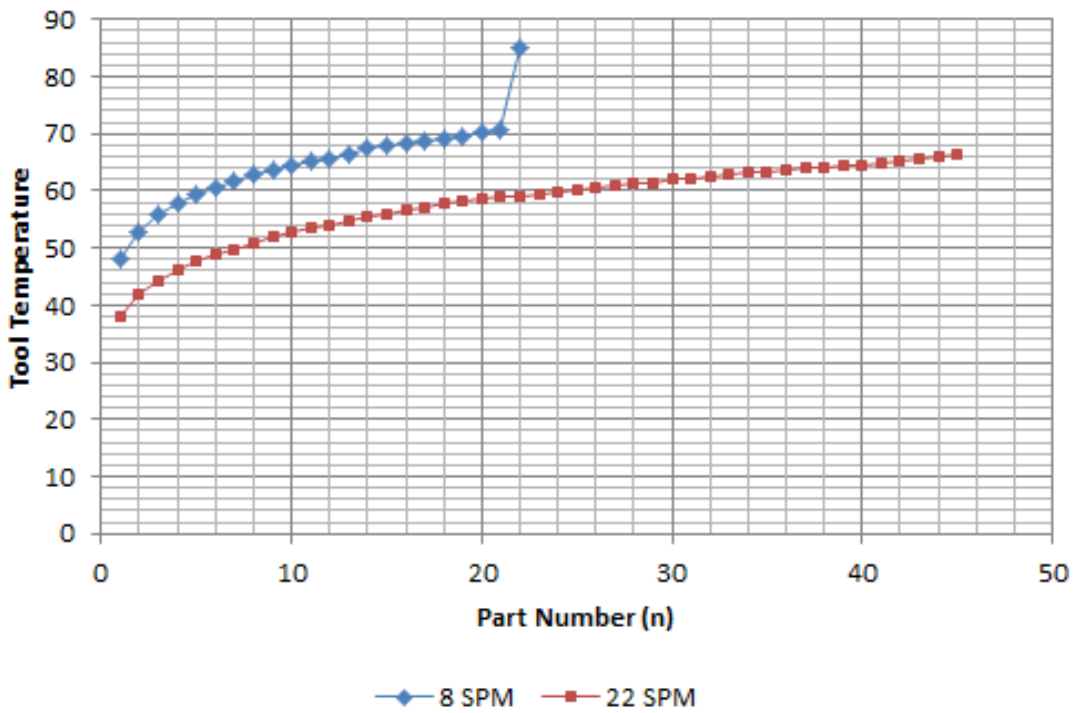


Figure 6.6. Tool Temperature Comparing 8 and 22 SPM for Link Press

Similar condition seen while comparing failure criterion for 8 SPM and 22 SPM given in Figure 6.7. While press speed 8 SPM, split issue seen earlier than 22 SPM because of FC value increased more.

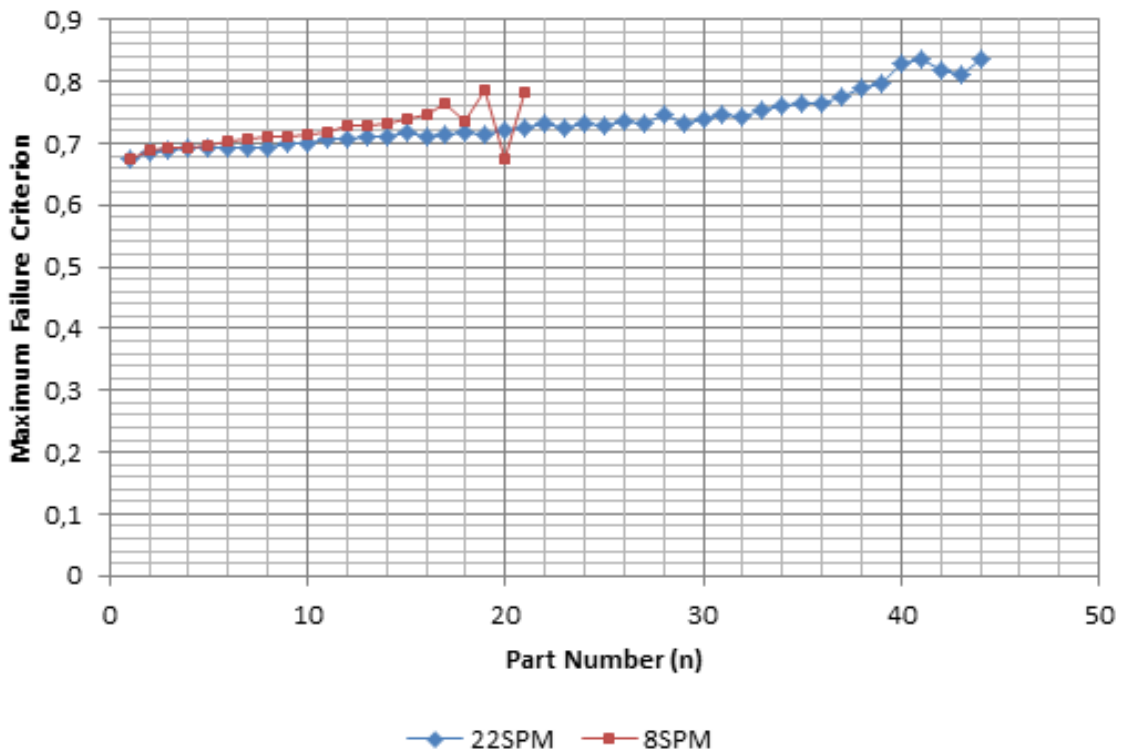


Figure 6.7. FC Comparing for 8SPM and 22 SPM for Link Press



Figure 6. 8 from mass production plant. That part bodyside inner panel of vehicle so that bigger than other parts. This big dimension restricted the automation and press speed, while part hit in 12 SPM, wall split issue seen more than higher press speeds. Besides low press speed effect efficiency of manufacturing lines negatively, also affect part quality.



Figure 6. 8.Wall Split Issue in Mass Production in 12 SPM

Figure 6. 6 shows the maximum local temperature of the cavities after each stroke, except for the fracture. As expected, blank temperatures were higher at 22 SPM. At low SPM, the cavity drawn in a compound agitation press will have a lower temperature. As with the HR values, the maximum temperatures seem to drop in the last strokes before the break. It is important to note that the material map only shows flow curves up to 100°C . An extrapolation was used above this temperature.

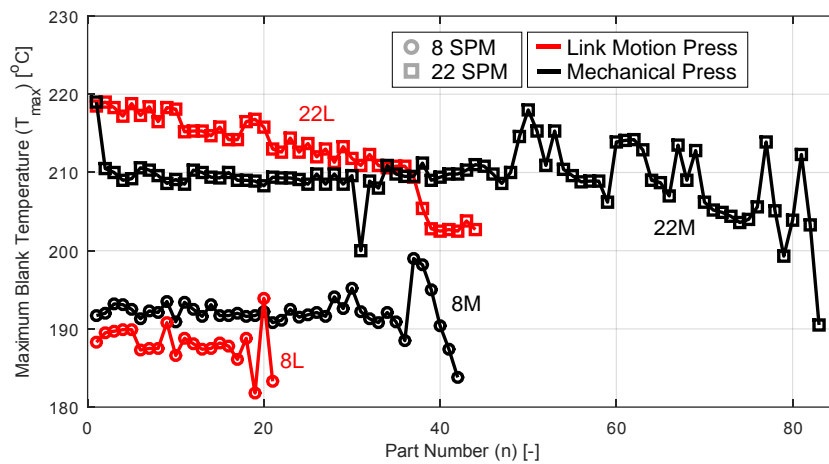


Figure 6. 9. Maximum Blank Temperature in All 4 Conditions

Additionally friction coefficient investigated during one operation as an example in Figure 6. 10. That is mean that; friction increased in multi-stroke operation so one point on blankholder selected randomly and friction coefficient investigated during draw operation from 11mm to 118mm draw height. Totally cup height is 170mm.

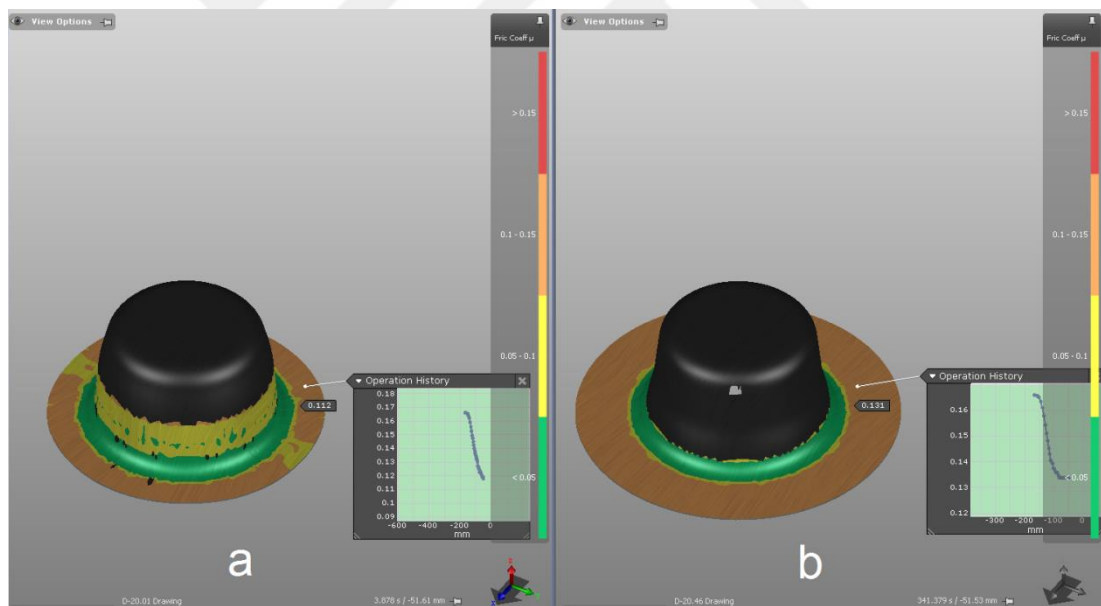


Figure 6. 10. Friction Coefficient a) 1st stroke b) 22th stroke

This cup can be drawn in 1st operation as 170mm but that have split issue in 23rd operation. Randomly one point selected in blankholder area and friction coefficient checked during operation for 1st operation and 23rd operation. That is also shown in Figure 6. 11, friction coefficient continues same up to 64mm draw height. But after than; 23rd stroke friction coefficient between die and sheet metal not decreased even 1st stroke continue to decrease. All parameters selected according to first

stroke results like all vehicle part feasibility. But when some inputs changed in process like friction coefficient, that effect directly to part quality.

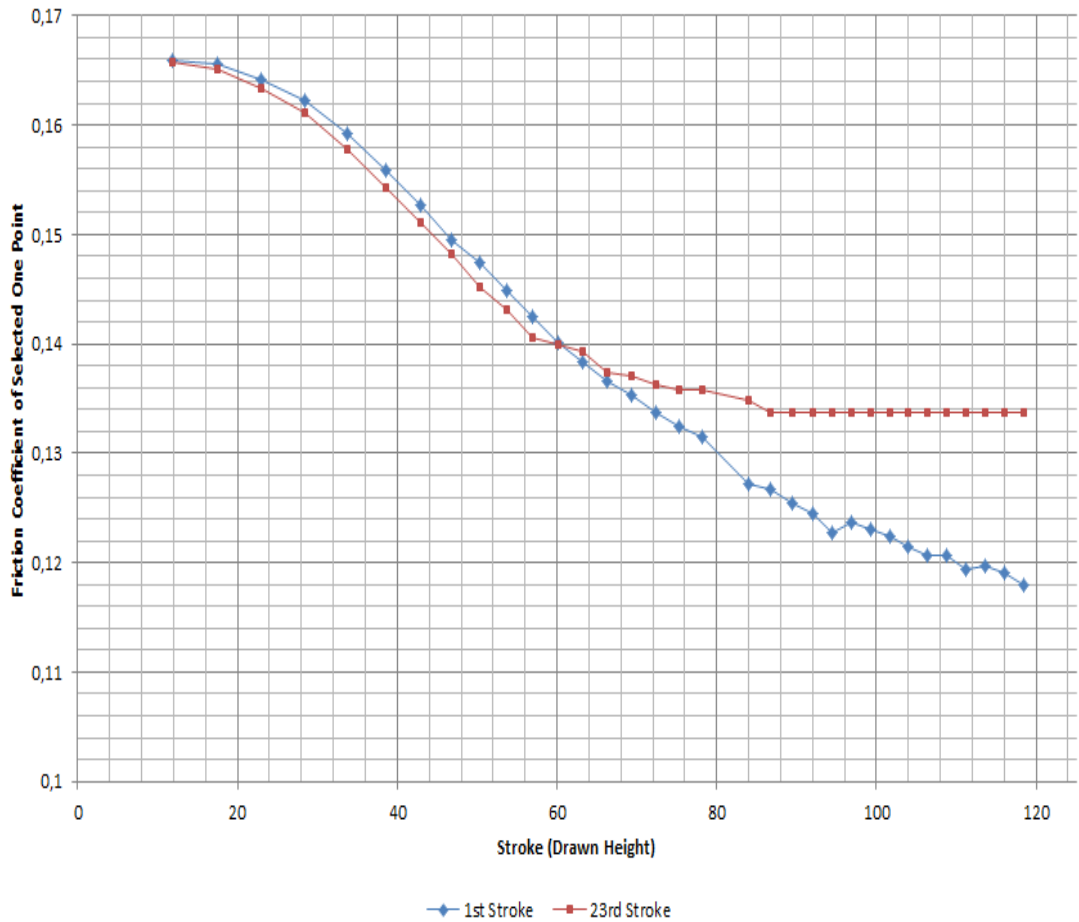


Figure 6. 11. Multi Stroke and Single Stroke Friction Effect

Multi stroke effects modeled in Figure 6. 12 that is called as Akcan Dead Loop with this study. That model shows that; first operation can start proper process conditions like oil, temperature and press specs and also all feasibility studies can be confirmed before die construction however after more operation, process condition changing that is uncontrolled area. One choice is to reduce automation speed. Namely; after getting part from die end of the operation, new blank should put the die after passing time that helps to reduce die temperature by air. That is not favorite method because of decrease mass production speeds.

Today all die manufacturer companies and automotive manufacturers should be aware of not correct to make a prediction with single stroke effects of die. Especially deep draw and high yield strength materials simulations should be simulated via real automation and multistroke input datas.

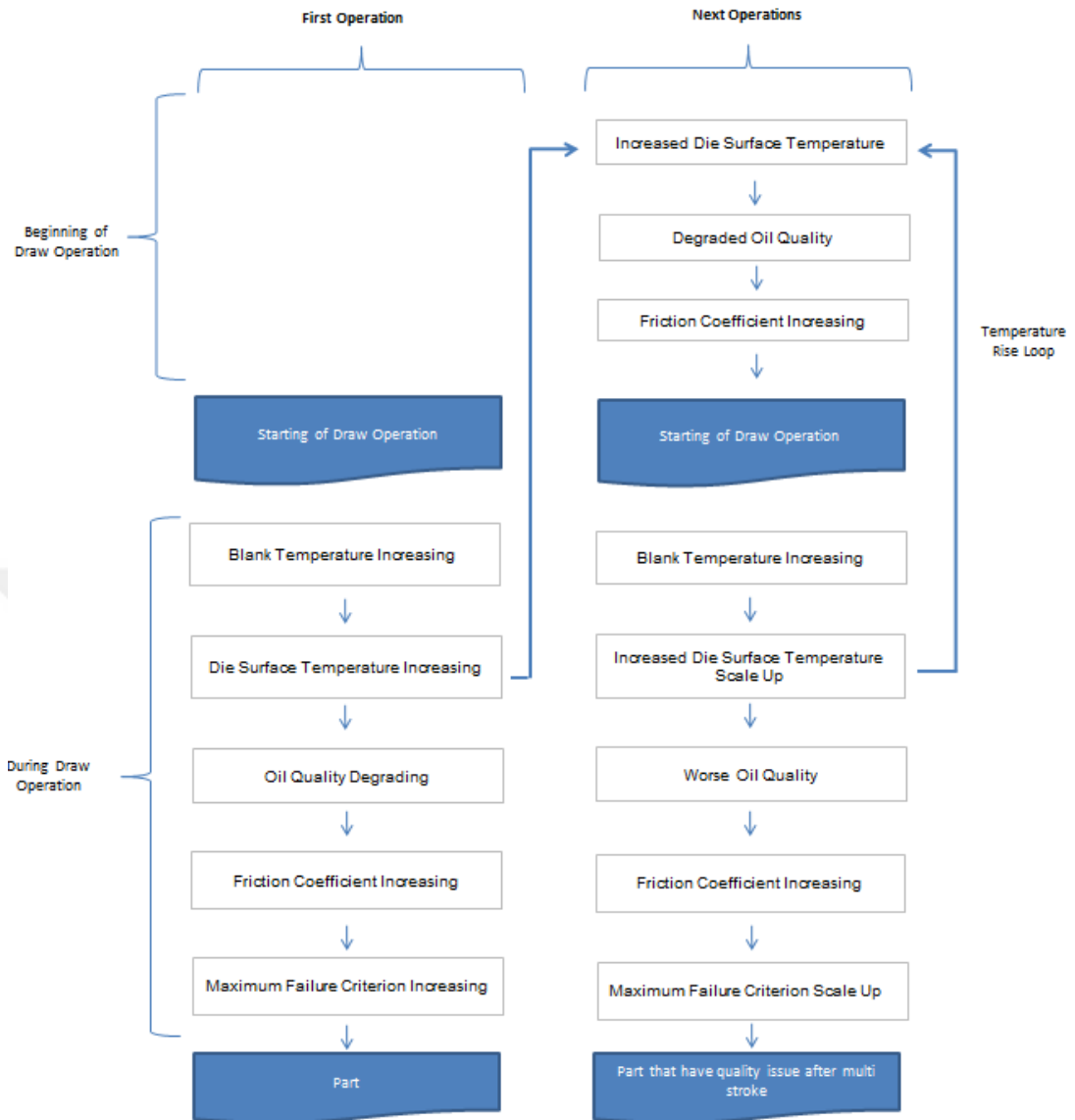


Figure 6. 12.Akcan Dead Loop

Figure 6.12 clearly shows that, same loop increase all negative factors and helps to obtained low quality parts.

## 7.COOLING SYSTEM FOR COLD STAMPING DIES

Conventional die design shown in Figure 7 .1 occurred with experience and engineering calculations by all automotive manufacturers or die makers. That includes rib dimension, die dimensions, standard parts, die materials, quality, coatings, bushes, electrical and air equipments, etc... It is mean that even lots of point of these standards is same for years, some of them added or revised after some experiences from press plants.

AHSS materials still hard for die makers because not predictable exactly for simulation softwares and not easy to change results because high point yield and tensile strengths. But automotive manufacturers and car design engineers want to work more with AHSS in order to get lighter house in the market. So die must be designed beyond the conventional die design methods.

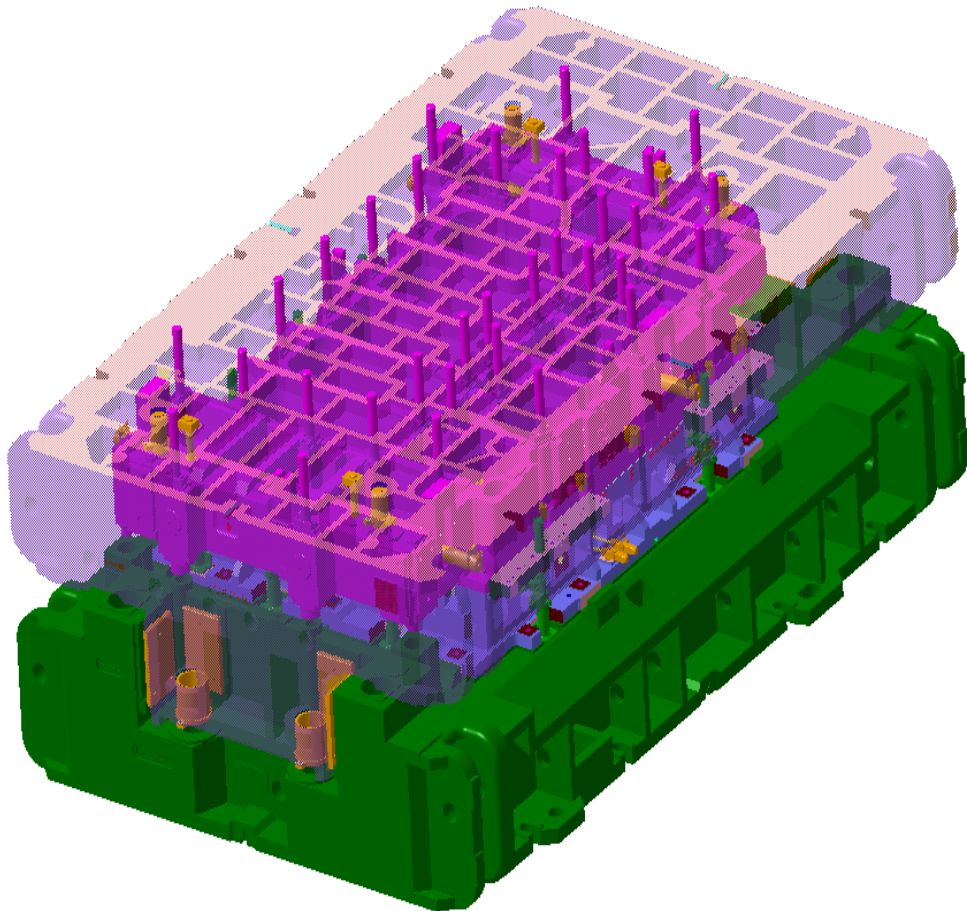


Figure 7. 1.Conventional Die Design Picture

While sheet metal temperature increasing during draw operation, temperature should be decreased with a system.

Hot stamping system has good examples for cooling in die. Hot stamping method occurs from three important points in drawing. The first step is heating the sheet metal parts that called the austenization station before draw operation. In austenization step; sheet metal temperature increased to 900°C-950°C that makes the part softer. After than part drawing by die and after drawing operation; sheet metal temperature decreased from 950°C to 850°C during handling and forming steps. Before die opening, cooling system try to reduce sheet metal temperature to 170°C. Generally each process steps can be summarized as austanization phase is 3-5minitues, handling of the components 5-10 seconds, cooling phase is 15-25 second. Each station duration is important to get proper part shown inFigure 7 .2.

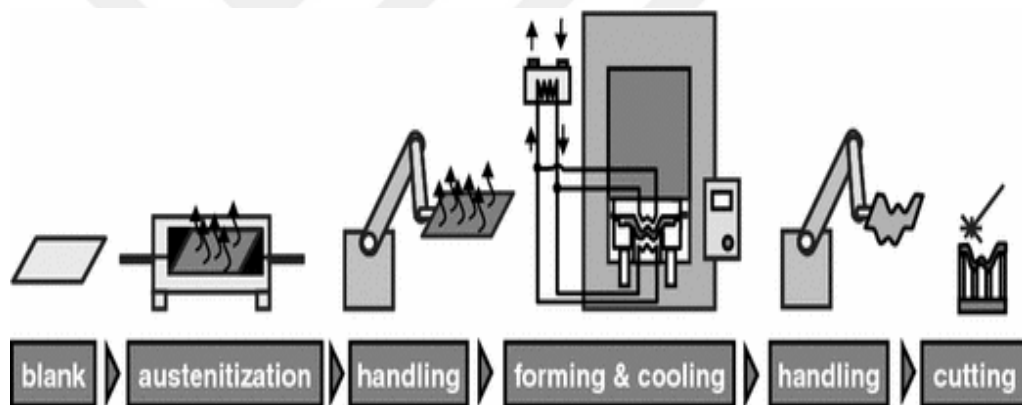


Figure 7. 2.Hot Stamping System [40]

That system developed by years by die makers in order to get faster system for efficiency in production line. Optimization studies and standards about hot stamping cooling system helps to design new cooling system for conventional cool drawing operation. [40] [41]

### 7.1.Cooling Channel

Convectional die design have two important factor about heat transfer that is heat transfer from sheet metal to die and second factor is heat transfer within die that's mean that die has big volume and mass so, temperature will distribute inside all volume that effect to receive heat amount and heat flux.

This system will be work in cool stamping system if pipes putting in die design phase in new project.

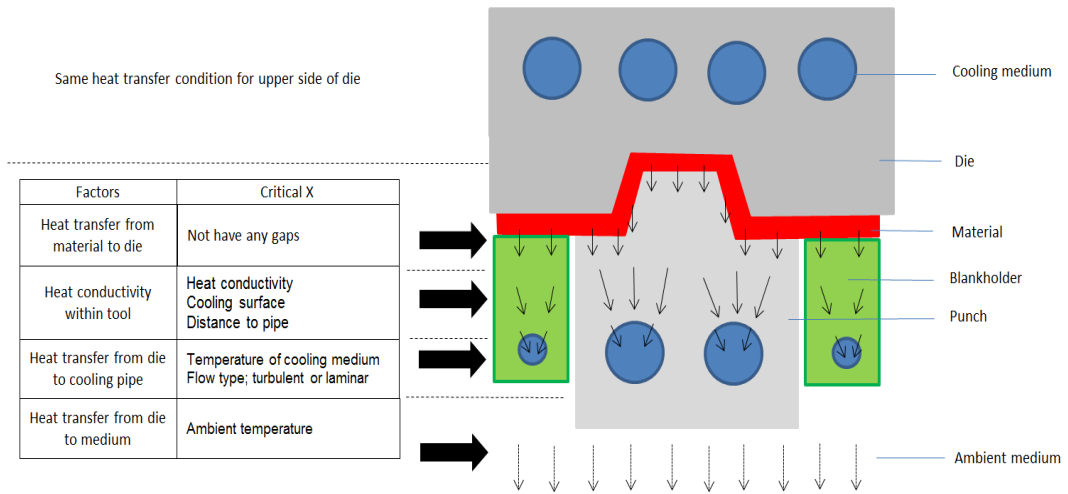


Figure 7. 3.Heat Transfer Condition In Case of Cooling Pipe

Even Steinbeiss, So, Michelitsch, Hoffmann study include first three step heat transfer mechanism not include from tool to ambient heat transfer that helps to reduce die temperature additionally ambient temperature will be effect to panel quality so that heat transfer mechanism added to this study in Figure 7 .3. Additionally; cooling rate accepted as 27K/second in that study. [41]

## 7.2.Laminar or Turbulent Flow

Pipe in the stamping die will be used in this study and coolant fluent will be used during process in simulation software. As a first step; water should be used in order to understand main effect and requirements in study and that will be changed according to results.

In a tube flow have two options as laminar or turbulent. These are have different results in process regarding heat transfer and flow condition. Reynold number defines the flow type that is laminar or turbulent flow. Fluent type, pipe diameter and flow velocity has important role to define flow type given to Equation 7.1;

$$Re = \frac{\rho v_m D}{\mu} = \frac{v_m D}{\nu} \quad (7. 1)$$

If Reynolds number lower than 2300, fluent type can be laminar. Flow not changed directly to turbulent flow, so this area called as transitional flow that is between 2300 and 10000. If Reynolds number higher than 10000 that is called as turbulent flow in process.



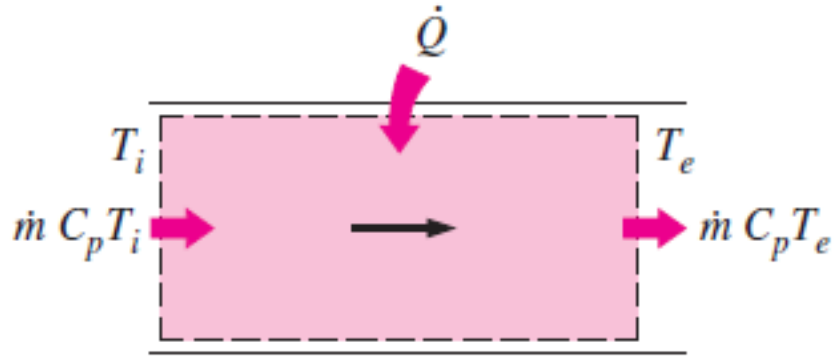


Figure 7. 4.Heat Transfer in Pipe Process

Heat transfer condition shows in Figure 7. 4. Pipe system reduces the temperature or increase the temperature according to medium temperature gap. If this gap is high, heat flux will be higher. Energy balance equation written as generally.

$$\dot{Q} = \dot{m}C_p(T_e - T_i) \quad (7. 2)$$

In laminar flow, velocity can be found like below;

$$\vartheta(r) = 2\vartheta_m(1 - \frac{r^2}{R^2}) \quad (7. 3)$$

so

$$\vartheta_{max} = 2\vartheta_m \quad (7. 4)$$

The stamping die coolant pipe system has lots of corner and high velocity so Turbulent flow investigation approach is better to find solution. Circular tube, laminar ( $T_s=$  constant) shown like below;

$$Nu = \frac{hD}{k} = 3,66 \quad (7. 5)$$

Nusselt relations between heat convection factors (h), pipe diameter (D) and conductivity of the coolant like below;

$$Nu_i = \frac{h_i D_h}{k} \quad (7. 6)$$

and

$$Nu_o = \frac{h_o D_h}{k} \quad (7. 7)$$

In case of turbulent flow in pipe system, heat convection factor written as hc and the important factors as below;



$d$  is diameter of the tube,  
 $C_p$  is the heat capacitance of the coolant,  
 $k$  is conductivity of the coolant,  
 $\rho$  is the density of the coolant,  
 $v_m$  is the mean velocity of the coolant,  
 $\mu$  is the viscosity of the coolant.

$$h_c = Nu \frac{k}{d} = 0.023(Re)^{0.8}(Pr)^{0.33} \frac{k}{d} \quad (7.8)$$

Re and Pr inserted to Equation 7.6;

$$h_c = 0.023 \left( \frac{\mu C_p}{k} \right)^{0.8} \left( \frac{v_m \rho}{\mu} \right)^{0.33} \frac{k}{d} \quad (7.9)$$

Hence,  $h_c$  received as below;

$$h_c = 15 \frac{kW}{m^2 \cdot K} \quad (7.10)$$

Heat transfer parameters entered to Autoform simulation program that calculate all variations during forming operation. Where average water temperature defined as 1°C, flow rate 50ml/min and pipe diameter is 14mm [27].

### 7.3.Cooling Channel Design

Conventional dies face heating issue and that increase failure criterion value and parts split issue seen in manufacturing lines. This issue seen automotive mass production lines and control by operators. Sometimes operator can't catch issue end of press line and vehicle would be manufactured in mass production and seen issue end of welding line or assembly line. That makes high cost effect and quality risk.

Ford Otosan which is one of the lighthouse automotive factory in the world set up whistle tracker system and try to catch splits part in press line. Additionally other automotive factories plans to set up image processing system in order to find deformed parts before sending them to other plant.

Cooling system offer to solve all split issue for AHSS and other sheet metal parts such as mild steel. Figure 7.5 shows the mass production issue of parts. Even end of press lines have inspection station, human can miss some issue in fast manufacturing speeds. First picture about door inner panel split issue, that can be

seen other station of vehicle. Figure 7 .6 shows the sheet metal part split issue and lastly Figure 7 .7 shows the big dimension part split issue.



Figure 7. 5.Sheet Metal Inner Part Split Issue



Figure 7. 6.Sheet Metal Split Issue



Figure 7. 7.Large Dimension Sheet Metal Part Split Issue

As a first step; cup draw test developed with cooling pipes in FE simulation software. Autoform R8 used for this study. Although that software heat transfer simulation developed for hot stamping die simulations, that used for cold stamping dies in this study.

Figure 7 .8 shows that new developed cold stamping dies that have cooling pipes. Punch and die have pipe system, blankholder not have any cooling system. This study aims to understand cooling effects to sheet metal parts quality and drawability.

Section 6 results gave information; sheet metal parts face split issue after multi operation that is change according to press speed and press type.

Cooling pipes should be inserted to die design before casting but before of that, die should be design properly to piping system. Especially split issue area seen in radius areas, so that surfaces should be defined in design phase. In design phase, designer should increase casting thickness according to this information.

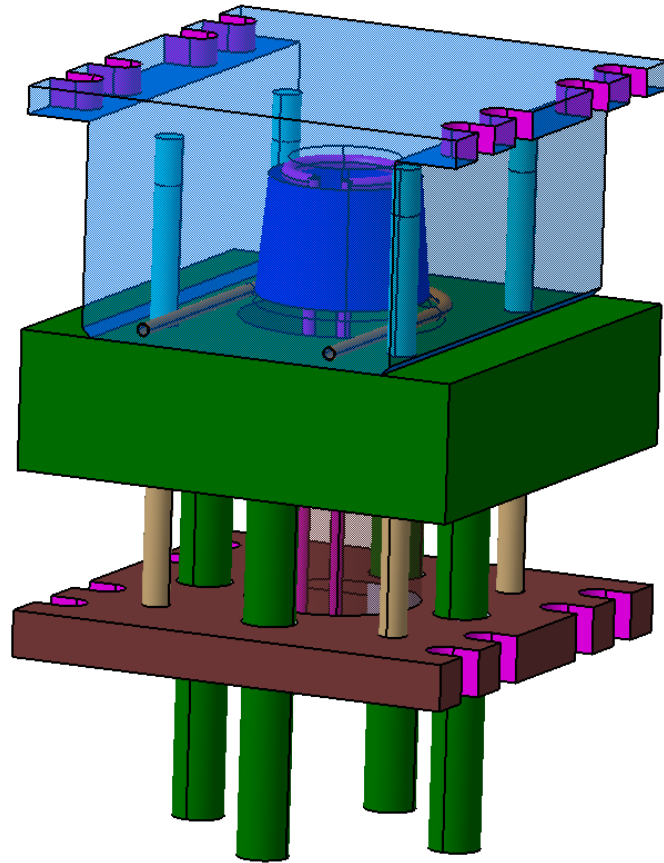


Figure 7. 8.Cup Drawing Model with Cooling Pipes

Figure 7 .8 shows die close position it is mean that sheet metal drawn in that position and upper die ready to go back for open position. In order to show better pipe routes, Figure 7 .9 and Figure 7 .10 shows the upper die and punch pipe pictures.

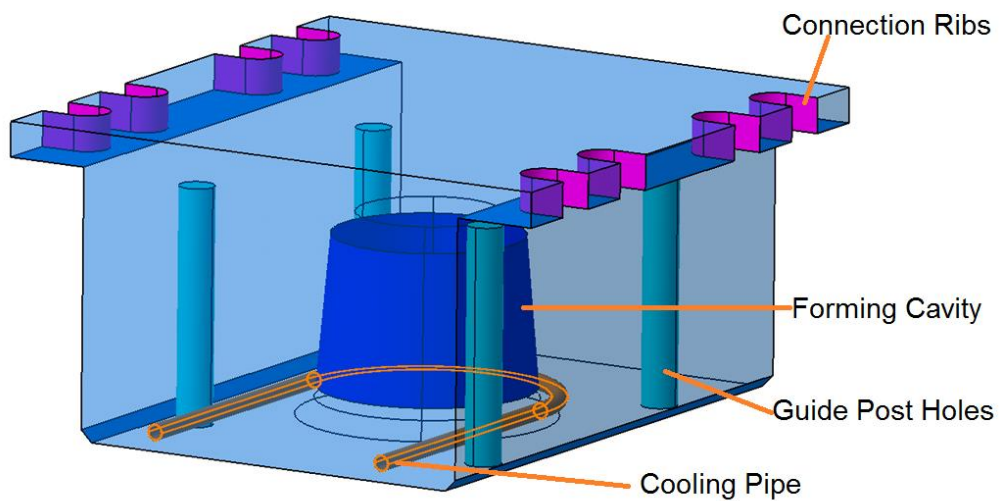


Figure 7. 9.Upper Die Pipe Route

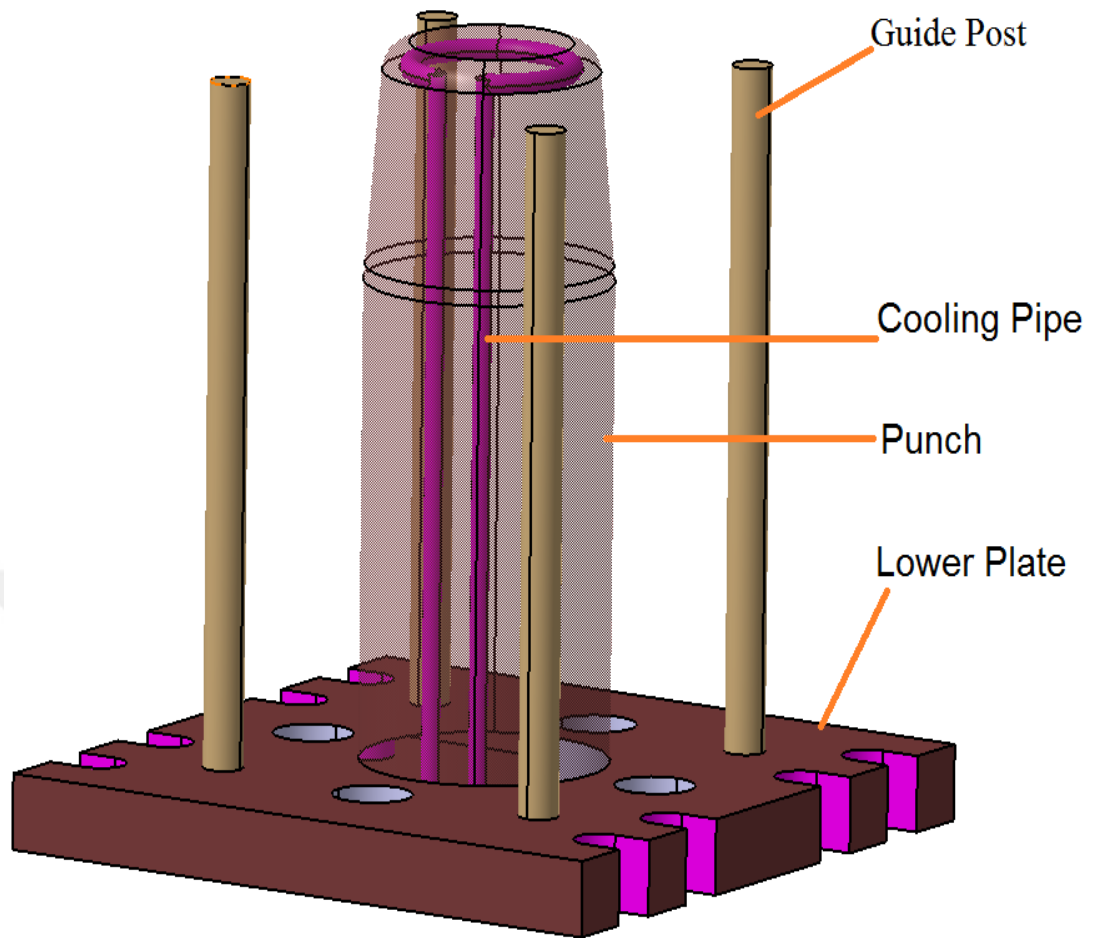


Figure 7. 10.Punch (Lower Die) Cooling Route

#### 7.4.Mathematical Model of Cooling Channel

Temperature increasing in draw operation and that increase the friction coefficient and die temperature. Increased die temperature affect the next cycle mill oil quality and that affect the draw quality. That is called as Akcan Dead Loop. Some precaution should be taken such as; automation speed decrease, extra oil added in before/after draw operation.

Second choice of precaution to be sent parts to customer is put an inspection point in end of the press lines. Normally; each press line have inspection point, sometimes human eyes missed the unsuitable parts, so automatic visual control or sound control application increasing day by day but none of them not solve the root cause.

Third precaution of this issue to control all input parameters before process such as; sheet metal thickness, mill oil volume, medium temperature, press speeds, etc. After defining optimum parameter tolerances, in case of out of tolerances, stopping the

process and parameters should be changed. That is hard system for mass production.

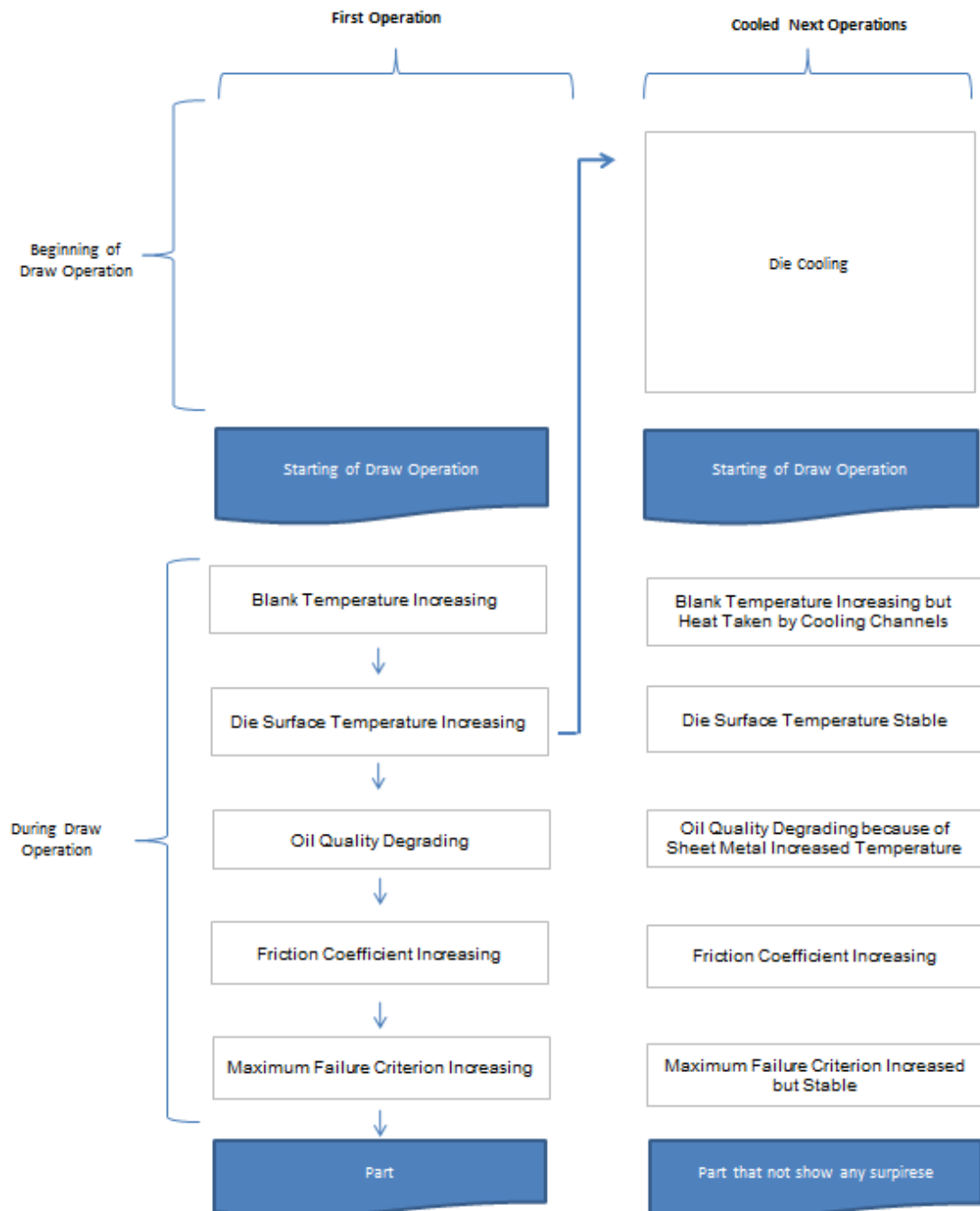


Figure 7. 11.Cooled Die Design Flow

That is sheet metal and tool temperature loop similar dilemma chicken came from egg or egg came from chicken. If reduce the temperature by using coolant pipe in draw operation; root cause will be removed before occurring.

### 7.4.1. Cooling channel formula

While defining some parameters before starting the cooling analyses mathematical model shown as below according to Figure 7.12.

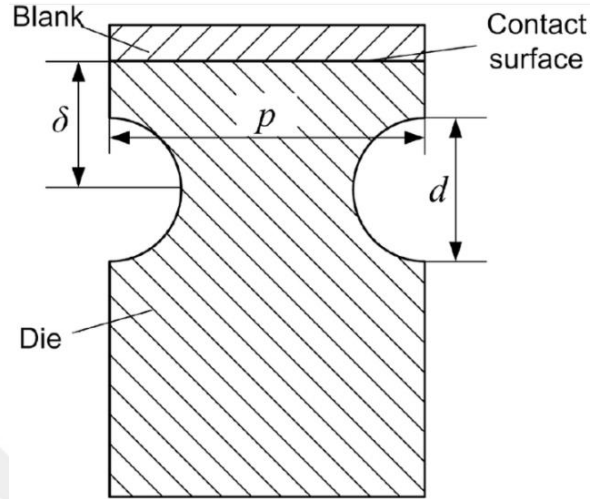


Figure 7. 12.Simple Model [15]

Pipe diameter, pipe distance from top surface and distance between two pipes is important parameters for especially bigger dies.  $Q_B$  is total blank heat loss given;

$$Q_B = C_{p,B} m_B (T_{B,1} - T_{B,2}) + m_B L \quad (7. 11)$$

Where  $C_{p,B}$  is the specific heat of the blank  $m_B$  is the mass of the blank,  $T_{W,1}$  initial temperature of sheet metal and  $T_{W,2}$  are the final temperature of the sheet metal part.

All heat not absorbed by water, so  $\varphi$  define the loss rate by water.  $Q_W$  define water heat absorption.

$$Q_W = \varphi Q_B \quad (7. 12)$$

Water total heat defines as;

$$Q_W = C_{p,W} m_W (T_{W,2} - T_{W,1}) \quad (7. 13)$$

Where  $C_{p,W}$  is the specific heat of the water,  $m_W$  is the mass of the water,  $T_{W,1}$  initial temperature of cooling system and  $T_{W,2}$  are the final temperature of the coolant fluent. Hence, for cooling system minimal coolant fluent need  $m_W$  that is water in our study;

$$m_{W,\min} = \frac{Q_W}{C_{p,W}(T_{W,2} - T_{W,1})} \quad (7. 14)$$

Additionally  $m_w$  can be calculated as below;

$$m_w = \frac{\pi}{4} n d^2 \vartheta t_c \rho_w \quad (7.15)$$

where cooling channel quantity defined as  $n$ , channel diameter defined as  $d$ , water speed defined as  $v$ , cooling time defined as  $t_c$ , water density defined as  $\rho_w$ . So;

$$\frac{\pi}{4} n d^2 \vartheta t_c \rho_w \geq \frac{Q_w}{c_{p,w}(T_{w,2}-T_{w,1})} \quad (7.16)$$

Cooling total area can be written like below;

$$A_c = n \pi d l \quad (7.17)$$

Cooling channel length defined as  $l$ , formula can be written as;

$$d \geq \frac{4 Q_w l}{c_{p,w} \vartheta t_c \rho_w (T_{w,out} - T_{w,in}) A_c} \quad (7.18)$$

where Equation (7.11) and Equation (7.12) can be added to Equation (7.18) as below;

$$d \geq \frac{4(C_{p,B} m_B (T_{B,2} - T_{B,1}) + m_B L) l}{c_{p,w} \vartheta t_c \rho_w (T_{w,out} - T_{w,in}) A_c} \quad (7.19)$$

Although turbulent flow increase to heat transfer, if  $Re$  over than 10 000, heat transfer effect decreasing, so upper and lower limit of Reynolds number can be restricted between 4 000 and 10 000 as below;

$$Re = \frac{d \rho_w \vartheta}{n_w} \quad (7.20)$$

where  $n_w$  is water viscosity coefficient. So  $d$  can be restricted because of flow type like below;

$$4000 \frac{n}{\rho_w \vartheta} \leq d \leq 10000 \frac{n}{\rho_w \vartheta} \quad (7.21)$$

As a summary Equation (7.19) and Equation (7.21) helps to find  $d$  diameter in draw operation. [15]

#### 7.4.2. Cooling channel quantity

In order to get enough cooling area, pipe area should be more than contact blank area. That can be written like below;

$$A_c = \alpha A_B \quad \alpha \geq 1 \quad (7.22)$$



If Equation (7.17) written to Equation (7.22), n can be written;

$$\mathbf{n} = \frac{\alpha A_B}{\pi d l} \quad (7.23)$$

Two pipe distance “p” can be determined after get cooling channel quantity “n”.

### 7.4.3. Cooling channel distance from contact surface

The heat flux written as below;

$$\Phi = \frac{\varphi Q_B}{t_c} \quad (7.24)$$

If die have just one channel, the heat flux can be written as;

$$\Phi_0 = \frac{\varphi Q_B}{n t_c} \quad (7.25)$$

Shape factor can be written as below;

$$\Phi_0 = \lambda_D S (T_{D,A} - T_{D,2}) \quad (7.26)$$

S is defined as shape factor, die surface temperature defined as  $T_{D,1}$ , wall of the cooling channel defined as  $T_{D,2}$ . According to this approach, contact between blank and die surface have zero air. That will be effect the heat transfer effectiveness. So making this calculation via paper not easy. Because each time; contact relation, heat transfer condition, temperatures changing. Following equation can be written;

$$T_{D,1} = T_{B,1} \quad (7.27)$$

Cooling channel wall temperature  $T_{D,2}$  can be thought average temperature of the water channels;

$$T_{D,2} = T_W = 0,5 (T_{W,1} + T_{W,2}) \quad (7.28)$$

Shape factor “S” can be written as;

$$S = \frac{\Phi_0}{\lambda_D (T_{B,1} - T_W)} \quad (7.29)$$

### 7.4.4. Cooling channel optimization

As soon as understanding, cooling effect and cooling channel need to cold stamping dies, pipe channel construction thought. Thanks to hot stamping works that helps to find the best method and feasibility studies. Cooling channels using in hot stamping dies for years but not have any information these are using for cold stamping dies or not.

Generally pipe diameter defines between 8mm to 20mm for hot stamping dies. Some practical studies show that small pipe dimension gave the better result for panel quality in hot stamping dies. Figure 7 .13 clearly shows the result by using Abaqus thermomechanical simulation results. Also some optimization method implemented that is related to cooling pipe positions that is necessary for get the best result. As mentioned above; calculating all heat transfer during mechanical simulation without software [15]. Abaqus, LS Dyna and Autoform are example models to get results.

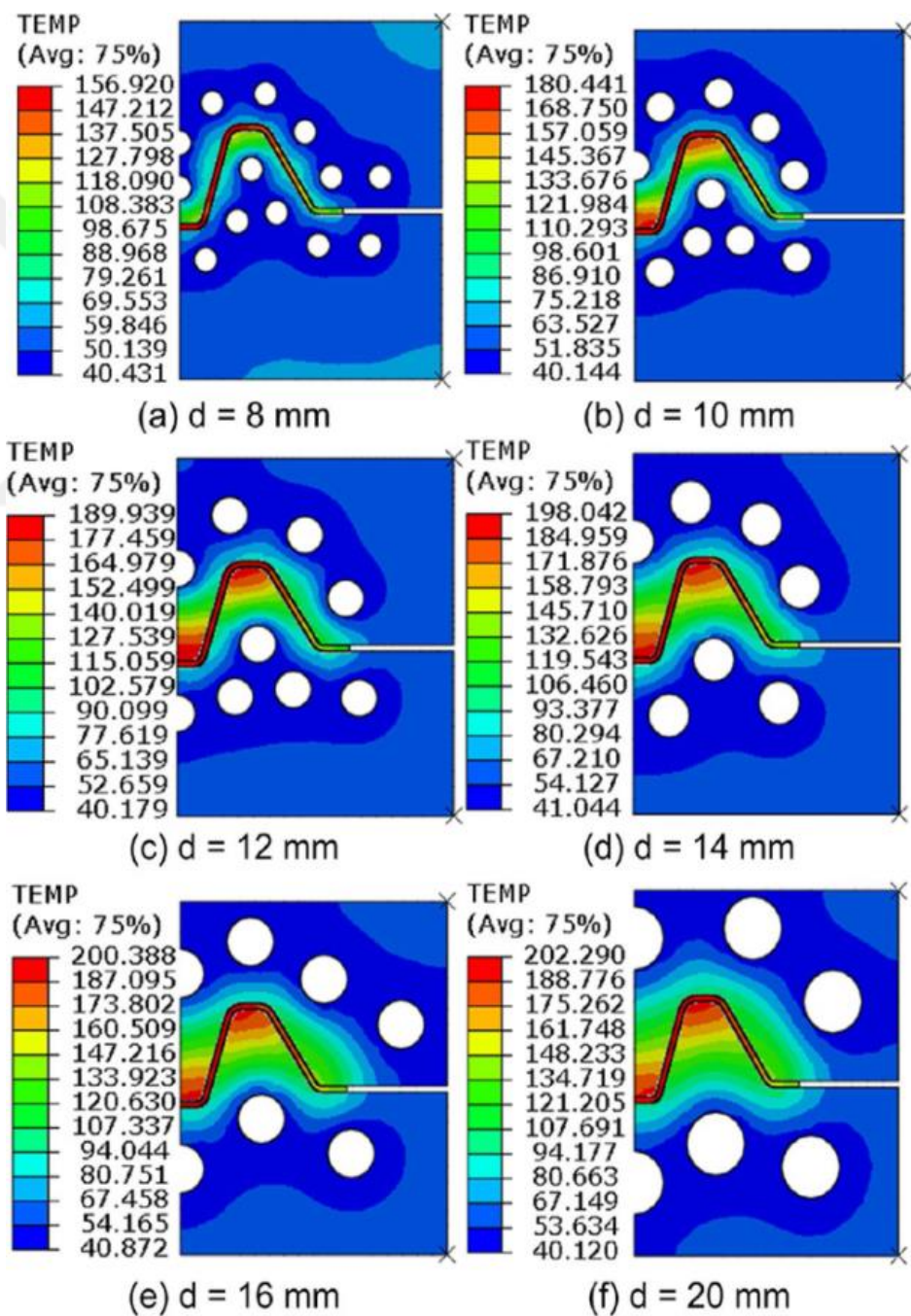


Figure 7. 13. Temperature Distribution After 8 Stroke [15]

One different study implemented by Shang and Pang [42] , they try to find the best pipe configuration by using FE simulation software. Figure 7. 14 clearly show that optimization effect to die surface temperature. Especially radius area faces the higher temperature because forming occurring in radius areas. In picture, pipe positions changed and maximum tool temperature decreased from 83,5°C to 69°C. [42]

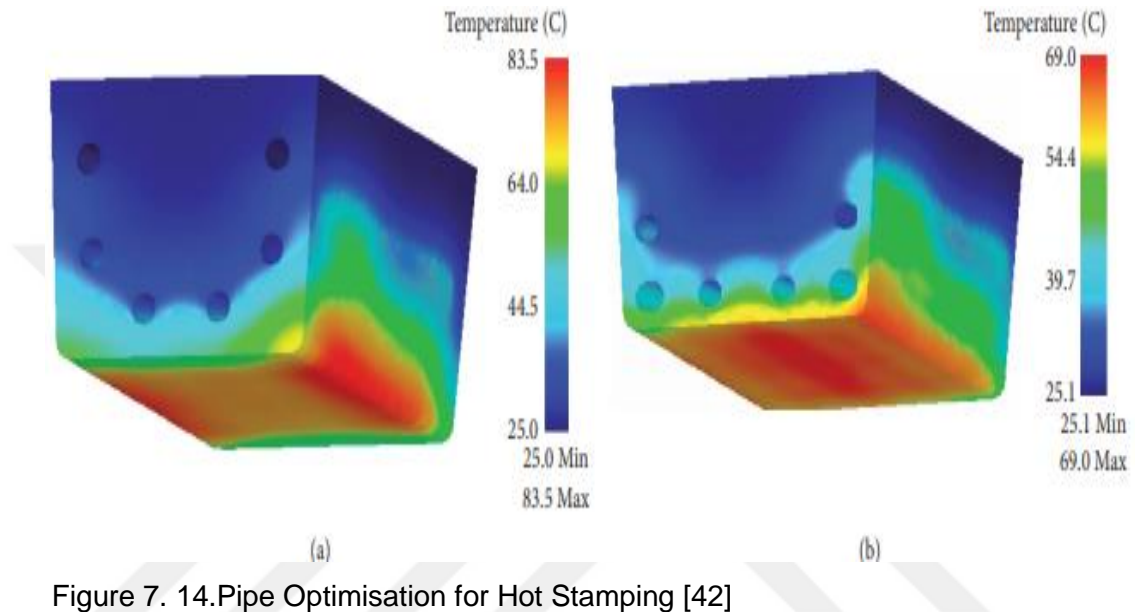


Figure 7. 14. Pipe Optimisation for Hot Stamping [42]

In this study, average pipe dimension prepared in order to see average effects of cooling systems, so 14mm dimension preferred.

Pipe inlet temperature defined as 1°C and outlet temperature is same in this software because that makes the simplification. According to software route is short so not have extra outlet temperature. Multi stroke repeat in same condition of Chapter 6. Cooling system working with same time starting of draw operation. Punch and die have cooling pipe and during closing and opening operation cooling of die continue.

### 7.5. Results of Cooling System in Multi Stroke

Multi stroke conditions are more close to real results. Same process conditions just not have cooling operation, blank material splits after 22th stroke. Because failure criterion increased stroke by stroke. Cooling system investigated and seen that although sheet temperature similar with uncooled system, die temperature and FC is in Appendix-E.

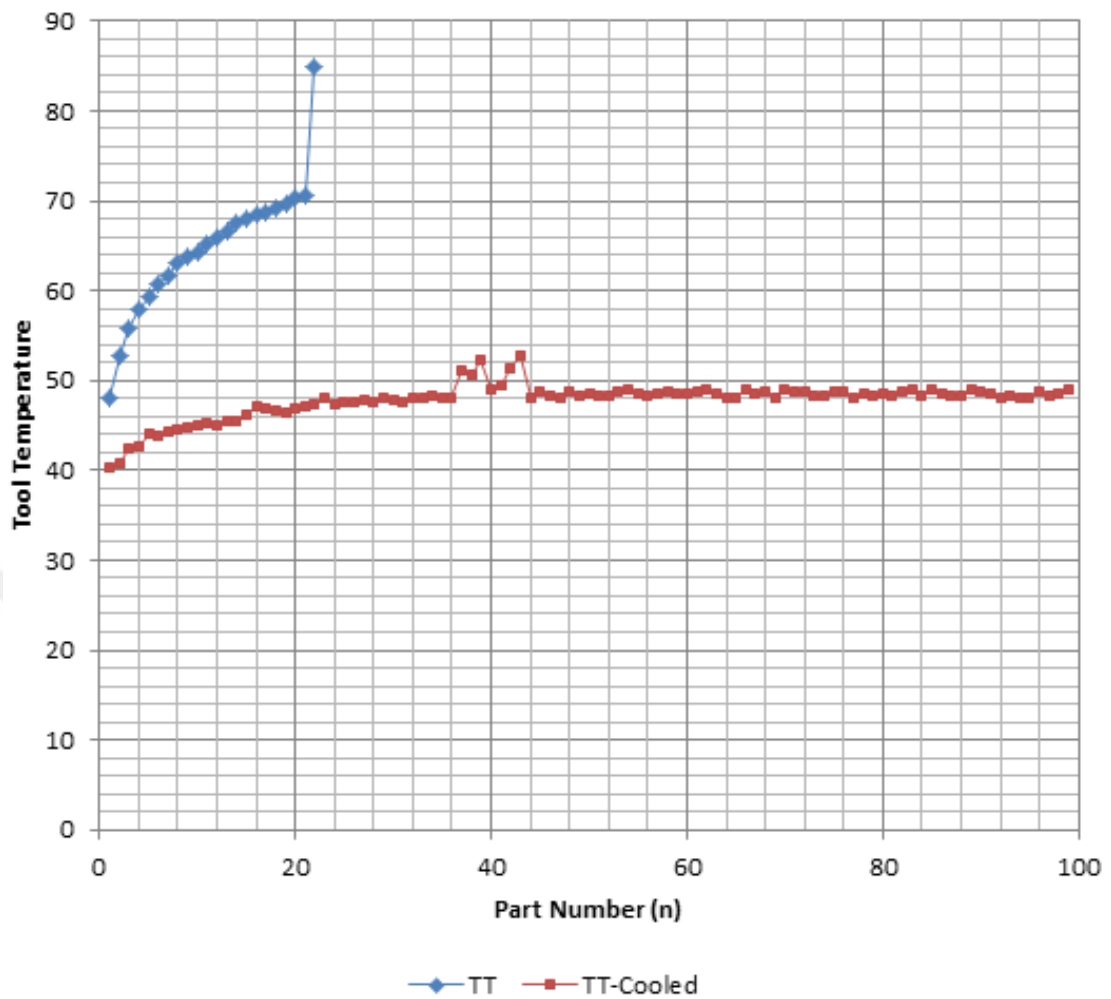


Figure 7. 15. Temperature Condition 8 SPM Link Press

8 SPM link press similar press type in mass production. Tool temperature (TT) is important item during draw operation because that affects oil quality and friction coefficient value negatively. While friction coefficient increasing, blank can not move between blankholder and upper die. Figure 7 .15 comparing tool temperature results not cooled and cooled die system. As written in section 6, part split issue seen 22th stroke so, tool temperature is not continue for next operation. In this section, die cooled during draw operation and not seen split issue for 99 strokes. Conventional draw operation; tool temperature increasing from 48°C to 70°C and after than increasing too much in split step. New cooling concept; die temperature start from 40°C that is first advantage fort his study. After increasing about 10°C temperature is not bigger than 50°C and steady stable condition seen clearly. Some parameters should be changed such as pipe dimension, fluent type and fluent temperature, pipe route,etc... that is optimization methods and better to find the best method for mass production die before design step.

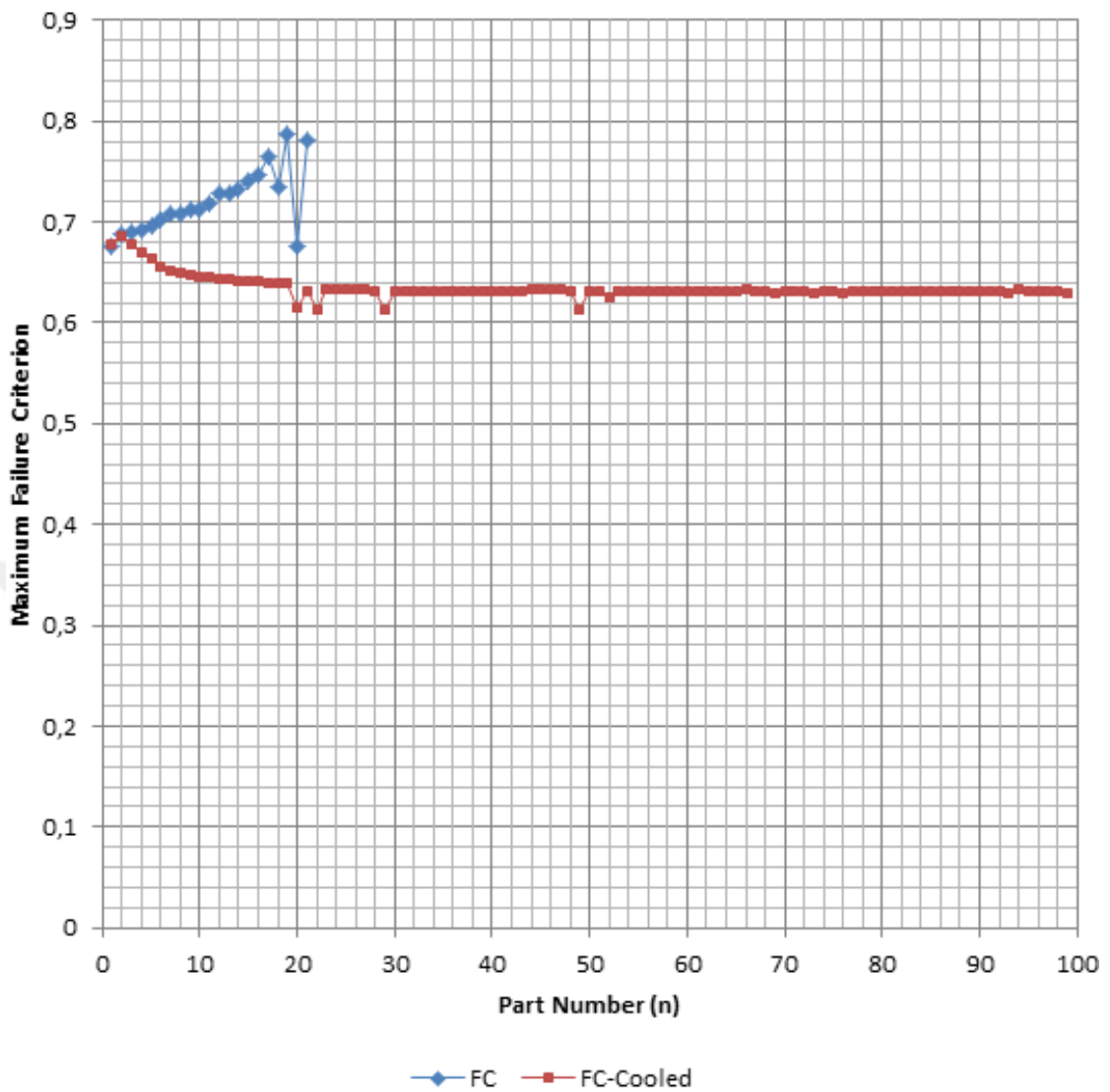


Figure 7. 16.FC Condition 8SPM Link Press

Similar condition seen in Figure 7 .16 results but inverse direction. It is mean that failure criterion (FC) increasing for conventional draw die operation that makes to parts split issue obviously. In new method of cooling die design shows that; FC value reduced in first 20 strokes. After that stable FC results received that is similar to temperature chart.

Mechanical press and link press have different stroke time so in order to understand mass production effects, trial repeat in mechanical press in Appendix-F.

Figure 7 .17 shows the totally 99 stroke operation for mechanical press that have same closing and opening time and results a little bit different. Sheet metal temperature seen stable during operation but FC and TT have different values. That condition explained in results.

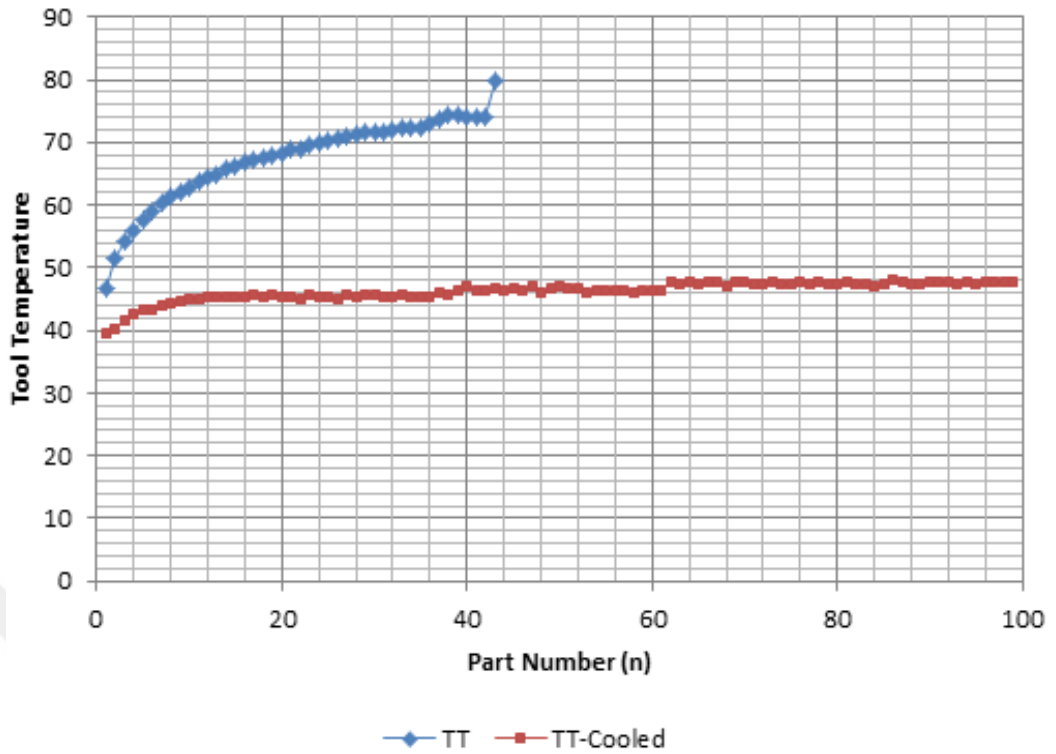


Figure 7. 17. Temperature Condition 8 SPM Mechanical Press

Conventional die temperature increasing during draw operation and in 8SPM mechanical press 43th stroke split condition seen so not continue the steps after 43th stroke. New cooling concept implemented for mechanical press and stable seen condition after 20th operation seen in Figure 7 .17

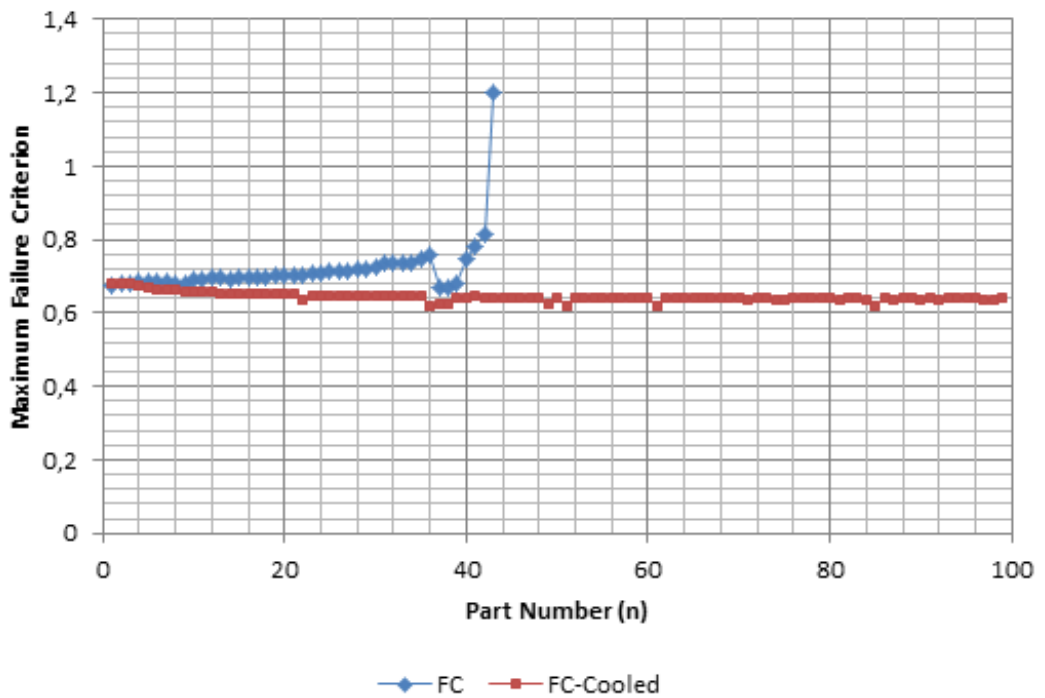


Figure 7. 18. FC Condition 8SPM Mechanical Press

FC without cooling system last value changed from over 3 to 1,2 in order to show better all Figure 7 .18. Similarly FC value increasing up to 43th operation but in cooling system, operation continue to 99th stoke. AutoForm software not allowed continuing over to 99th but that will be developed for next years.

22 SPM include high press speed in mass production, automotive manufacturer companies want to produce with higher velocity their products with robot system. Table include simulates mass production condition, that shows that FC value started as 0,676 and reduced to 0,646 sheet metal temperature started as 218,2°C and temperature continue similar during operation and completed with 216,8°C tool temperature started with 33,22°C and completed with 42,28 after 99 stroke.

Tool temperature compared with conventional die and cooled die according to FE results in Figure 7 .19. Conventional die temperature started with 38,15°C to process and that increasing stroke by stroke gradually. Last operation 44th operation and temperature reached to 65,85°C. And split issue seen 45th operation in process. Cooling system graph investigated during 99th process and correct parts get for all process. Tool temperatures continue to increase and close to be stable condition but Autoform simulation program restrict to make more process even needed. Whatever; temperature increasing slower than the conventional method and FC result also showed that works to get enough quality parts on time.

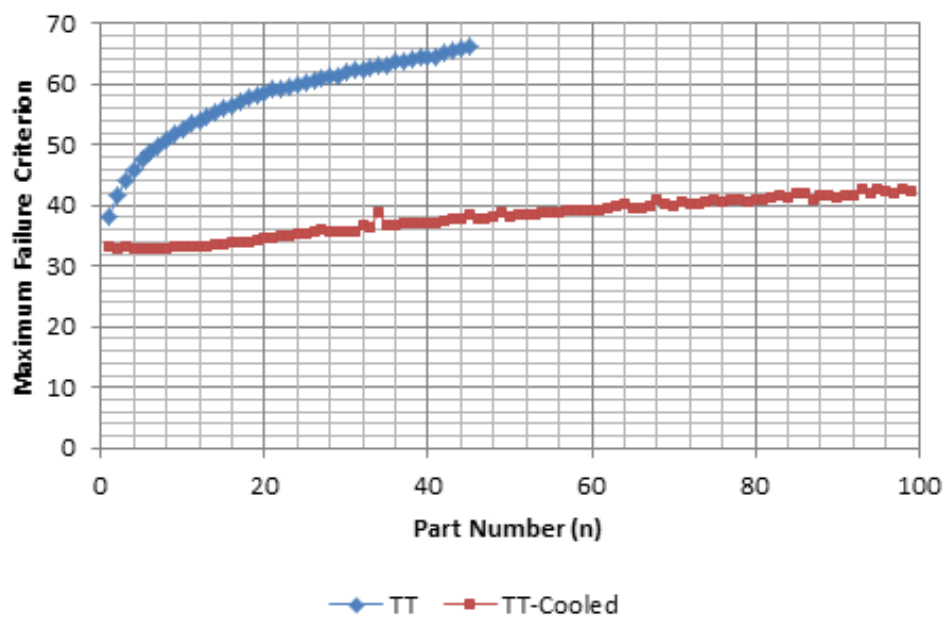


Figure 7. 19.Tool Temperature Condition 22 SPM Link Press

Conventional die FC value started to process as 0,676 and over 0,8 values is not preferable to get enough quality part. Process completed over 3 FC value but in



order to get better graph in Figure 7. 20, value reduced to 1,2. FC value increasing gradually in conventional die and that is over in 45th operation. Cooled die investigated and FC value increasing from 0,676 to 0,686 and reduce after stable temperature and process conditions. While FC value reduced panel thinning and quality is better level in process.

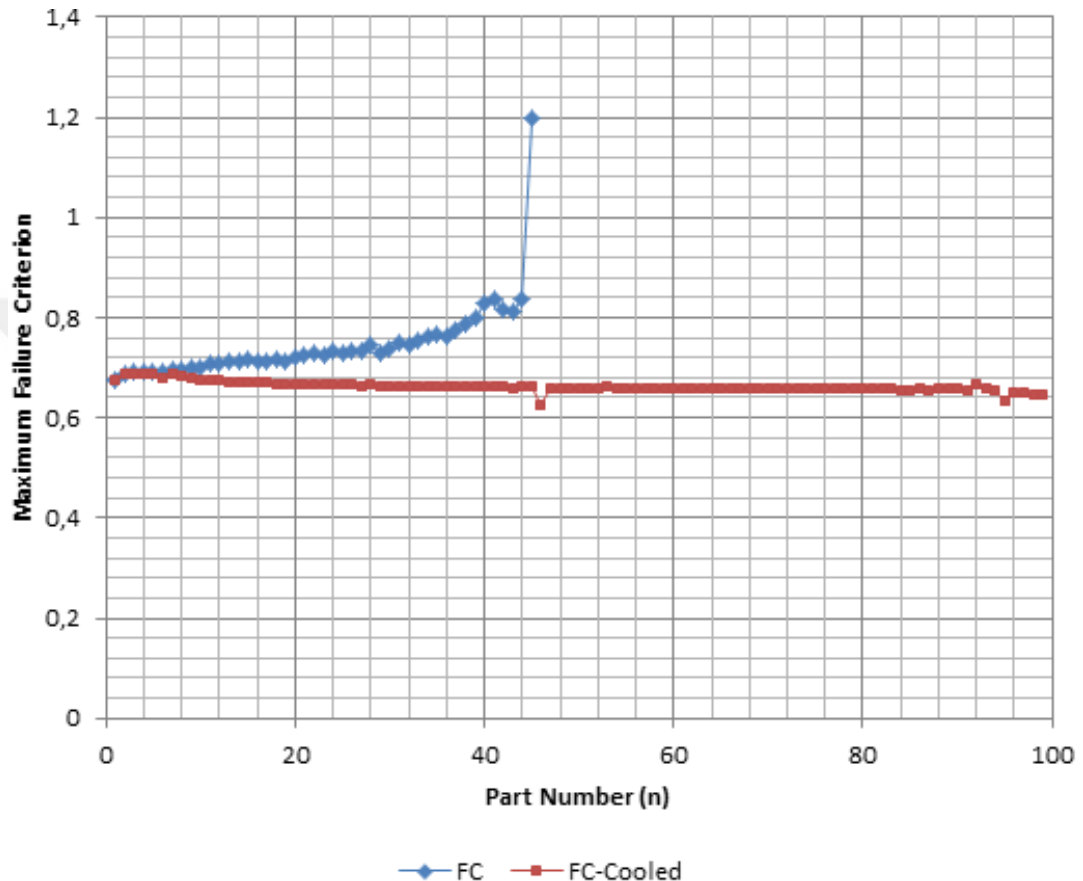


Figure 7. 20. FC Condition 22SPM Link Press

Last condition of this FE experiment 22SPM mechanical press condition given in Appendix-H. FC value started as 0,68 and completed with 0,64 so decreasing of FC value clearly seen in this table. Additionally sheet metal temperature started as 191°C that is lower than link press sheet metal temperature value that is 218°C. That is related with different press curves and material card properties up to 100°C. Over than 100°C extrapolation method used in software.

Tool temperature increasing in conventional die per part shown in Figure 7 .21. That is similar for all uncooled conventional die system. Although process occurred longer than other 8SPM Mechanical, 8SPM Link and 22SPM Link presses, part split issue seen in 84th operation and die surface temperature increasing excessively.



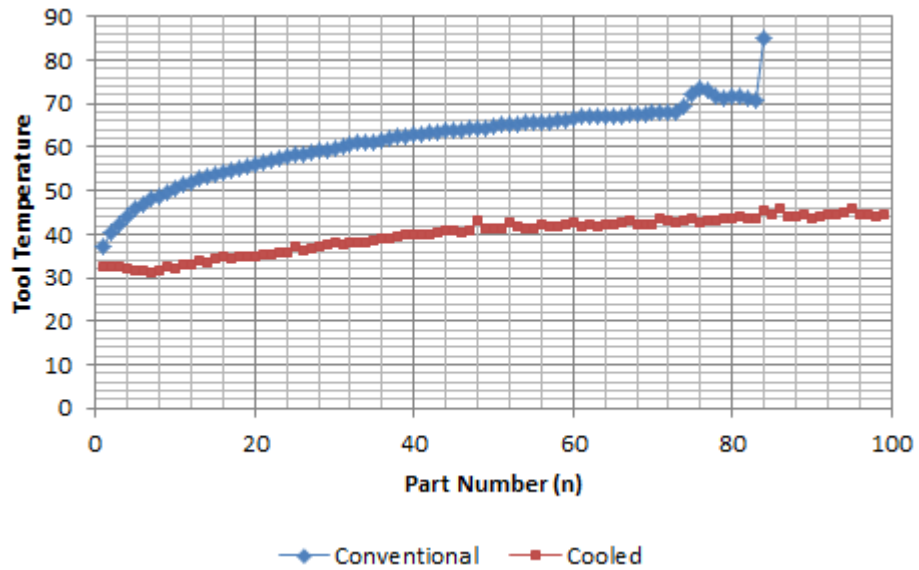


Figure 7. 21.Tool Temperature Condition 22 SPM Mechanical Press

Cooled tool temperature started lower than conventional system because 1°C inlet temperature water entered to punch and upper die system and reduce the first temperature of tool and try to reduce die temperature even sheet metal try to increase die temperature. Tool temperature not over to 50°C but not reach stable condition after 99th stroke.

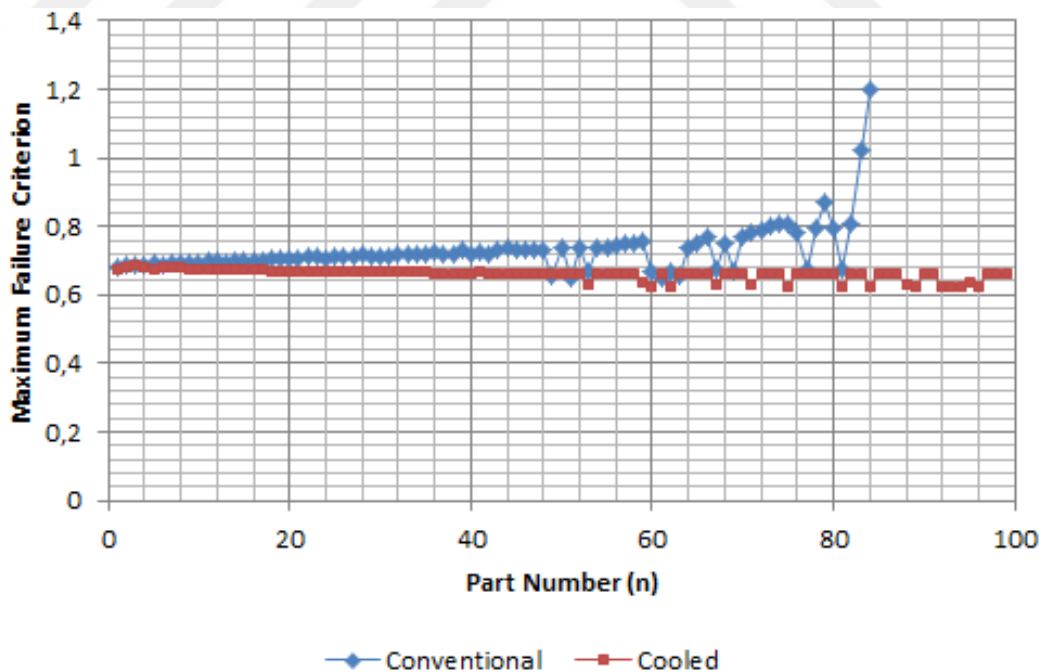


Figure 7. 22.FC Condition 22SPM Mechanical Press

Maximum failure criterion value decreased similarly of others because that affects the graph profile in Figure 7 .22. FC value increasing in conventional method and have big deviation after 45th stroke. In cooled system, FC value have small

increasing in first step and decreasing in next steps but in this process, that is closer to 0,7 even coolant system implementation. Coolant flow will be changed from water to better fluent in order to send to die lower from 0°C. That will affect positively parts quality.

### **7.6.Cooling System Design and Construction**

Cooling system for stamping dies using in hot stamping dies but not have clear information that is using for cold stamping dies. Conventionally that is not normal concept for cold stamping process so not has enough experiences to design dies according to this system.

However hot stamping dies using cooling system in draw operation for years and system can be copied from there. Hot stamping die system explained in Figure 7 .2. and need cooling system. For hot stamping dies, heat rate must be above 27°C/sec in order to get martensitic material after draw operation so all system must be design perfectly. Today all manufacturer use water as cooling fluent that have two important reasons. First reason that is cheaper and the second one is safer than other coolants [43].

Two different manufacturing methods using for cooling system. The first method is drilling die parts and closes the hole by seals and covers. The second one is pre-embedded system; hose putting the sand process before casting. These are both having advantages and disadvantages. [44]



Figure 7. 23.Cooling Pipe System in Hot Stamping [5]

Drilling die parts not implemented to complex part shape dies but has advantage to make bigger channels that increase to heat transfer surfaces. That can be implemented just simple die parts, for example for cup draw die that can be applied.

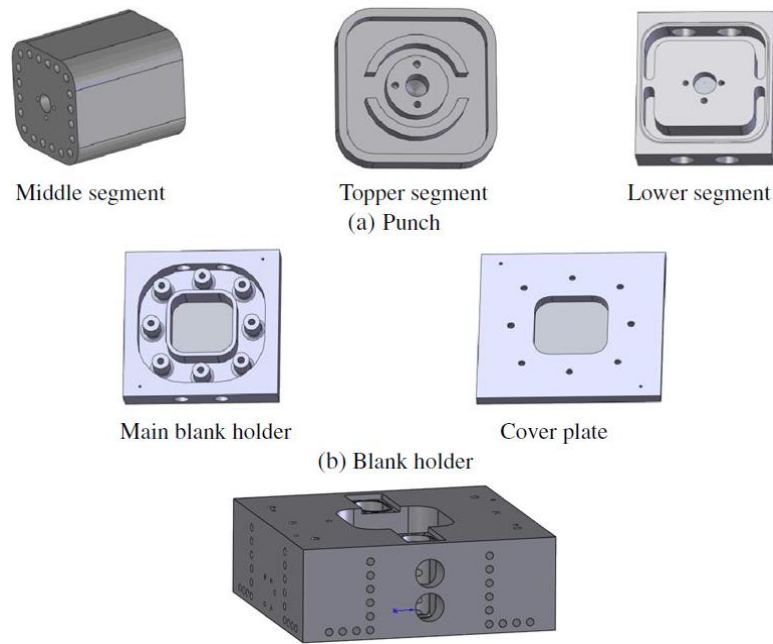


Figure 7. 24.Drilling Method Implementation Example [43]

The other important point of drilling method, seal implementation is not easy. That must be thought in design phase. In this method, some die parts must be designed as divided. For example Figure 7 .24a shows that punch occurs from 3 main parts one is middle segment and second is topper segment and the last one is lower segment. Similarly blank holder occurs from main blank holder and cover plate. All holes should be closed with seals and must be checked in mass production because seals will be deformed after some cycles especially face with hot water. [44] [43]

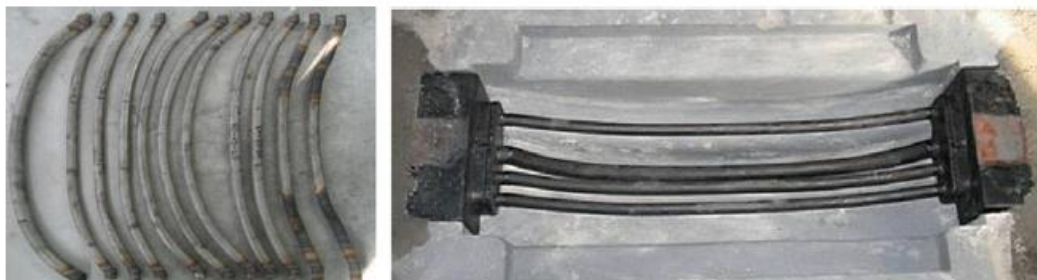


Figure 7. 25.Pre-Embedded Pipes [43]

Second manufacturing method of cooling system is pre-embedded system that is using for complex shape parts and more expensive than drilling method. Because manufacturing method is not easy but today using pre-embedded system is an obligation shown in Figure 7 .25. Cooling pipe types, cooling pipe quantity, cooling point locations, inlet and outlet points defined according to experienced guidelines and FE simulations. Pipes melting points are higher than casting material, so that is working after to get casted dies. [43] [45]

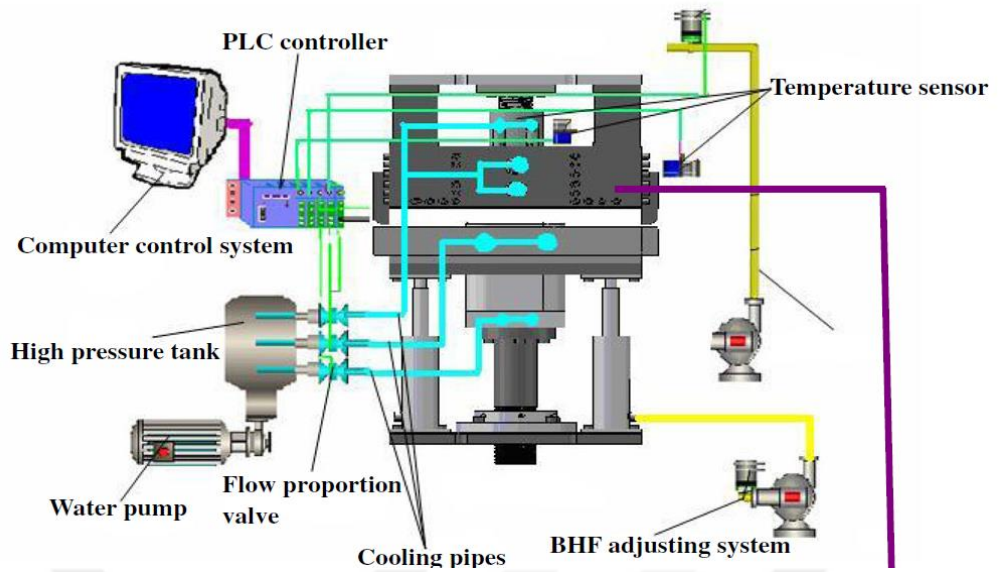


Figure 7. 26. Standard Hot Stamping Test System [43]

Optimization studies continue for all process in order to get correct part quality after operation. Die system design shown in Figure 7 .26 that use simple water pump for circulation.

## 8. CONCLUSIONS AND FUTURE WORK

A mathematical model for heat generation has been developed and validated with experiments from literature. After the first hit, the temperature predictions were within  $\pm 2^\circ\text{C}$ .

Once this model is validated, single stroke investigated as the highest cup geometry in order to learn limits of the draw operation. Two different material thickness, two different press velocity and two different die temperature, one is cooled and other is conventional put FE simulation by using DP800 material and 170mm draw height. After observing cooling effect more than other variables, different die temperatures effects measured to thickness and one press velocity. This study clearly shows that cooling of die improves drawability of sheet metal parts.

As a next step, a multi-cycle model is generated for link press and mechanical press models. Two different press speeds also used as 8SPM and 22SPM to understand speed effects to part quality. The die design and material selection were done to speed up the heat generation, such that, after only 22 to 83 hits failures were observed. This study shows that; even first part have enough quality, 22th part will face split issue in mass production that is seen today not just for AHSS materials also mild steels in mass production. So this study should help to all big and deep part draw operation positively.

While understand parts quality effected in mass production randomly, if reduce the die temperature by adding coolant pipes to punch and upper die radius area, what part quality is in FE simulation. Failure criterion, tool temperature and sheet metal temperature checked for 4 different processes as 8SPM mechanical press, 8SPM link press, 22SPM mechanical press and 22SPM link press. Each operation set up to 99<sup>th</sup> operation and failure criterion value decreasing stroke by stroke gradually that shows that system stables.

Draw die cooling system investigated for standard cold dies and hot stamping die cooling system examined.

Several improvements could be done in the mathematical model, such as:

- 1) Temperature dependent FLC may be required to further improve FC-value predictions,
- 2) Higher temperature flow curves could reduce the error due to extrapolation,
- 3) Correction of idle times on the tools may change the tool temperatures,
- 4) Friction model requires further investigation,
- 5) All results should be better if Autoform can allow to more than 99 strokes for stamping FE simulation.
- 6) Coolant temperature effectiveness will be checked with lower from 1°C
- 7) Optimization should be made about pipe diameter, pipe configuration, pipe dimension to part surface

After the proposed work done, it is possible to find the best possible process window to improve productivity (higher SPM) and reduce costs (due to scrapping of failed parts). A draw die with built-in cooling channels is planned for further experimental studies.

This study has two main profits to sheet metal manufacturers;

- Remove all scrap issue from draw operation even some small parameter changed during operation such as mild steel oil distribution, die surface roughness, sheet metal thickness tolerances, etc...
- Possibility to be manufactured; big dimension, deep, complex and high durability materials drawability via cold stamping system.

## REFERENCES

- [1] Ghassemieh E., Materials in Automotive Application State of the Art and Prospects *New Trends and Developments in Automotive Industry*, ISBN: 978-953-307-999-8, 2011.
- [2] Fekete J., Hall J., Design of auto body: Materials perspective, *Automotive Steels*, Radhakanta Rana and Shiv Brat Singh, Eds., Woodhead Pub.,1-18, 2017, <http://www.sciencedirect.com/science/article/pii/B9780081006382000018> (visiting date: 25 April 2020).
- [3] Kimchi M. Keeler S., Advanced High Strength Steel Application Guidelines Verison 6.0, 2017.
- [4] Meyers,K., Chawla, M., *Mechanical Behaviour of Materials*, Second Edition, Cambiridge Universty Press, New York, 2009.
- [5] Zmik J., Recent Progress in High Strength Low Carbon Steels, *Metalurgija-Sisak then Zagreb*, **45**(4), 323-331, 2006.
- [6] Posco, *Automotive Steel Data Book*, 2016.
- [7] Fallahiarezoodar A., Peker R.,Altan T., Temperature Increase in Forming of Advanced High-Strength Steels Effect of Ram Speed Using a Servodrive Press, *Journal of Manufacturing Science and Engineering*, **138**(9) 094503\_1-094503\_7, 2016.
- [8] Groover M.P., *Fundamentals of Modern Manufacturing*, 4th Edition, John Wiley & Sons Inc., USA, 2010.
- [9] Capan L., *Metallere Plastik Şekil Verme*, Çağlayan Kitabevi, İstanbul, 1999.
- [10] Edward M., *Metal Working science and Engineering*, McGraw-Hill, USA, 1991.
- [11] Suchy I., *Handbook of Die Design*, The McGraw Hill Companies, New York, 2006.
- [12] Varol G.E.,Yılmaz S., Yaşacan A., Geliştirilmiş Yüksek Mukavemetli Otomotiv Çelik Kaliteleri, *Metal Dünyası Dergisi*, **271**, 2016.
- [13] Abspoel M.,Scholting J.,Droog M., A New Method for Predicting Forming Limit Curves from Mechanical Properties, *Journal of the Material Precessing Technology*, **213**, 759-769, 2012.

- [14] Verband Der Automobilindustrie E.V.(VDA), *Material Specifications*, 2016.
- [15] Zhengwei G., Xin, L., Hong X., Mengmeng L., Optimal Design for Cooling System of Hot Stamping Dies, *ISIJ International*, **56** (12), 2250-2258, 2016.
- [16] Fallahiarezoodar A., Peker R., Altan T., Heat Generation in Forming of AHSS, *Stamping Journal*, 12-13, 2015.
- [17] Voestilpine steels, <https://www.voestalpine.com/stahl/en/Products/Steel-strips/Hot-dip-galvanized-steel-strip>, (visiting date: 10 September 2020).
- [18] Özkan F., Bach, A., Future Trends and Challenges in Using AHSS in Body Structure, *Presented at PHS Suppliers Forum*, Troy, MI, September 2019.
- [19] Billur E. and Altan, T., Challenges in forming advanced high strength steels, *Proceedings of New Developments in Sheet Metal Forming*, 285–304, 2010.
- [20] Cengel Y., *Heat Transfer A Practical Approach*, Güven, İzmir, 2011.
- [21] Pereira B., Rolfe, M., Temperature Conditions During ‘Cold’ Sheet Metal Stamping, *Journal Materials Processing Technology*, **214**(8), 1749–1758, 2014.
- [22] Kim Q., Altan T., Yan H., Evaluation of Stamping Lubricants in Forming Advanced High Strength Steels (AHSS) Using Deep Drawing and Ironing Tests, *Journal of Materials Processing Technology*, **209**(8), 4122–4133, 2009.
- [23] Farren G., Taylor W., *The Heat Developed During Plastic Extension of Metals*, Proc. R. Soc., London, 1925.
- [24] Cengel, Y., Boles, M., *Thermodynamics An Engineering Approach*, Güven, İzmir, 2008.
- [25] Marangaloub J.H., Kott M., Gastebois S., Hol J. Waandersa D., Temperature Dependent Friction Modelling: The Influence of Temperature on Product Quality, *Procedia Manufacturing*, **47**, 535-540, 2020.
- [26] Jeffery J., Kenny F., Infante D. D., Altan T. Hoschouer C., Evaluating Lubricant Using the Cup Drawing Test, *Stamping Journal*, **16-17**, September/October 2016.
- [27] Billur E., Fundamentals and Applications of Hot Stamping Technology for Producing Crash-Relevant Automotive Parts, *PhD Dissertation*, The Ohio State University, 2013.



- [28] Hilditch T., Souza P., Hodgson T., Properties and automotive applications of advanced high-strength steels (AHSS), in *Welding and Joining of Advanced High Strength Steels (AHSS)*, Mahadev Shome and Muralidhar Tumuluru, Eds. Woodhead Publishing, 9-28, 2015, <http://www.sciencedirect.com/science/article/pii/B9780857094360000023> (visiting date: 15 May 2020).
- [29] Ermanno Ceron and Niels Bay, Testing and prediction of limits of lubrication in sheet metal forming, *Lightweighting: Possibilities & Challenges*, 251–257, SMF, 2012.
- [30] Thompson, A., Salisbury, M., Worswick, I., Van Riemsdijk, R., Mayer, S., Winkler I., Strain Rate and Temperature Effects on the Formability and Damage of Advanced High-Strength Steels, *Metallurgical and Materials Transactions*, **39**(6), 1350-1358, 2008.
- [31] «CR\_DP800-GI\_Vegter+thermo\_1.2-1.6.mtb,» AutoForm Material Card, Tata Steel, 2019.
- [32] Billur E., Saraç H. İ., Akcan K, Temperature Effects in Deep Drawing of Advanced High Strength Steels, *Journal of Research on Engineering Structures and Materials*, 2021, **1**, DOI:<http://dx.doi.org/10.17515/resm2021.218me1004>, (visiting date: 24 March 2021).
- [33] Vegter H., Boogaard A., A plane stress yield function for anisotropic sheet material by interpolation of biaxial stress states, *International Journal of Plasticity*, **22**, 557-580, 2006, <http://www.sciencedirect.com/science/article/pii/S0749641905000926> (visiting date: 18 July 2020).
- [34] Vegter H., Horn, M., Abspoel C., The Corus-Vegter Lite Material Model: Simplifying Advanced Material Modelling, *International Journal of Material Forming*, **2**, 511, December 2009, <https://doi.org/10.1007/s12289-009-0640-4> (visiting date: 09 December 2020).
- [35] Reinberg A., Mokashi S., Naseri, Y., Demiralp Y., Golovashchenko N., Drawbead Restraining Forces in Sheet Metal Drawing Operations, *Stamping Journal*, November/December 2020.
- [36] Ju T., Mao J., Malpica L., Altan, T., Evaluation of Lubricants for Stamping of Al 5182-O Aluminum Sheet Using Cup Drawing Test, *Journal of Manufacturing Science and Engineering*, vol. **137**, September 2015.
- [37] Asnafi N., Tooling and Technologies for Processing of Ultra High Strength Sheet Steels, *The International Conference of Automotive Manufacturing Solutions*, India, 2011.

- [38] Basril M.A.M., Teng M.A., The Effect of Heating Temperature and Methods Towards the Formability of Deep Drawn Square Metal Cup, *IOP Conference Series Materials Science and Engineering*, **210**(1), June 2017.
- [39] Kurtulus N., "New Developments in Sheet Metal Forming Simulations, *Proceedings of the 2nd Metal Forming Technology Day*, 2019.
- [40] Wang Y., Chang T., Mille R., Liasi E. Sheng Z., Deep Drawing by Indirect Hot Stamping, *SAE 2013 World Congress and Exhibition*, 1172, January 2013.
- [41] So H., Michelitsch T., Hoffmann H. Steinbeiss H., Method for Optimizing the Cooling Design of Hot Stamping Tools, *Production Engineering*, **1**, 149-155, 2007.
- [42] Pang L. Shang X., Optimization Design of Insert Hot Stamping Die's Cooling System and Research on the Microstructural Uniformity Control of Martensitic Phase Transitions in Synchronous Quenching Process, *Advances in Materials Science and Engineering*, 2020.
- [43] Chengxi L., Zhongwen X. Hongsheng L., Cooling System of Hot Stamping of Quenchable Steel BR1500HS: Optimization and Manufacturing Methods, *The International Journal of Advanced Manufacturing Technology*, **69**, 211–223, 4 May 2013.
- [44] Ying L. Hu P., Numerical Investigation on Cooling Performance of Hot Stamping Tool with Various Channel Design, *Applied Thermal Engineering*, **96**, 338-351, 2016.
- [45] Vollmerb R., Aspachera J., Gharbib M. Palm C., Increasing Performance of Hot Stamping Systems, *International Conference on the Technology of the Plasticity*, **207**, 765–770, 17-22 September 2017.
- [46] Herich A., Die Science: Stamping 101-Die Basics, *Stamping Journal*, 2008.



**APPENDIX**

Appendix-A

Table A.1. 8Spm Mechanical Press Results

8 Spm Mechanical Press			
Exp.	Failure Critarion	Sheet Temperature	Tool Temperature
1	0,677	191,7	46,84
2	0,68	192	51,5
3	0,683	193,2	54,06
4	0,684	193,1	56,06
5	0,686	192,5	57,69
6	0,688	191,3	59
7	0,685	192,3	60,28
8	0,682	192,1	61,28
9	0,683	193,5	62,22
10	0,691	190,9	62,84
11	0,693	193,4	63,81
12	0,695	192,5	64,44
13	0,695	191,6	64,88
14	0,689	193,1	65,81
15	0,696	191,7	66,12
16	0,698	191,7	66,75
17	0,698	192	67,06
18	0,698	191,6	67,5
19	0,701	191,7	68,06
20	0,702	192,2	68,38
21	0,703	190,8	68,88
22	0,704	191,1	69,06
23	0,711	192,5	69,5
24	0,708	191,5	70
25	0,714	191,8	70,25
26	0,716	192,1	70,62
27	0,716	191,6	71
28	0,719	194,1	71,31
29	0,721	192,6	71,62
30	0,725	195,2	71,5
31	0,735	192,2	71,75
32	0,737	191,3	72,12
33	0,739	190,8	72,25
34	0,739	192,1	72,5
35	0,749	190,9	72,5
36	0,759	188,5	72,88
37	0,672	199	73,69
38	0,671	198,2	74,25
39	0,678	195	74,38

<b>40</b>	0,748	190,4	73,94
<b>41</b>	0,779	187,4	73,88
<b>42</b>	0,817	183,8	74,06
<b>43</b>	3,009	320,9	80



## Appendix-B

Table B.1. 8Spm Link Press Results

8 spm Link Press			
Exp.	Failure Criterion	Sheet Temperature	Tool Temperature
1	0,675	188,3	48,12
2	0,688	189,5	52,81
3	0,691	189,7	55,75
4	0,693	189,9	57,81
5	0,697	189,9	59,31
6	0,703	187,3	60,66
7	0,708	187,5	61,72
8	0,709	187,5	63,06
9	0,712	190,8	63,69
10	0,713	186,6	64,31
11	0,719	188,8	65,12
12	0,729	188,1	65,81
13	0,728	187,4	66,56
14	0,733	187,5	67,5
15	0,741	188,2	68
16	0,746	187,8	68,38
17	0,764	186,1	68,81
18	0,734	188,8	69,19
19	0,787	181,8	69,56
20	0,675	193,9	70,25
21	0,782	183,3	70,5
22	2,914	279,8	85

## Appendix-C

**Table C.1. 22Spm Mechanical Press Results**

<b>8 Spm Mechanical Press</b>			
<b>Exp.</b>	<b>Failure Criterion</b>	<b>Sheet Temperature</b>	<b>Tool Temperature</b>
1	0,679	219	37
2	0,685	210,5	40,38
3	0,689	210	42,44
4	0,688	209	44,28
5	0,691	209,2	45,81
6	0,69	210,6	46,84
7	0,693	210,3	48,06
8	0,692	209,6	48,88
9	0,694	208,6	49,75
10	0,692	209,1	50,53
11	0,697	208,5	51,31
12	0,698	210,3	51,97
13	0,696	210	52,62
14	0,697	209,4	53,19
15	0,701	209,3	53,81
16	0,697	210	54,31
17	0,701	209	54,75
18	0,706	209	55,28
19	0,708	208,9	55,75
20	0,706	208,3	56,22
21	0,707	209,4	56,69
22	0,71	209,3	56,94
23	0,711	209,3	57,38
24	0,707	209,1	57,84
25	0,712	208,5	58,16
26	0,713	209,8	58,41
27	0,711	208,5	58,84
28	0,717	209,8	59,22
29	0,712	208,5	59,44
30	0,714	209,6	59,97
31	0,715	200	60,31
32	0,718	208,9	60,59
33	0,719	208	60,91
34	0,718	210,9	61,12
35	0,721	209,8	61,34
36	0,725	209,5	61,69
37	0,718	209,5	62
38	0,722	211,2	62,31
39	0,731	209	62,56

40	0,719	209,4	62,81
41	0,727	209,8	63,09
42	0,722	209,8	63,28
43	0,732	210,3	63,59
44	0,735	211	63,69
45	0,733	210,8	63,81
46	0,734	209,8	64
47	0,734	208,6	64,19
48	0,734	210	64,44
49	0,655	214,6	64,38
50	0,735	218	64,75
51	0,651	215,3	65,25
52	0,736	210,9	65,12
53	0,667	215,3	65,31
54	0,736	210,4	65,5
55	0,738	209,6	65,56
56	0,745	208,8	65,75
57	0,748	208,9	65,88
58	0,753	208,9	66
59	0,756	206,2	66,19
60	0,669	213,9	66,5
61	0,651	214,1	67
62	0,669	214,2	66,94
63	0,658	212,9	67,19
64	0,738	209	67,19
65	0,751	208,7	67,06
66	0,768	207	67,19
67	0,672	213,5	67,62
68	0,752	209	67,62
69	0,671	212,8	67,69
70	0,769	206,2	67,81
71	0,78	205,2	67,81
72	0,788	204,9	68
73	0,802	204,4	67,94
74	0,81	203,6	69,19
75	0,809	204	72,12
76	0,783	205,6	73,56
77	0,672	213,9	72,94
78	0,792	205,1	71,56
79	0,871	199,3	71,19
80	0,797	203,9	71,56
81	0,672	212,3	71,94
82	0,81	203,3	71,44
83	1,02	190,5	70,88



84	4,48	479,1	85
----	------	-------	----



## Appendix- D

**Table D.1. 22Spm Link Press Results**

<b>8 Spm Link Press</b>			
<b>Exp.</b>	<b>Failure Criterion</b>	<b>Sheet Temperature</b>	<b>Tool Temperature</b>
1	0,676	218,5	38,15
2	0,686	219	41,81
3	0,69	218,3	44,23
4	0,692	217,2	46,03
5	0,691	218,8	47,56
6	0,693	217,3	48,83
7	0,694	218,4	49,86
8	0,694	216,5	50,88
9	0,699	218,3	51,85
10	0,7	218,1	52,7
11	0,707	215,2	53,46
12	0,707	215,3	54,1
13	0,711	215,3	54,81
14	0,712	214,7	55,37
15	0,716	215,8	55,96
16	0,712	214,2	56,54
17	0,713	214,2	57,07
18	0,716	216,5	57,72
19	0,713	216,8	58,16
20	0,721	215,8	58,62
21	0,726	213	59,1
22	0,731	212,6	59,09
23	0,724	214,4	59,42
24	0,732	212,6	59,86
25	0,728	213,7	60,15
26	0,734	212	60,65
27	0,733	213	60,91
28	0,747	211,3	61,23
29	0,731	213,3	61,45
30	0,739	211,8	62,02
31	0,748	210,9	62,29
32	0,744	212,3	62,49
33	0,752	210,9	62,86
34	0,762	210,6	63,12
35	0,766	210,8	63,25
36	0,763	210,8	63,67
37	0,774	209,4	63,88
38	0,789	205,4	64,24
39	0,798	202,8	64,35

<b>40</b>	0,828	202,5	64,48
<b>41</b>	0,836	202,7	64,66
<b>42</b>	0,818	202,5	65,08
<b>43</b>	0,812	203,8	65,46
<b>44</b>	0,837	202,7	65,85
<b>45</b>	3,595	396,9	66,34



Appendix- E

Table E.1. 8Spm Link Press Results with Cooled System

Exp.	77 kN-8 spm Link Press-Cooled		
	Failure Criterion	Sheet Temperature (°C)	Sheet Temperature (°C)
1	0,678	188,8	40,38
2	0,685	186,8	40,88
3	0,678	188,9	42,44
4	0,67	187,8	42,62
5	0,663	188,3	44,12
6	0,656	187,9	43,75
7	0,652	188,2	44,25
8	0,649	188,9	44,47
9	0,648	187,2	44,66
10	0,645	185,6	44,94
11	0,645	185,9	45,19
12	0,644	190,7	45,09
13	0,643	190,6	45,41
14	0,642	187,8	45,53
15	0,641	187,2	46,12
16	0,641	188,1	47,12
17	0,64	187,8	46,81
18	0,64	187,7	46,62
19	0,639	187,3	46,34
20	0,615	192,8	46,97
21	0,631	189,4	47,16
22	0,614	194,7	47,34
23	0,633	191,4	48
24	0,634	191,3	47,28
25	0,634	190,8	47,5
26	0,633	190,6	47,62
27	0,633	188,9	47,75
28	0,632	191,5	47,69
29	0,613	194,6	47,97
30	0,632	189	47,81
31	0,632	190	47,69
32	0,631	190,2	48,06
33	0,632	188,8	48
34	0,632	188,8	48,19
35	0,631	189,5	48,09
36	0,631	188,6	48,06
37	0,632	189,4	51,13
38	0,632	187,9	50,68

39	0,631	190,7	52,19
40	0,632	187,4	48,94
41	0,632	194,3	49,41
42	0,631	187,5	51,27
43	0,631	186,7	52,73
44	0,634	192,8	48,08
45	0,634	188,9	48,81
46	0,633	194,8	48,40
47	0,633	189,9	48,15
48	0,632	187,2	48,65
49	0,613	189,7	48,31
50	0,632	186,5	48,59
51	0,632	189,9	48,28
52	0,626	192,0	48,28
53	0,631	191,0	48,86
54	0,631	188,1	48,92
55	0,632	189,4	48,49
56	0,632	187,2	48,23
57	0,631	186,9	48,54
58	0,631	189,7	48,66
59	0,632	190,3	48,60
60	0,632	186,3	48,44
61	0,631	186,5	48,86
62	0,632	189,6	48,96
63	0,632	190,2	48,55
64	0,631	190,6	48,06
65	0,631	190,8	48,08
66	0,634	192,8	48,94
67	0,631	193,2	48,59
68	0,631	190,8	48,69
69	0,63	189,1	48,12
70	0,632	188,0	48,88
71	0,631	189,1	48,77
72	0,631	192,4	48,71
73	0,63	191,6	48,35
74	0,631	192,6	48,27
75	0,631	190,5	48,68
76	0,63	190,2	48,87
77	0,632	192,2	48,07
78	0,632	188,4	48,60
79	0,631	186,6	48,33
80	0,632	194,4	48,43
81	0,632	189,6	48,33
82	0,631	191,7	48,75

<b>83</b>	0,631	194,7	48,90
<b>84</b>	0,632	193,1	48,22
<b>85</b>	0,632	186,3	48,89
<b>86</b>	0,631	186,2	48,41
<b>87</b>	0,632	193,7	48,27
<b>88</b>	0,632	194,4	48,36
<b>89</b>	0,631	193,4	48,89
<b>90</b>	0,631	195,0	48,85
<b>91</b>	0,631	186,9	48,52
<b>92</b>	0,631	191,9	48,16
<b>93</b>	0,63	193,7	48,23
<b>94</b>	0,633	192,9	48,11
<b>95</b>	0,632	186,6	48,05
<b>96</b>	0,631	190,7	48,66
<b>97</b>	0,631	189,0	48,31
<b>98</b>	0,631	192,6	48,54
<b>99</b>	0,63	187,6	48,89

Appendix- F

Table F.1. 8Spm Mechanical Press Results with Cooled System

Exp.	78 kN-8 Spm Mechanical Press-Cooled		
	Failure Criterion	Sheet Temperature (°C)	Sheet Temperature (°C)
1	0,68	191,0	39,66
2	0,68	191,9	40,28
3	0,678	191,3	41,66
4	0,675	190,3	42,75
5	0,672	191,6	43,16
6	0,666	191,6	43,34
7	0,664	191,8	43,94
8	0,662	193,6	44,44
9	0,658	195,2	44,56
10	0,66	194,3	44,91
11	0,659	196,1	45,06
12	0,659	195,9	45,31
13	0,655	198,8	45,25
14	0,653	190,4	45,5
15	0,652	191,7	45,44
16	0,652	194,4	45,22
17	0,652	191,1	45,74
18	0,651	196,3	45,47
19	0,651	191,3	45,53
20	0,651	191,9	45,42
21	0,651	198,8	45,33
22	0,634	195,8	45,02
23	0,649	197,4	45,84
24	0,649	196,0	45,26
25	0,649	191,8	45,33
26	0,648	199,0	45,14
27	0,648	196,6	45,74
28	0,647	196,2	45,27
29	0,648	198,0	45,76
30	0,647	198,4	45,57
31	0,647	190,5	45,40
32	0,647	197,8	45,22
33	0,647	192,5	45,64
34	0,646	196,9	45,37
35	0,646	195,6	45,45
36	0,621	196,1	45,46
37	0,624	190,7	45,99
38	0,623	198,0	45,77

39	0,643	195,4	46,27
40	0,644	193,3	46,90
41	0,645	196,9	46,53
42	0,644	195,4	46,42
43	0,643	198,1	46,88
44	0,643	197,9	46,51
45	0,644	197,7	46,61
46	0,644	191,3	46,29
47	0,643	192,7	46,93
48	0,642	192,8	46,20
49	0,624	196,4	46,76
50	0,641	196,1	46,99
51	0,62	197,0	46,85
52	0,641	196,4	46,59
53	0,643	192,3	46,12
54	0,641	192,1	46,26
55	0,642	192,4	46,24
56	0,642	198,7	46,48
57	0,641	195,6	46,42
58	0,641	194,4	46,02
59	0,64	191,7	46,27
60	0,641	194,9	46,34
61	0,619	192,4	46,52
62	0,64	197,5	47,67
63	0,64	195,9	47,50
64	0,64	197,5	47,65
65	0,64	191,6	47,35
66	0,64	197,0	47,82
67	0,64	197,9	47,64
68	0,64	192,2	47,10
69	0,64	193,1	47,85
70	0,64	192,9	47,66
71	0,638	190,2	47,25
72	0,64	197,3	47,37
73	0,64	191,3	47,71
74	0,637	196,6	47,51
75	0,638	192,9	47,49
76	0,641	196,9	47,73
77	0,64	192,1	47,51
78	0,64	191,9	47,67
79	0,639	191,4	47,54
80	0,64	194,7	47,53
81	0,638	193,4	47,88
82	0,64	195,0	47,35



<b>83</b>	0,639	193,0	47,55
<b>84</b>	0,638	197,5	47,12
<b>85</b>	0,618	190,4	47,22
<b>86</b>	0,64	191,6	47,95
<b>87</b>	0,636	198,3	47,66
<b>88</b>	0,64	192,4	47,56
<b>89</b>	0,64	195,5	47,56
<b>90</b>	0,638	198,8	47,69
<b>91</b>	0,639	192,9	47,62
<b>92</b>	0,637	195,7	47,69
<b>93</b>	0,64	193,3	47,56
<b>94</b>	0,64	199,7	47,62
<b>95</b>	0,639	193,8	47,56
<b>96</b>	0,64	198,1	47,62
<b>97</b>	0,638	195,5	47,69
<b>98</b>	0,638	196,8	47,65
<b>99</b>	0,64	194,8	14,62

**Appendix- G**

**Table G.1. 22Spm Link Press Results with Cooled System**

Exp.	80 kN-22 Spm Link Press-Cooled		
	Failure Criterion	Sheet Temperature (°C)	Sheet Temperature (°C)
1	0,676	218,2	33,22
2	0,686	218,2	32,94
3	0,689	217,4	33,31
4	0,688	217,8	33,06
5	0,689	217,2	32,94
6	0,68	219,3	32,97
7	0,686	218,2	33
8	0,683	218,1	33
9	0,679	218,5	33,16
10	0,677	218,1	33,16
11	0,676	219	33,22
12	0,675	219	33,19
13	0,673	218,7	33,12
14	0,669	218,1	33,62
15	0,673	217,6	33,5
16	0,67	217,6	33,81
17	0,669	218,1	34,06
18	0,668	217,4	33,88
19	0,668	218,3	34,16
20	0,667	217,5	34,53
21	0,666	217,7	34,5
22	0,666	217,7	35,16
23	0,666	218	35
24	0,665	217,7	35,31
25	0,666	217,5	35,25
26	0,666	218,6	35,56
27	0,664	218,1	36
28	0,665	217,8	35,78
29	0,664	218,9	35,72
30	0,664	217,9	35,84
31	0,663	219,6	35,81
32	0,662	217,3	36,59
33	0,662	218,4	36,34
34	0,662	217,6	38,69
35	0,662	218,5	36,66
36	0,662	217,2	36,69
37	0,662	217,5	36,94
38	0,661	217,8	37,06

39	0,661	218,1	37,03
40	0,661	218,5	37,22
41	0,661	217,6	37,25
42	0,661	217,3	37,41
43	0,66	219,5	37,69
44	0,661	217,8	37,81
45	0,661	218,7	38,44
46	0,625	219,0	37,69
47	0,66	218,9	37,75
48	0,659	218,8	38,19
49	0,66	217,4	38,97
50	0,66	217,5	38,31
51	0,66	218,0	38,56
52	0,659	217,6	38,66
53	0,661	217,4	38,47
54	0,66	217,1	38,81
55	0,659	220,0	38,81
56	0,659	218,1	39,03
57	0,659	217,8	39,06
58	0,66	217,2	39,34
59	0,659	218,1	39,38
60	0,658	219,0	39,16
61	0,659	218,0	39,16
62	0,659	217,7	39,5
63	0,658	218,5	40,03
64	0,659	217,7	40,25
65	0,658	217,7	39,44
66	0,658	217,2	39,66
67	0,657	218,2	39,97
68	0,658	218,3	41,03
69	0,658	218,3	40,44
70	0,658	217,8	39,91
71	0,657	218,7	40,66
72	0,657	218,6	40,12
73	0,658	217,3	40,25
74	0,658	217,8	40,59
75	0,658	217,3	41
76	0,659	218,3	40,59
77	0,658	217,7	40,88
78	0,657	218,0	41,09
79	0,658	217,6	40,72
80	0,657	218,1	41
81	0,657	218,6	41,09
82	0,657	217,1	41,22

<b>83</b>	0,657	217,2	41,53
<b>84</b>	0,655	218,2	41,44
<b>85</b>	0,656	218,8	42,03
<b>86</b>	0,657	217,4	41,97
<b>87</b>	0,656	218,1	41,12
<b>88</b>	0,657	218,5	41,72
<b>89</b>	0,657	217,6	41,78
<b>90</b>	0,657	217,1	41,28
<b>91</b>	0,656	217	41,72
<b>92</b>	0,665	217,5	41,66
<b>93</b>	0,657	216,8	42,75
<b>94</b>	0,656	217,1	42,12
<b>95</b>	0,632	217	42,84
<b>96</b>	0,65	216,9	42,47
<b>97</b>	0,649	217	41,91
<b>98</b>	0,647	217,5	42,72
<b>99</b>	0,646	216,8	42,28

Appendix- H

Table H.1. 22Spm Mechanical Press Results with Cooled System

Exp.	87kN-22 Spm Mechanical Press-Cooled		
Exp.	Failure Criterion	Sheet Temperature (°C)	Sheet Temperature (°C)
1	0,675	211,2	32,47
2	0,684	209,6	32,38
3	0,686	209,6	32,41
4	0,684	209,8	31,88
5	0,677	215,1	31,72
6	0,681	209,7	31,62
7	0,68	209,2	31,38
8	0,68	210	31,56
9	0,676	214,1	32,34
10	0,676	212,1	32,19
11	0,677	210,3	32,94
12	0,674	210,6	32,88
13	0,674	211,8	34,01
14	0,675	210,6	33,53
15	0,673	210,7	34,28
16	0,672	211,7	34,88
17	0,673	211,8	34,56
18	0,67	210,7	34,66
19	0,671	211,3	35,06
20	0,67	210	35,09
21	0,67	210,3	35,12
22	0,668	211,2	35,34
23	0,668	211,3	35,94
24	0,668	211,1	35,81
25	0,667	211,1	36,97
26	0,668	210,4	36,31
27	0,668	210,9	36,91
28	0,668	212,3	37,19
29	0,667	210,9	37,78
30	0,666	212,2	37,97
31	0,666	210,6	37,75
32	0,666	213,6	38,12
33	0,666	209,8	38,22
34	0,666	209,8	38,16
35	0,666	213,9	38,38
36	0,665	213,0	39,06
37	0,665	212,6	39,16
38	0,665	213,4	39,44

39	0,665	210,0	39,91
40	0,665	211,5	39,91
41	0,666	214,8	40,12
42	0,665	211,2	39,97
43	0,665	210,3	40,56
44	0,665	214,0	40,88
45	0,665	213,6	40,97
46	0,665	214,2	40,34
47	0,664	211,9	41
48	0,665	212,0	43,19
49	0,664	210,5	41,28
50	0,664	212,2	41,16
51	0,664	209,5	41,53
52	0,664	214,4	42,59
53	0,631	211,2	41,78
54	0,664	210,1	41,31
55	0,663	209,5	41,47
56	0,663	209,1	42,09
57	0,664	213,6	41,56
58	0,662	210,1	41,97
59	0,635	212,8	42,38
60	0,624	210,5	42,69
61	0,662	213,9	41,59
62	0,623	210,0	42,12
63	0,662	211,0	41,97
64	0,662	201	42,34
65	0,662	212,8	42,25
66	0,663	212,3	42,53
67	0,631	214,8	43,06
68	0,661	210,5	42,22
69	0,66	211,9	42,12
70	0,66	209,9	42,38
71	0,63	214,3	43,44
72	0,662	212,5	43,06
73	0,661	211,4	42,91
74	0,662	211,9	43,25
75	0,623	213,8	43,66
76	0,661	212,8	42,72
77	0,662	211,9	43,31
78	0,661	211,9	43,38
79	0,661	213	43,59
80	0,661	211,8	43,75
81	0,626	213,6	44,19
82	0,66	212,5	43,54

<b>83</b>	0,661	211,3	43,69
<b>84</b>	0,627	214,3	45,25
<b>85</b>	0,661	212,2	44,59
<b>86</b>	0,661	211,3	45,97
<b>87</b>	0,66	210,3	43,88
<b>88</b>	0,628	214,6	44,25
<b>89</b>	0,623	215,8	44,53
<b>90</b>	0,659	212,2	43,72
<b>91</b>	0,66	211,5	44,28
<b>92</b>	0,625	214,5	44,62
<b>93</b>	0,623	214,3	44,41
<b>94</b>	0,623	214,6	45,03
<b>95</b>	0,635	214,2	45,84
<b>96</b>	0,623	214,1	44,47
<b>97</b>	0,659	211,3	44,41
<b>98</b>	0,659	212,4	44,12
<b>99</b>	0,66	212,4	44,41

## PERSONAL PUBLICATIONS AND WORKS

Billur E., Saraç H., **Akcan K**, E., Temperature Effects in Deep Drawing of Advanced High Strength Steels, *Journal of Research on Engineering Structures and Materials*, 2021,; **1**, DOI:<http://dx.doi.org/10.17515/resm2021.218me1004>, (visiting date: 24 March 2021).





## **VITA**

Kadir Akcan studied in Beyođlu Fındıklı High School. He graduated from Kocaeli University Mechanical Engineering Department in 2010 as the second grade student of department. He graduated from İstanbul Technical University in post graduate Aeroplane-Space Engineering Department in 2013. He has been die design team leader responsibility in Ford Otosan.

